CATALYTIC EVALUATION OF Ru(II) AND Co(II) SALICYLALDIMINE COMPLEXES FOR TRANSFER HYDROGENATION OF ACETOPHENONE

Dakalo Lorraine Ndou

UNIVERSITY OF THE
WITWATERSRAND,
JOHANNESBURG

A Dissertation submitted to the Faculty of Science, University of the Witwatersrand, in partial fulfilment of the requirements for the degree of Master of Science

Johannesburg; 2017

Declaration

I declare that this Dissertation entitled **Catalytic Evaluation of Ru(II) and Co(II) Salicylaldimine Complexes For Transfer Hydrogenation of Acetophenone** is my own, unaided work. It is being submitted for the Degree of Master of Science at the University of the Witwatersrand, Johannesburg. It has not been submitted before for any degree or examination at any other University.

(Signature of candidate)

_____28th_____day of_____May_____2017__in_Johannesburg_____

Abstract

N-(aryl) salicylaldimine ligands were prepared by the condensation of salicylaldehyde and aniline, 2,6 – dimethylaniline, 2,6 – diisopropylaniline and N,N-diethyl-p-phenylenediamine to give the desired ligands in good yields (70 - 93 % yield). The synthesised ligands were characterised by NMR spectroscopy, FTIR spectroscopy, ESI mass spectrometry and elemental analysis. The purity of these ligands was determined by determining the meting points. Co(II) and Ru(II) complexes were prepared from $Co(OAc)_2.4H_2O$ and $[RuCl_2(\eta^6\text{-}p\text{-cymene})]_2$ to afford the *N*-(aryl) salicylaldiminato complexes **Co1** – **Co4** and **Ru1** – **Ru4** with yields in the range 60 – 66 % and 90 – 97 %, respectively. These complexes were characterised by NMR spectroscopy, FTIR, ESI mass spectrometry, elemental analysis and TGA. The purity of these complexes was also determined by determining the melting point.

The transfer hydrogenation of acetophenone was studied using 2-propanol as the hydrogen source and KOH as the base with the Ru (II) and Co (II) complexes as catalyst precursors. The catalytic activity of these complexes was evaluated using ^{1}H-NMR and GC - MS. Preliminary studies were performed for 6 h at 82 ^{o}C and the conversion was evaluated using ^{1}H-NMR. Due to the low catalytic activity of these complexes, the reaction time was increased to 48 h. Increasing the reaction time resulted in improvements in the conversion of the complexes. The catalysis was also evaluated at various temperatures to study the effect it has on the activity of the complexes. Temperature was found to not have a significant effect on the conversion. The ruthenium complexes were found to be active towards the transfer hydrogenation of acetophenone but the cobalt complexes were observed to have no catalytic activity in the transfer hydrogenation of acetophenone.

The ruthenium complexes were investigated in an ionic liquid – organic biphasic system with the aim of separating the metal complexes in order to reuse the catalysts. Toluene was the

organic phase and [BMIM]BF_4 was the ionic liquid which afforded a biphasic system. Three cycles were performed and the performance of **Ru1** – **Ru3** decreased with each cycle but **Ru4** behaved differently as the performance increased with each cycle.

Acknowledgements

First and foremost I would like to thank the **Almighty God** for giving me the strength throughout this programme and for seeing me through it.

I would also like to express my thanks to my entire family, especially my parents, for always supporting and encouraging me all these years. Their love for me has proved to be unconditional.

I would also like to thank those in the Department of Chemistry, University of the Witwatersrand, who contributed in making this project a success through their assistance in the technical aspects of the project. I would mostly like to thank Thapelo for his assistance with the GC-MS and for his patience.

I would also like to thank my colleagues Pamela Khuzwayo and Tebogo Mokgehle for their invaluable assistance and all the fun times we shared.

Lastly, I would like to thank my supervisor, Dr Juanita van Wyk, for all the assistance.

Table of Contents

Declaration i

Abstract ii

List of schemes x

List of tables xi

Abbreviations xii

CHAPTER 1 1

LITERATURE REVIEW: TRANSFER HYDROGENATION PROCESS USING HOMOGENEOUS AND HETEROGENISED TRANSITION METAL CATALYSTS 1

1.1 Introduction 2

1.2 Transfer hydrogenation 4

1.2.1 The direct hydrogen transfer route 7

1.2.2 The hydridic route 8

1.2.3 Homogeneous transition metal catalysts for transfer hydrogenation 9

1.2.4 Heterogenized transition metal catalysts for transfer hydrogenation 15

1.2.4.1 Inorganic supports 16

1.2.4.2 Polymer supports 19

1.2.4.3 Biphasic system 21

1.3 Aim and objectives of this study 25

1.3 References 26

CHAPTER 2 29

SYNTHESIS AND CHARACTERISATION OF SALICYLALDIMINE LIGANDS AND THEIR RESPECTIVE COBALT AND RUTHENIUM COMPLEXES 29

2.1. Introduction 30

2.2 Experimental 31

2.2.1 Materials and instrumentation 31

2.2.2 General procedure for the synthesis of salicylaldimine ligands 32

2.2.3 General procedure for the synthesis of cobalt complexes Co1 - Co4 32

2.2.4 General procedure for the synthesis of ruthenium complexes Ru1 - Ru4 33

2.3 Results and discussion 33

2.3.1 Synthesis and characterisation of salicylaldimine ligands 33

2.3.1.1 ^{1}H-NMR spectroscopy studies of the salicylaldimine ligands 34

2.3.1.2 {^{1}H} ^{13}C-NMR studies of the salicylaldimine ligands 35

2.3.1.3 Infrared spectroscopy, elemental analysis and mass spectrometry studies of the ligands 35
2.3.2 Synthesis and characterisation of cobalt salicylaldiminato complexes 40
2.3.2.1 FTIR, mass spectrometry and elemental studies of the cobalt salicylaldiminato complexes 41
2.3.2.2 TGA studies of the cobalt salicylaldiminato complexes 43
2.3.3 Synthesis of ruthenium salicylaldiminato complexes 44
2.3.3.1 ^{1}H-NMR spectroscopy studies of the ruthenium salicylaldiminato complexes 45
2.3.3.2 {^{1}H} ^{13}C-NMR spectroscopy studies of ruthenium salicylaldiminato complexes 48
2.3.3.3 FTIR, mass spectrometry and elemental analysis studies of the ruthenium salicylaldiminato complexes 51
2.3.3.4 TGA studies of the ruthenium salicylaldiminato complexes 53
2.4 Conclusion 54
2.5 References 55
CHAPTER 3 57
CATALYTIC EVALUATION OF Co(II) AND Ru(II) SALICYLALDIMINATO COMPLEXES AS CATALYSTS IN TRANSFER HYDROGENATION OF ACETOPHENONE 57
3.1 Introduction 58
3.2 Experimental 61
3.2.1 Materials and instrumentation 61
3.2.2. General procedure for the transfer hydrogenation of acetophenone 62
3.2.3 The development of a biphasic system for the transfer hydrogenation of acetophenone 62
3.3 Results and discussion 63
3.3.1 Transfer hydrogenation of acetophenone using Ru(II) and Co(II) salicylaldimine complexes 63
3.3.2. Catalytic studies using an ionic liquid – organic system in the transfer hydrogenation of acetophenone 71
3.4 Conclusion 74
3.5 References 75
CHAPTER 4 76
Summary 76
Appendix 79

List of figures

Chapter 1

Figure 1.1: Structures of $[Rh((Ph_2P)_2NCH_2\text{-}C_4H_3S)_2]BF_4$ (**1**), $[Rh((Ph_2P)_2NCH_2\text{-}C_4H_3O)_2]BF_4$ (**2**), $[Rh((Ph_2P)_2N\text{-}C_6H_4\text{-}R\text{-}(cod)]BF_4$ (**3-4**) and $[Rh((Ph_2P)_2N\text{-}C_6H_4\text{-}R]BF_4$ (**5-6**) complexes used to convert acetophenone to 1-phenylethanol.

Figure 1.2: Chiral multidentate ligands (*R*) - **7** and (*R*) – **8**.

Figure 1.3: Structures of 2,6-Bis(4-substituted-5-thioxo-4,5-dihydro-1,2,4-triazol-3-yl)pyridines (**9a – 9d**), Mannich bases (**10a – 10d**) and $[C_{13}H_{19}N(OPR_2\text{-}Ru(\eta^6\text{-}p\text{-}cymene)Cl_2)_2]$ (**11 – 12**).

Figure 1.4: Iron pre-catalyst used in the transfer hydrogenation of acetophenone.

Figure 1.5: Structures of the (*R, R*)-TsDPEN ligand (**19**), the silica derivative of the (*R, R)*-TsDPEN ligand (**20**) and the silica supported ligand (**21**).

Figure 1.6: Structure of the chiral polymer supported (1,2-diamine monosulfonamide)-ruthenium complex.

Figure 1.7: Structures of the (a) POLYDMAP structure and (b) 4-DMAP structure.

Figure 1.8: Ruthenium catalysts applied in transfer hydrogenation in the presence of an ionic liquid.

Figure 1.9: Structures of (i) acetophenone derivatives converted to secondary alcohols and (ii) TsDPEN-coordinated Ru(II) catalysts **27.**

Chapter 2

Figure 2.1: General structure of (a) a salicylaldimine ligand and (b) a tetracoordinate metal complex derived from a salicylaldimine ligand.

Figure 2.2: Thermogram of the TGA results of the cobalt complexes **Co1 - Co4**.

Figure 2.3: ^{1}H-NMR spectra of (a) **L1** and (b) **Ru1** displaying the aromatic region and the chemical shift of **H**C=N for both compounds.

Figure 2.4: ^{1}H-NMR spectrum of the protons on the cymene ring in (a) the [(η^6-*p*-cymene)$RuCl_2$]$_2$ and (b) **Ru1** compounds.

Figure 2.5: {^{1}H} ^{13}C-NMR spectrum of the cymene ring carbon signals on (a) the **Ru1** complex and (b) the [(η^6-*p*-cymene)$RuCl_2$]$_2$ dimer.

Figure 2.6: Thermogram of the TGA data of the ruthenium complexes **Ru1 - Ru4**

Chapter 3

Figure 3.1: The (η^6-Arene) ruthenium (II) complex used for the transfer hydrogenation of acetophenone.

Figure 3.2: Representation of the [RuCl(PPh3)(DHAphen)] complex.

Figure 3.3: Cobalt complex that showed excellent catalytic activity in the hydrogenation of ketones, aldehydes, and imines with good yields**.**

Figure 3.4: The catalyst precursors (**Ru1 - Ru4** and **Co1 - Co4**) used in the conversion of acetophenone to 1-phenylethanol.

Figure 3.5: ^{1}H-NMR spectrum of (a) acetophenone and (b) 1-phenylethanol converted using catalyst precursor **Ru2**.

Figure 3.6: GC chromatogram of acetophenone.

Figure 3.7: GC chromatogram showing the elution of (a) 1-phenylethanol and (b) acetophenone.

Figure 3.8: Representation of **(A)** The mass spectrum of 1-phenylethanol (molar mass = 122) and **(B)** The mass spectrum of acetophenone (molar mass = 120).

Figure 3.9: The effect of time on the catalytic activity of complexes **Ru1 - Ru4** and **Co1 - Co4**.

Figure 3.10: The catalytic activity of the catalyst precursors when dissolved in the [BMIM]BF_4 ionic liquid.

List of schemes

Chapter 1

Scheme 1.1: General representation of the transfer hydrogenation reaction using 2-propanol as the hydrogen donor.

Scheme 1.2: The transfer hydrogenation process using formic acid/trimethylamine couple as a hydrogen donor.

Scheme 1.3: The MPV reduction as proposed for the direct transfer route.

Scheme 1.4: Catalytic cycle of the dihydridic route in transfer hydrogenation of ketones.

Scheme 1.5: Synthetic procedure for the immobilization of amino-alcohol ligands on silica.

Scheme 1.6: The synthesis of the ionic liquid **28**.

Chapter 2

Scheme 2.1: Synthesis of salicylaldimine ligands.

Scheme 2.2: Synthesis of Co(II) salicylaldiminato complexes.

Scheme 2.3: Synthesis of reduced Ru(II) salicylaldiminato complexes.

Scheme 2.4: Synthesis of reduced Ru(II) salicylaldimine complexes.

List of tables

Chapter 2

Table 2.1: ^{1}H-NMR chemical shifts δ (ppm) for the salicylaldimine ligands **L1 - L4**.

Table 2.2: {^{1}H} ^{13}C-NMR chemical shifts δ (ppm) for the salicylaldimine ligands **L1 - L4**.

Table 2.3: Elemental analysis, mass spectrometry and FTIR data for the salicylaldimine ligands **L1 - L4**.

Table 2.4: Elemental analysis, mass spectrometry and FTIR data for the cobalt complexes **Co1 - Co4**.

Table 2.5: ^{1}H-NMR chemical shift δ (ppm) for the ruthenium complexes **Ru1 - Ru4**.

Table 2.6: {^{1}H} ^{13}C-NMR chemical shift δ (ppm) for the [(η^{6}-*p*-cymene)$RuCl_2$]$_2$ and ruthenium complexes, **Ru1 - Ru4**.

Table 2.7: Elemental analysis, mass spectrometry and FTIR data for the ruthenium complexes **Ru1 - Ru4**.

Chapter 3

Table 3.1: The catalytic activity of the catalyst precursors in the transfer hydrogenation of acetophenone.

Table 3.2: Effect of temperature on the catalytic activity of complexes **Ru2** and **Co3**.

Table 3.3: The effect of the ionic liquid on the catalytic activity of **Ru1 - Ru4** and **Co3.**

Abbreviations

α	alpha
β	beta
bp	boiling point
br	broad
[BMIM]BF_4	1-butyl-3-methylimidazolium tetrafluoroborate
[BMIM]PF_6	1-butyl-3-methylimidazolium hexafluorophosphate
cod	1,4-cyclooctadiene
cy	Cymene
^oC	degree Celsius
d	doublet
dd	doublet of doublets
4-DMAP	4-(dimethylamino) pyridine
DMSO	dimethylsulfoxide
dppp	1,3-bis(diphenylphosphino)propane
η	eta
ESI-MS	electrospray ionization mass spectrometry
FT-IR	fourier transform infrared spectroscopy
GC-MS	gas chromatography – mass spectroscopy
GC	gas chromatography
hrs	hours
HCl	hydrochloric acid
pH	hydrogen ion concentration in solution
i-PrOH	isopropanol
i-Pr	isopropyl
L	ligand
µl	microlitre
min	minute
ml	millilitres
mmol	millimoles
m	multiplet
MCM-41	mobil composition of matter no. 41

Me	methyl
MeOH	methanol
$MgSO_4$	magnesium sulphate
MHz	megahertz
MPV	Meerwein-Ponndorf-Verley
MS	mass spectroscopy
TsDPEN	*N*-(*p*-toluenesulfonyl)-1,2-diphenylethylene diamine
NMR	nuclear magnetic resonance
KOH	potassium hydroxide
p	para
Ph	phenyl
ppm	parts per million
POLYDMAP	poly 4-(dimethylamino) pyridine
q	quartet
s	singlet
sec	second
Sal	salicylaldimine
SBA-15	Santa Barbara Amorphous no. 15
NaOAc	sodium acetate
NaOH	sodium hydroxide
t	triplet
td	triplet of doublets
t-Bu	tertiary-butyl
T	temperature
TEAF	formic acid/trimethylamine
TGA	thermogravimetric analysis
THF	tetrahydrofuran
cm^{-1}	wavenumber

CHAPTER 1

LITERATURE REVIEW: TRANSFER HYDROGENATION PROCESS USING HOMOGENEOUS AND HETEROGENISED TRANSITION METAL CATALYSTS

1.1 Introduction

Saving the environment and its resources is of vital importance because life is dependent on these. There are a number of factors that impact the environment negatively and among these is the chemical industry.[1] Wastes that are generated by the chemical industry are toxic and volatile and are thus harmful to the environment. The problem with wastes that are generated by the chemical industry can be solved by applying the principles of green chemistry. Green chemistry is also called sustainable chemistry and is defined as *'a philosophy of chemical research and engineering that promotes the designing of products and processes that reduce the use and generation of hazardous substances'*.[2] This initiative helps in pollution prevention and industrial ecology. By applying the principles of green chemistry, chemical industries can then have less impact on the environment.[3]

Current research that is being done to improve the sustainability and environmental impact of industrial processes includes the development of new catalysts.[1, 4] It is desired that the newly developed catalysts be environmentally friendly and exhibit better catalytic activity than the existing ones. Improved activity and selectivity of the catalysts are key factors in improving the quality of the products produced and reducing the quantity of by-products, which also reduces waste production. It is also desired that the newly developed catalysts be renewable so that they can be regenerated and reused with minimal or no loss in activity or properties.[1] Optimizing synthetic methods is of vital importance to synthetic chemists for economical and ecological reasons. The aim of optimizing synthetic methods is to maximize efficiency and minimize production costs. It is ideal for the synthetic procedure to produce 100% yield and to have good selectivity.[5]

Catalysts can be classified as homogeneous and heterogeneous depending on their interaction with the phase of reaction in which they are involved.[4] In a homogeneous process the

reactants, products, and catalyst are all in one phase whilst in a heterogeneous process the reactants and products are in one phase and the catalyst is in a different phase.[6] Industrially, heterogeneous processes are favoured because these systems allow easy separation of the catalyst from the products and reactants thus facilitating the recycling of the catalyst.[1] Major disadvantages of heterogeneous processes, however, are that the molecular interaction of the catalyst with the substrate(s) is not well understood and these processes usually require harsh reaction conditions such as high temperature and pressure.[6] Although homogeneous catalysts have disadvantages such as poor product/catalyst separation and poor thermal stability, they also have good advantages. These advantages include high activity and selectivity. In addition, the molecular structure of the catalyst is known, thus it can be fine-tuned for process optimization.[6] Homogeneous processes produce high yields and they are performed under mild reaction conditions. These are desirable properties for an economical synthetic route. Also, the steric and electronic properties of these catalysts can be tuned by varying the metal centre, ligand or both. However; despite their good properties, the application of homogeneous catalysts in industry is very limited. This is because of the difficulty in separating the products from the reaction mixture, the need for volatile organic solvents and the recovery of the catalysts are disadvantageous in these processes.[5] A convenient method of solving the problem of product/catalyst separation for homogeneous processes is the immobilization or anchoring of the catalysts on a support or in a solvent.[4]

Immobilization of homogeneous catalysts combines the benefits of homogeneous and heterogeneous systems. Researchers have investigated various methods of immobilizing homogeneous catalysts. Some of these methods include anchoring the catalyst on polymer supports,[4] zeolites,[7] inorganic supports[7] and biphasic systems.[4] Biphasic systems make use of two immiscible liquids where the catalyst is soluble in the one solvent and the reactants and products are soluble in a second solvent. This strategy has been successfully employed

commercially in the Ruhrchemie/Rhône-Poulenc hydroformylation process. In this process a water-soluble catalyst is used, which is retained in the aqueous phase, while reactants and products are retained in an organic solvent.[8]

Lately, there has been research focused on developing new methods which allow catalyst recovery and further having sustainable catalysts for organic transformations. One such example is hydrogenation reactions. These reactions are performed using H_2 gas which is disadvantageous because it is flammable and requiring harsh conditions.[9-10] Transfer hydrogenation, on the other hand, employs 2-propanol or formic acid as the hydrogen source, which are environmentally friendly, and it operates under mild reaction conditions. It is therefore regarded as a convenient method in large scale synthesis because it does not require high hydrogen pressure or the use of hazardous reducing agents.[10] The objective of this chapter, therefore, is to outline the work done in transfer hydrogenation over the years as published in literature and the common transition metals used as active catalysts in the transfer hydrogenation of carbonyl compounds and heterogenised transition metal catalysts that have been developed for transfer hydrogenation processes.

1.2 Transfer hydrogenation

Transfer hydrogenation can be defined as the reduction of unsaturated organic compounds with the aid of a hydrogen source such as an alcohol in the presence of a catalyst.[11] The transfer hydrogenation of carbonyl compounds to their respective alcohols is a fundamental molecular transformation. The asymmetric reduction of unsaturated compounds introduces new functionalities and stereogenic centres in the structure of organic compounds.[12-13] Transfer hydrogenation of ketones has been more extensively studied than aldehydes because aldehydes are more readily reduced than ketones in the transfer hydrogenation with 2-

propanol. However, reducing aldehydes to primary alcohols is considered difficult because the catalytic transfer hydrogenation of aldehydes leads to side reactions which occur under basic conditions and thus the catalytic transfer hydrogenation of aldehydes is occasionally studied. On the other hand, the transfer hydrogenation of ketones using 2-propanol as the hydrogen source results in an acetone by-product being formed (Scheme 1.1.); which is readily removed.[12, 14]

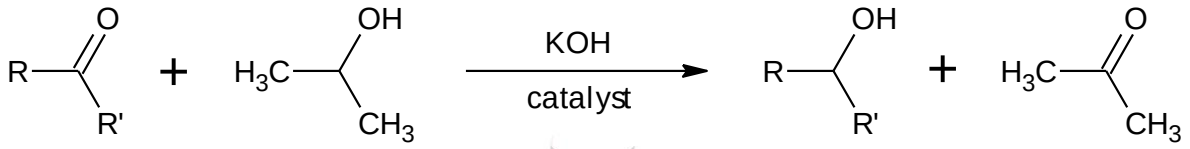

R = alkyl or aromatic group

R' = alkyl or aromatic group

Scheme 1.1: General representation of the transfer hydrogenation reaction using 2-propanol as the hydrogen donor.

The transfer hydrogenation process requires a source of hydrogen in order to reduce carbonyl compounds. Such sources include 2-propanol, formic acid, dihydropyrirdine,[15] HCO_2Na.[16] The most common used hydrogen sources, however, are 2-propanol and formic acid.

2-Propanol is used as a hydrogen source because it has favourable properties such as stability, non-toxicity, environmentally friendly, easy to handle (bp = 82 ^oC), inexpensive and the ability to dissolve many organic compounds. 2-Propanol is oxidized to acetone during the reaction as depicted in Scheme 1.1.[12, 17] The reduction of ketones by 2-propanol is a reversible process where the equilibrium is regulated by the oxidation potentials of the relevant carbinol/ketone couples and this reversibility is what prevents complete

conversion.[12] When 2-propanol is used as the hydrogen donor, a base is required to activate the starting complex to catalysis. Sodium or potassium carbonates, hydroxides or alkoxides have been employed for this purpose at various concentrations.[12]

Another common hydrogen donor for transfer hydrogenation is formic acid/trimethylamine (TEAF) which has been shown to be a better hydrogen donor than 2-propanol. This is due to the evolution of CO_2 as shown in Scheme 1.2 which is generated in an open system and it is also inexpensive.[12-13] TEAF also has a range of advantages such as its solubility with many solvents at 20 – 60 ^{o}C. It allows high substrate concentrations and it also results in high conversions in favouring the forward reaction. The use of TEAF, however, has some restrictions. The major disadvantage is that most of the complexes easily decompose in formic acid while some completely lose their catalytic activity. This was accounted to the fact that the acid inhibits one of the steps of the activation process that is promoted by the base.[13] Transfer hydrogenation can occur according to two mechanisms, i.e. direct hydrogen transfer or the hydridic route. The hydridic route is promoted by transition metals while the direct hydrogen transfer route is usually promoted by non-transition metals.[13]

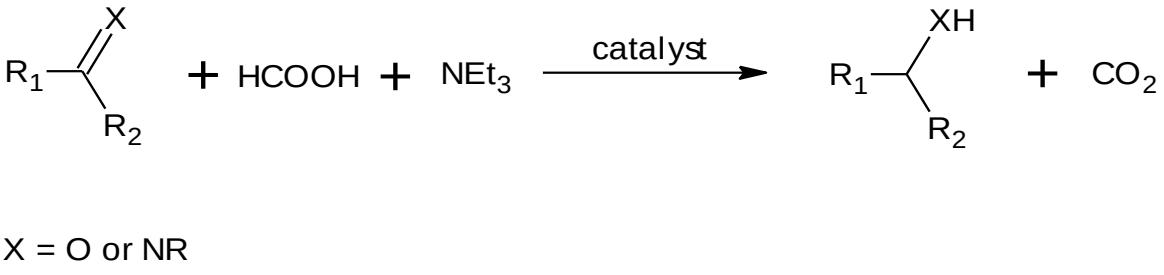

Scheme 1.2: The transfer hydrogenation process using formic acid/trimethylamine couple as a hydrogen donor.

1.2.1 The direct hydrogen transfer route

The mechanism of the direct transfer route was proposed by Meerwein-Ponndorf-Verley and is commonly referred to as the MPV reduction. Originally, in the MPV reduction aluminium isopropoxide was used as the promoter for the transfer of hydrogen from isopropanol to the ketone. This mechanism does not require metal hydride intermediates.[18] The direct hydrogen transfer route proceeds via a complex wherein both the donor and the acceptor are bound to the metal and are held in close proximity as shown in Scheme 1.3. Once the substrate coordinates to the metal, it is activated towards the nucleophilic attack of the hydride. The metal provides the reactants with the correct orientation for the transfer of the hydride to be feasible.

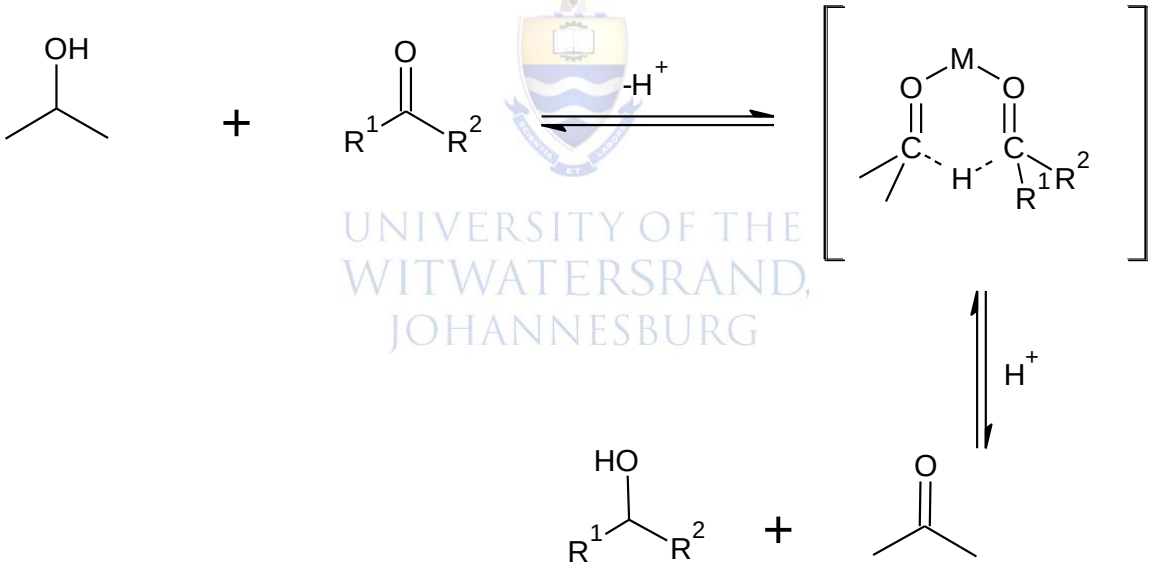

Scheme 1.3: The MPV reduction as proposed for the direct transfer route.[18]

In the MPV reduction the carbonyl oxygen of the substrate and the oxygen of the alcohol are coordinated to the metal to afford the tetra-coordinated intermediate. The hydride is then transferred to the carbonyl via a pericyclic mechanism to afford the new alcohol and the new carbonyl.[19]

1.2.2 The hydridic route

The hydridic route involves the interaction of the catalyst with the hydrogen donor to form a metal hydride, which is then followed by transfer of the hydride from the metal hydride to the substrate. Therefore, the donor and the acceptor interact with the metal at different stages of the reaction.[13, 20] The hydridic route can further be divided into a dihydridic or a monohydridic route. In the dihydridic route (Scheme 1.4), the C-H and O-H from the hydrogen donor lose their identity when they are transferred to the ketone because they are scrambled between the carbon and the oxygen. The reason for their loss in identity has been explained to be due to the fact that these hydrogens become equivalent once they have been transferred to the metal to give the dihydride. In the monohydridic route, however, the C-H from the hydrogen donor still remains as the C-H in the product. The C-H hydrogen on the donor forms the hydride on the metal and then transfers to the carbonyl carbon of the substrate while the O-H from the donor adds to the carbonyl oxygen of the ketone substrate.[13, 18, 21]

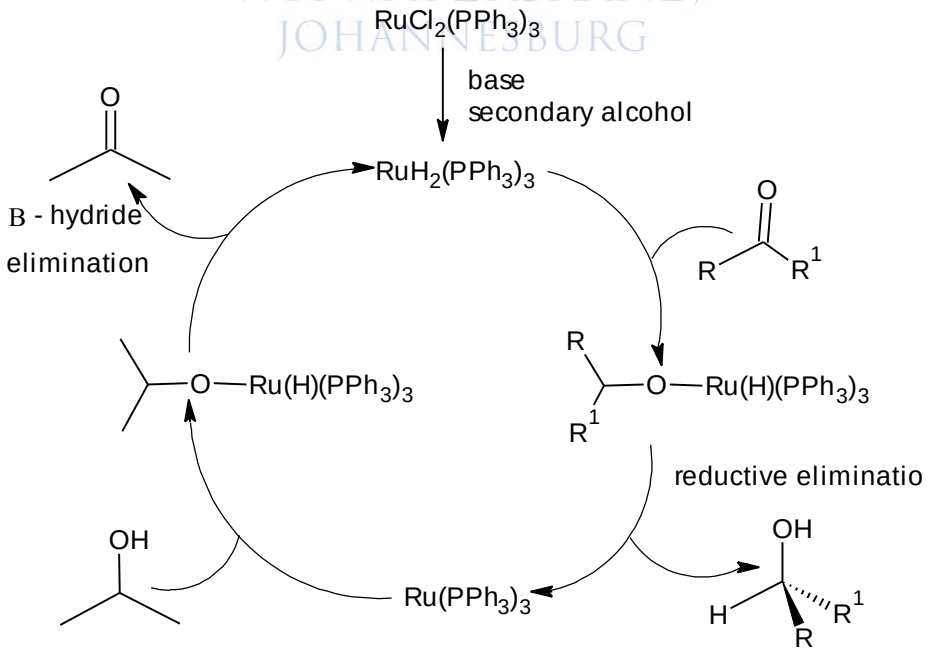

Scheme 1.4: Catalytic cycle of the dihydridic route in transfer hydrogenation of ketones.[13]

In the dihydridic route, the two hydrogens from the alcohol are transferred to the metal to give the dihydride complex. The carbonyl is then coordinated to the metal dihydride species via π-coordination and one hydride is inserted to the carbonyl carbon to afford a C-H bond. The remaining hydride is inserted to the carbonyl oxygen to give an O-H bond and the product is released through reductive elimination. Coordination of the alcohol to the metal results in a metal hydride and the metal dihydride is regenerated by β-hydride elimination.[21]

1.2.3 Homogeneous transition metal catalysts for transfer hydrogenation

The transfer hydrogenation process is a widely studied metal catalysed homogeneous process.[22] The transition metals that have been applied in this process include rhodium, ruthenium, iridium and some lanthanoid complexes.[23-25] This section highlights the application of these transition metals in the transfer hydrogenation of carbonyl compounds.

As reported by Malacea and co-workers dichlorobis(1,4-cyclooctadiene)diiridium, ($[Ir(COD)Cl]_2$, has been used as a pre-catalyst in the transfer hydrogenation of various ketones using 2-propanol as the hydrogen source in the presence of a variety of ligands. It was noted that the nature and structure of the chiral ligands had a significant effect on the activity and selectivity of the Ir(I) systems.[26] Sakaguchi and co-workers reported on the activity of $[Ir(cod)Cl]_2$/phosphine/Cs_2CO_3 system for the reduction of α,β-unsaturated carbonyl compounds in the presence of 2-propanol as the hydrogen source. In the case of an α,β-unsaturated ketone, it was noted that the iridium catalysts preferred to coordinate to the double bond than the carbonyl group.[27] The $[Ir(cod)Cl]_2$/dppp/Cs_2CO_3 (dppp = 1,3-bis(diphenylphosphino)propane) combined system was reported to have accomplished the chemoselective transfer hydrogenation of unsaturated carbonyl compounds to saturated compounds. In a 1:1 reaction containing a mixture of a conjugated enone and a saturated

ketone using $[Ir(cod)Cl]_2$/dppp/Cs_2CO_3 as the catalyst, the reduction of the α,β-unsaturated ketone was preferred over the saturated ketone.[27] Although there is still room for improvement, it has been concluded that iridium catalyst systems are efficient in terms of activity and enantioselectivity in the transfer hydrogenation of ketones.[26]

Rhodium catalysts have also been applied in the transfer hydrogenation of acetophenone. At room temperature and in the absence of base, no formation of 1-phenylethanol could be traced. However, at 82 ^{o}C and in the presence of base, conversion of >95 % was observed for the rhodium catalysts. Aydemir and co-workers reported on the activity of six synthesized rhodium catalytic systems (**1 - 6**) shown in Figure 1.1 that displayed high conversions. Optimization studies indicated that excellent conversions were obtained in reducing acetophenone to 1-phenylethanol when the substrate-catalyst ratio was 100:1 in 2-propanol at 82 ^{o}C. It was also noted that the activity of the catalyst increased with an increase in the bulkiness of the ligand.[28] Chiral rhodium complexes, i.e. Cp*RhCl[(*R*,*R*)-Tsdpen], were reported by Ikariya and Blacker to be highly reactive in the reduction of a variety of ring substituted α-chloroacetophenones. Using TEAF as the hydrogen source, the mixture with the rhodium catalyst proceeds the corresponding chiral alcohol with 96 % ee.[25]

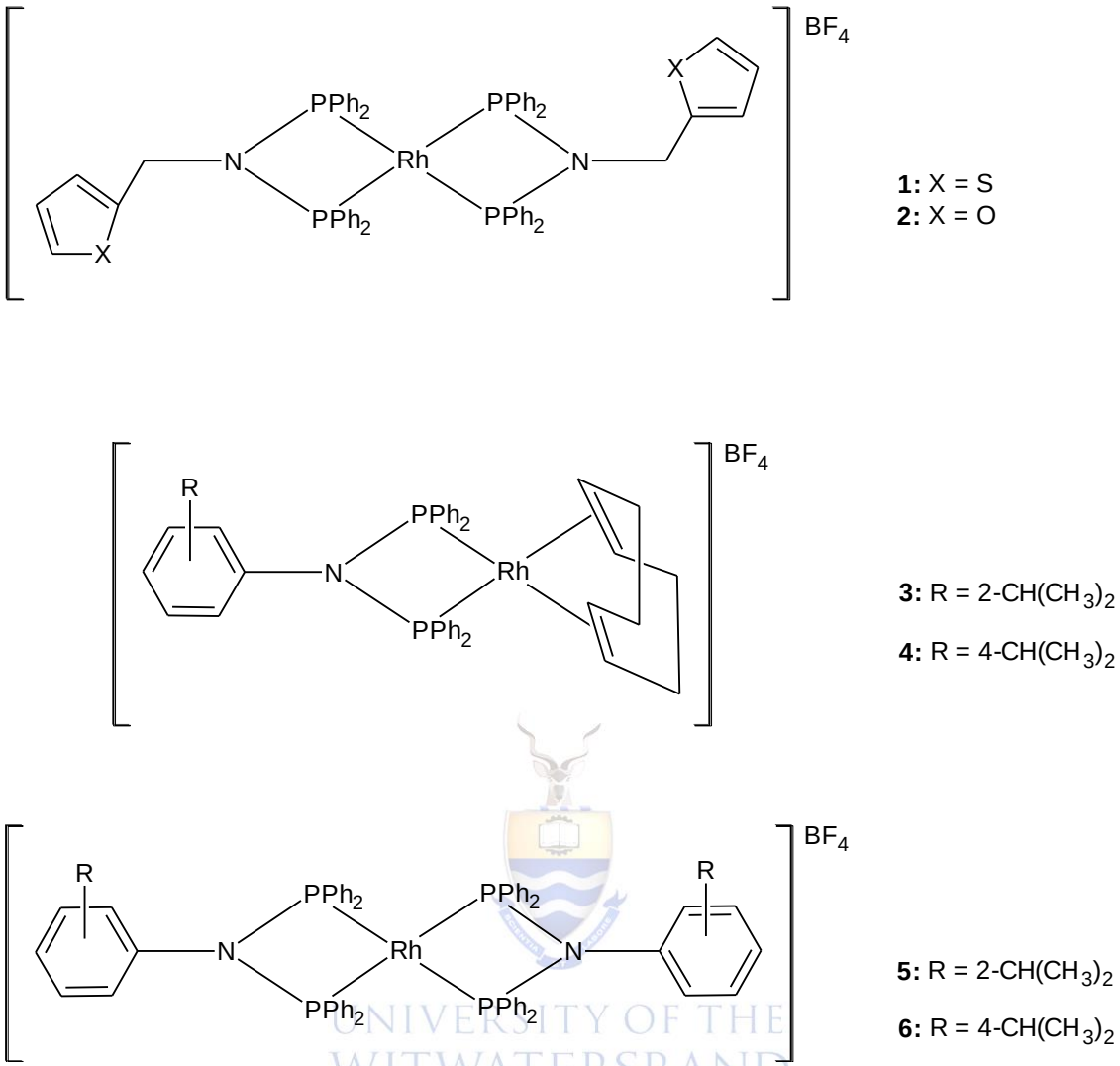

Figure 1.1: Structures of $[Rh((Ph_2P)_2NCH_2\text{-}C_4H_3S)_2]BF_4$ (**1**), $[Rh((Ph_2P)_2NCH_2\text{-}C_4H_3O)_2]BF_4$ (**2**), $[Rh((Ph_2P)_2N\text{-}C_6H_4\text{-}R\text{-}(cod)]BF_4$ (**3-4**) and $[Rh((Ph_2P)_2N\text{-}C_6H_4\text{-}R]BF_4$ (**5-6**) complexes used to convert acetophenone to 1-phenylethanol.[28]

Trivalent samarium compounds with bidentate and tridentate chiral ligands have been utilised in the transfer hydrogenation of ketones. Evans *et al* reported samarium species generated in situ by treating a dilithio salt of (*R*)-**7** (Figure 1.2) with SmI_3 mediated the reduction of aryl ketones.[29] Ohno and co-workers reported that the enantioselectivity and the catalytic activity of the samarium species were sensitive to the purity of *n*-BuLi. It was also pointed out that the presence or absence of the salt is responsible for the catalytic activity of the lanthanoid compounds. Ohno and co-workers further anticipated that salt-free dinuclear compounds of

samarium with the chiral multidentate ligand (*R*)-**8** (Figure 1.2) could display good catalytic activity for the transfer hydrogenation of aryl ketones. Salt-free samarium complex has also been applied in the transfer hydrogenation of acetophenone to obtain (*R*)-1-phenylethanol with 95 % enantioselectivity but with low conversion. It was also noted that the catalytic activity and enantioselectivity is also sensitive to the substituents of acetophenone. For halogenated acetophenone derivatives, the *ortho*-substituted derivatives were more readily reduced than the *meta*- and *para*-substituted derivatives with high enantioselectivities.[30] With the application of lanthanoid catalyst systems, the enantioselectivity decreased with increasing atomic radii in the order La ≈ Ce < Nd < Pr << Sm.[30]

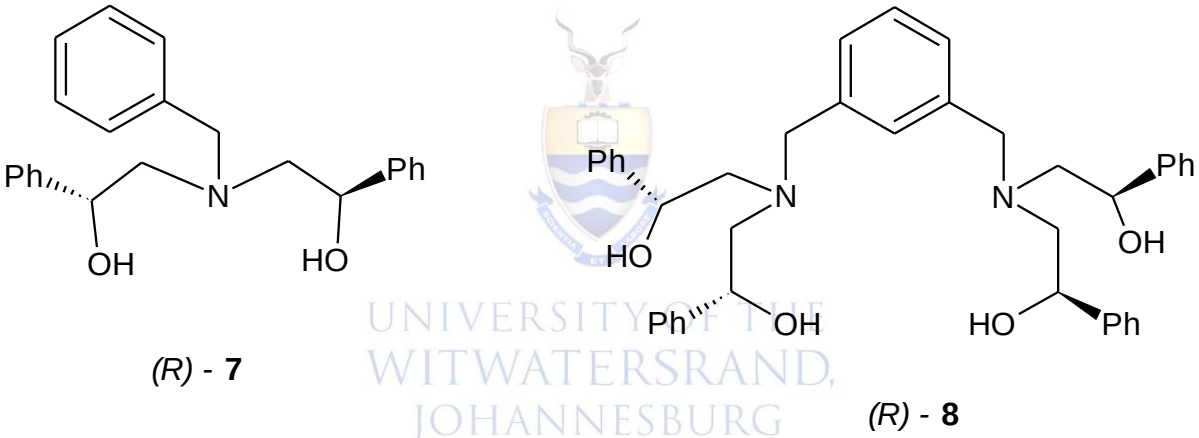

(R) - **7** *(R)* - **8**

Figure 1.2: Chiral multidentate ligands (*R*) - **7** and (*R*) – **8**. [30]

Ruthenium (II) complexes are the most used catalysts for transfer hydrogenation of ketones. Ahmet and Osman reported on the application of ruthenium (II) complexes that bear pyridine-bridged triamine ligands as highly efficient transfer hydrogenation catalysts. They also reported on *in situ* generated catalytic systems of 2,6-bis-(5-thioxo-4,5-dihydro-1,2,4-triazole-3-yl)pyridines and Ru(II) salts and they were found to be active in transfer hydrogenation yielding secondary alcohols with good conversions. It was noted that the catalytic activity decreased upon the introduction of bulky groups in the triazole fragment of the ligand due to steric effect (**9(a - d)** - **10(a - d)**) (Figure 1.3).[31] Furthermore, Aydemir and

co-workers reported on the activity of ruthenium (II)-arene complexes with functionalised phosphinites in the catalytic transfer hydrogenation (**11** and **12** in Figure 1.3). These catalysts reduced acetophenone to the corresponding ((*R*), (*S*)-1-phenylethanol) in the presence of NaOH as the promoter. These catalysts displayed low conversion at room temperatures but upon increasing the temperature to 50 ^{o}C, high conversion and good enantioselectivity were observed.[24]

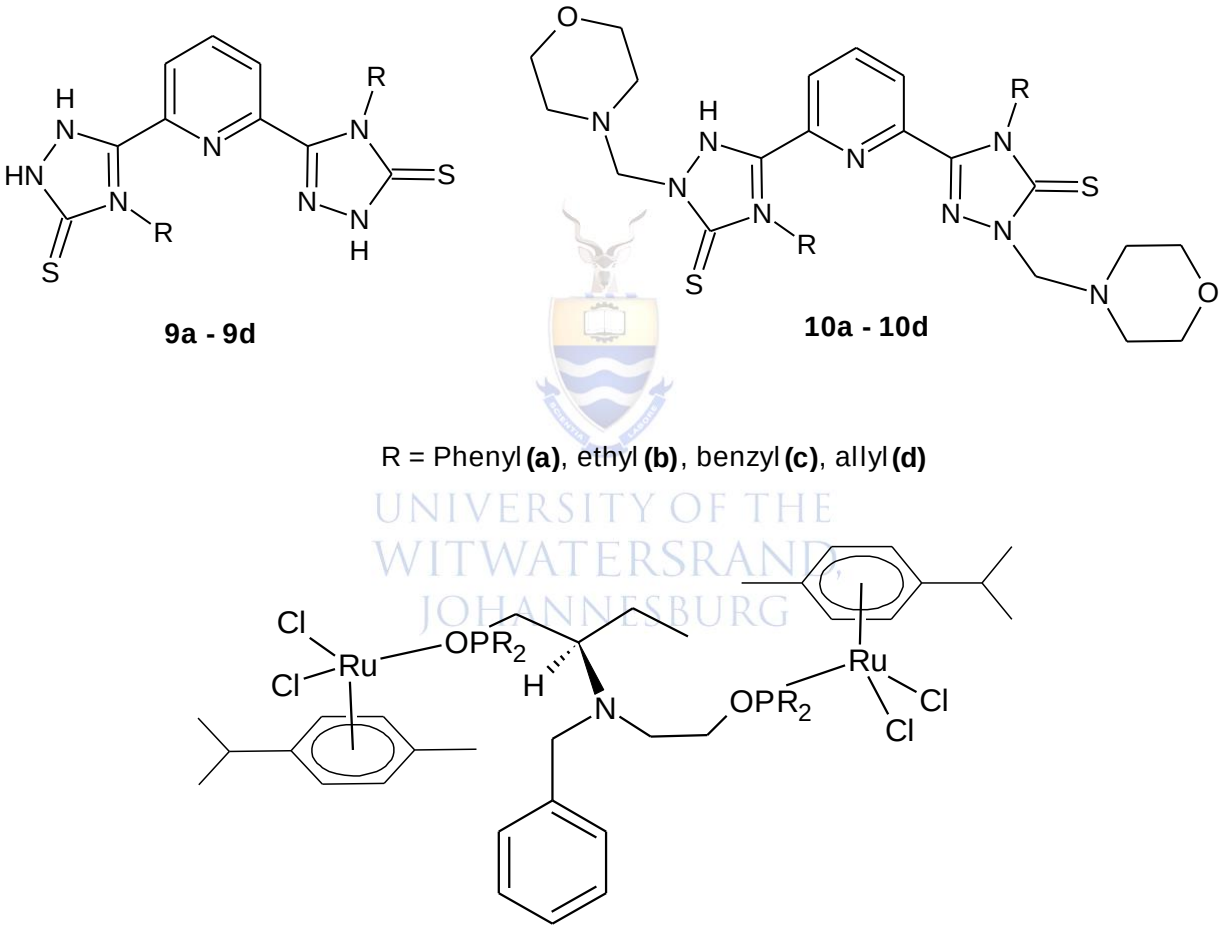

Figure 1.3: Structures of 2,6-Bis(4-substituted-5-thioxo-4,5-dihydro-1,2,4-triazol-3-yl)pyridines (**9a – 9d**), Mannich bases (**10a – 10d**) and [$C_{13}H_{19}N$(OPR_2-Ru(η^6-*p*-cymene)Cl_2)$_2$] (**11 – 12**).[24]

Apart from the metals mentioned above, iron has also been applied in the transfer hydrogenation of ketones. The advantages of using iron complexes in place of the platinum group metals in organic transformations are that they have low toxicity, low cost and are highly abundant. The iron complexes in Figure 1.4 that contain Cy and *i*Pr substituents (**13-16**) were deemed inactive while those containing ethyl substituents (**17** and **18**) were deemed active in the catalytic transfer hydrogenation of acetophenone. Complex **18**, however, was observed to have a higher activity than complex **17** because of the Ph substituents on the NN-linker backbone. Complexes **13 - 16** were inactive because there was too much steric bulk at the phosphorus donor atoms of the ligand. Although complex **18** had good activity, the enantioselectivity was poor. Lagaditis and co-workers concluded that the reason for this observation was because there is a degree of steric bulk that is required.[32] Morris and co-workers reported on the activity of the dihydrogen complex cis-$[FeH(H_2)\{P(CH_2CH_2PPh_2)_3\}]BPh_4$. This complex catalysed the transfer of hydrogen from cyclopentanol to benzylideneacetone and had good selectivity. This complex was also reported to have reduced 3-methyl-2-cyclohexenone to the unsaturated alcohol with 31 % conversion while it also reduced 72 % of 2-cyclohexanone to a mixture of the saturated and unsaturated alcohol. However, some of the α,β-unsaturated ketones were reduced at the C=C double bond which resulted in a saturated ketone as the product while other α,β-unsaturated ketones were not reduced at all. The iron complexes were shown to be attractive in transfer hydrogenation because of their low cost and low toxicity.[33]

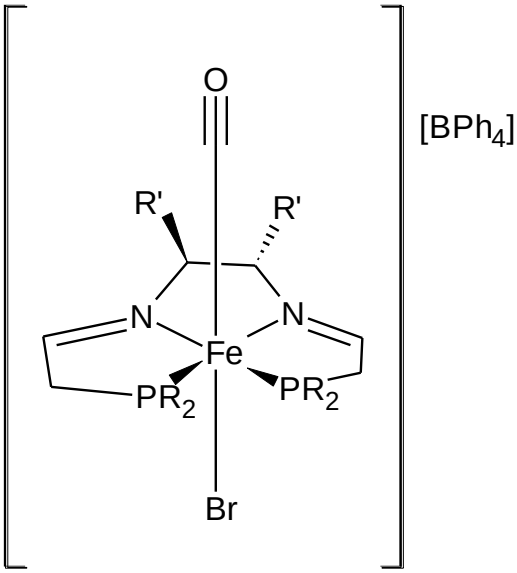

13: R = Cy; R' = H (*S,S*)**-14:** R = Cy; R' = Ph

15: R = *i*Pr; R' = H (S,S)**-16:** R = *i*Pr; R' = Ph

17: R = Et; R' = H (S,S)**-18:** R = Et; R' = Ph

Figure 1.4: Iron pre-catalyst used in the transfer hydrogenation of acetophenone.[32]

1.2.4 Heterogenized transition metal catalysts for transfer hydrogenation

Transfer hydrogenation is one method that can be accomplished with homogeneous and heterogenized catalysts.[34] Studies concerning the immobilization of transition metal ion complexes on solid supports have been reported. It has been reported that the activity of the catalysts is dependent on the type of support; such as alumina, silica-alumina, and cation exchange resins. Supporting a metal complex may alter the property of the complex in a way that is beneficial for it.[35] There are a number of ways to immobilize metal complexes, i.e. the use of inorganic supports, polymer supports, and biphasic systems.[35-36] Immobilizing the chiral catalyst onto a solid support often affords good recyclability, but the enantio-selectivity is usually lower than in the homogeneous or biphasic cases.[37]

1.2.4.1 Inorganic supports

Catalysts immobilised onto silica inorganic supports possess good advantages since they do not swell or dissolve in organic solvents and they also exhibit thermal and mechanical stability under the catalytic conditions.[38-39] The application of silica as supports for the immobilization of homogeneous catalyst systems has been reported in literature. Sandee *et al* reported silica as a valuable support for transfer hydrogenation using ruthenium catalysts. When these catalysts were immobilized on a silica support they were observed to be slightly more active than the homogeneous analogues. This can be attributed to the physical and chemical properties of the support.[38]

A NH-3-(trimethoxysilyl)benzyl-(1*R*, 2*S*)-norephedrine ligand was immobilized on silica (Scheme 1.5) and this silica loaded ligand was reacted with the (*p*-cymene)-ruthenium(II) chloride dimer ($RuCl_2(\eta^6$-*p*-cymene)). The ruthenium complex of the NH-3-(trimethoxysilyl)benzyl-(1*R*, 2*S*)-norephedrine ligand immobilized on silica displayed good results in the transfer hydrogenation of acetophenone.[38] This catalyst obtained a conversion of 20 % after an hour, which is two to three times faster than the homogeneous analogue. It was also noted that initially the rate was not completely dependent on the concentration of the substrate but at higher conversions, however, the rate was dependent on the concentration of the substrate. This observation was also noted for the homogeneous analogues. The effect of the inorganic support was investigated by performing a blank reaction i.e. a reaction in the absence of the ligand. When silica and $RuCl_2(\eta^6$-*p*-cymene) were mixed in the absence of the ligand, it was observed that the precursor adsorbs onto the silica and this was concluded by observing the change in colour. However, the reactivity of the Ru(II) species was negligible (0.2 % conversion). It was hence concluded that immobilization is not effective without the ligand.[38]

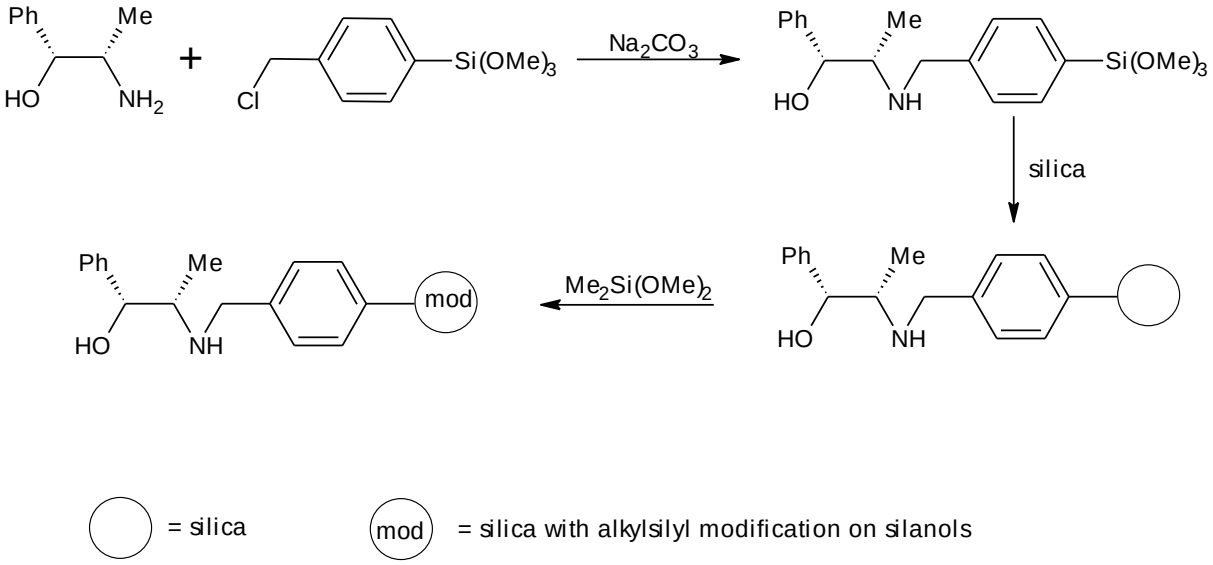

Scheme 1.5: Synthetic procedure for the immobilization of amino-alcohol ligands on silica.[38]

In efforts to develop practical, efficient and highly recyclable catalytic systems, novel heterogenized ruthenium catalysts have been designed and synthesised by grafting a chiral TsDPEN derivative onto the surface of an amorphous silica gel and mesoporous silicas of MCM-41 and SBA-15 and they provided successful application for the asymmetric transfer hydrogenation of a series of ketones.[39]

The synthesized ligands (Figure 1.5) were anchored onto amorphous silica gel and mesoporous silicas of MCM-41 and SBA-15. The heterogenized ruthenium complexes were afforded by reacting the supported ligands with $[RuCl_2(p\text{-cymene})]_2$ in situ. Ru-**21** (the complex of ruthenium and ligand **21**, Figure 1.5) showed excellent catalytic activity (>99 % yield after 6 h) and excellent enantioselectivity (97 % ee). These results were not different from the ruthenium catalysts of ligands **19** and **20** (Figure 1.5). The immobilized catalysts were shown to be recovered by centrifugation and still maintained high enantioselectivity after the fifth use with minimal loss in activity. The loss in activity after five runs was accounted to the leaching of the Ru metal. Upon reducing the temperature, the enantioselectivity was increased to 98 % but the catalytic activity decreased to <99 % after 9

h while for the homogeneous catalyst a reaction time of 20 h was needed. However, upon increasing the temperature, the catalytic activity increased and the enantioselectivity decreased. A series of ketones were also chosen for the transfer hydrogenation using Ru-**21** under optimum conditions, i.e. 40 ^{o}C and s/c = 100:1. It was shown that Ru-**21** gave high catalytic activity and good enantioselectivities for all the ketones when compared to the homogeneous catalyst.[39]

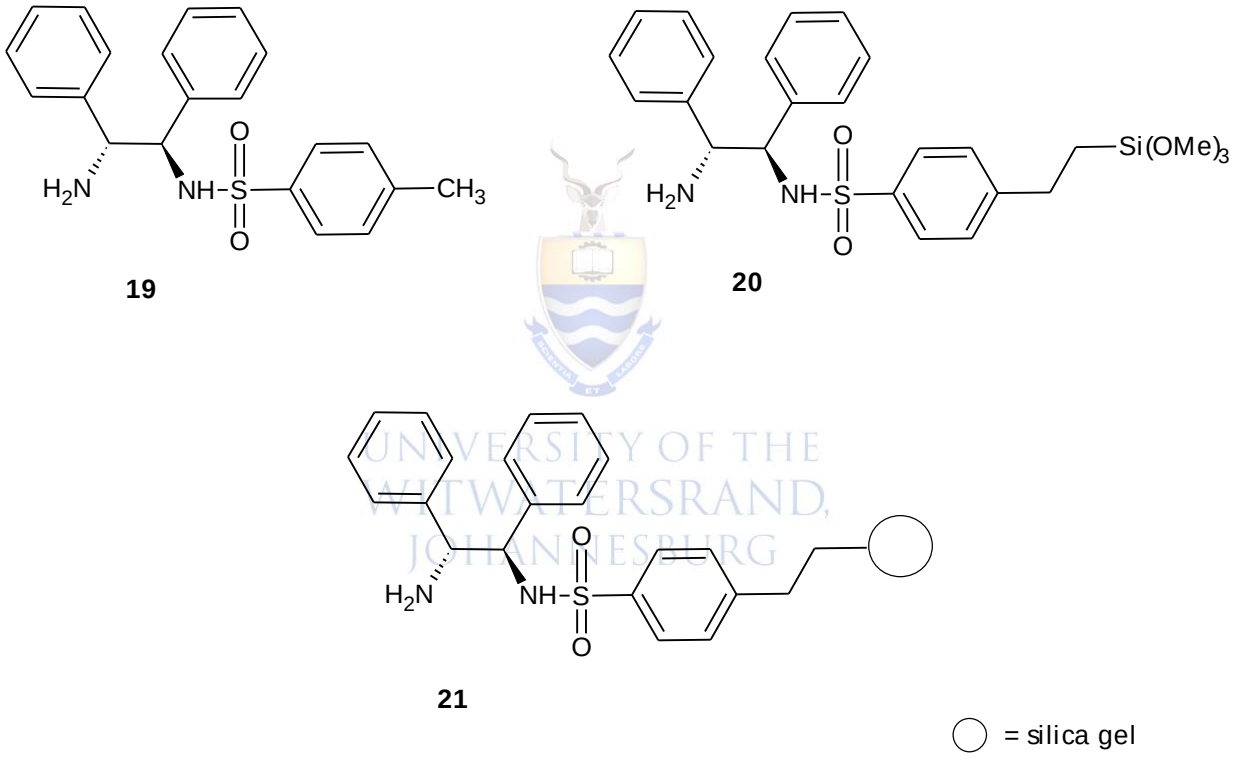

Figure 1.5: Structures of the (*R, R*)-TsDPEN ligand (**19**), the silica derivative of the (*R, R)*-TsDPEN ligand (**20**) and the silica supported ligand (**21**).[39]

1.2.4.2 Polymer supports

The use and relevance of polymers have evolved over the past half century. They have found use as supports in catalysis.[40-41] A hydrophilic polymer-supported N-toluenesulfonyl-1,2-diphenylethylenediamine (TsDPEN) ruthenium catalyst has been used as a successful method for asymmetric transfer hydrogenation of imines as reported by Haraguchi and co-workers.[42] Kann incorporated a pendant quaternary ammonium sulfate group onto the polymer backbone which rendered the polymer hydrophilic and applied the catalyst in the transfer hydrogenation of acetophenone in water. It was noted that using highly cross-linked polymers as the catalyst support afforded product in high yield.[42] A ruthenium (II) complex was anchored to a polymer-bound ligand (Figure 1.6) and applied in the reaction of both aromatic and aliphatic epoxides and gave essentially complete conversion. The polymer-supported catalyst can be recycled up to ten times with no loss of catalytic activity.[42]

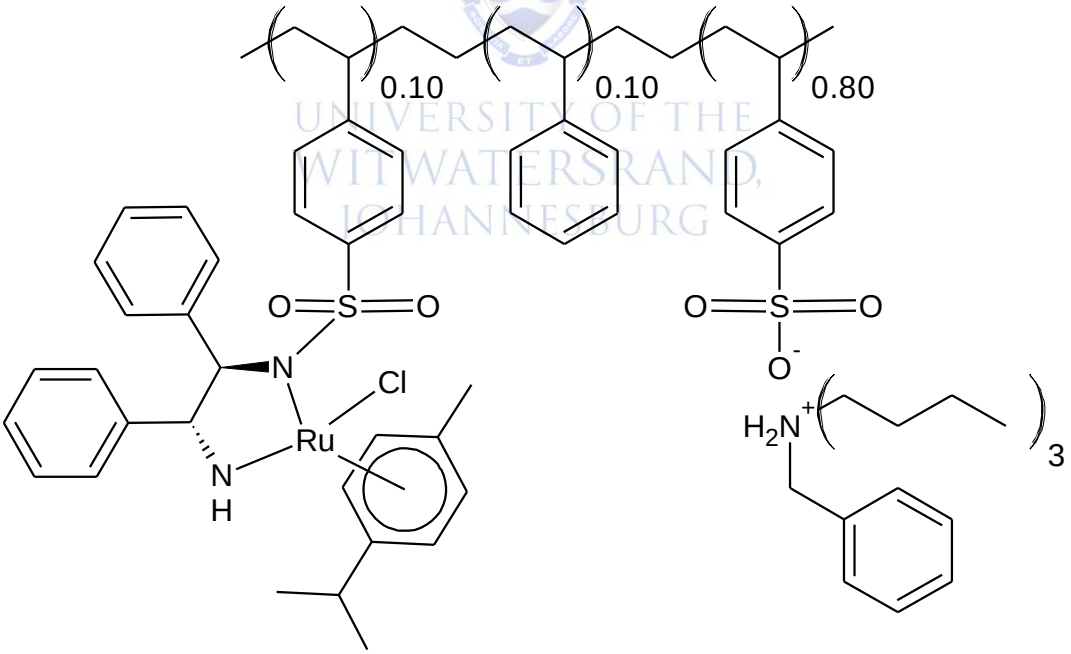

Figure 1.6: Structure of the chiral polymer supported (1,2-diamine monosulfonamide)-ruthenium complex.[42]

The catalyst system consisting of $Rh_6(CO)_{16}$ and amines (Rh-amine catalyst system) has also been heterogenized to form a polymer-bound Rh-cluster complex that displayed good performance of recoverable and reusable catalysts. Mizugaki and co-workers reported the Rh-amine catalyst system that could be heterogenized with POLYDMAP (Figure 1.7 (a)) as an aminated polystyrene support. This heterogenized catalyst could be recycled without loss of high activities and selectivities in the transfer hydrogenation of α,β-unsaturated aldehydes. Making use of a polymer-bound metal complex as a catalyst simplifies the process of purification of products.[43] The Rh-amine catalyst was heterogenized by using POLYDMAP as the polymer support instead of 4-DMAP (4-(dimethylamino)pyridino) (Figure 1.7 (b)) as in the homogeneous case (POLYDMAP has a 4-DMAP moiety on the para-position of the styrene unit in the cross-linked polystyrene support).[43]

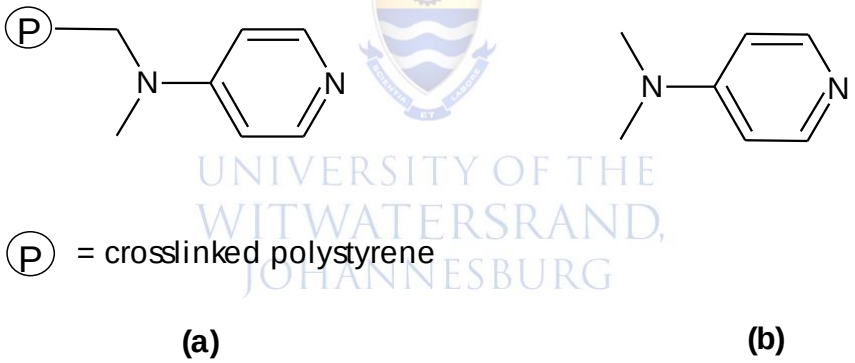

Figure 1.7: Structures of the (a) POLYDMAP structure and (b) 4-DMAP structure.[43]

In the homogeneous transfer hydrogenation, in order to obtain unsaturated alcohols in good yields, a large amount of 4-DMAP had to be used while for the heterogeneous transfer hydrogenation; only a small amount of POLYDMAP was used and produced good yields. For example, a low conversion of cinnamaldehyde was observed in the homogeneous case than in the heterogeneous case. The heterogenized rhodium catalysts can simply be separated from the reaction mixture by filtration. The polymer-bound Rh catalysts were recycled and still maintained good chemoselectivity even after the fourth cycle.[43]

1.2.4.3 Biphasic system

Attempts have been made in developing biphasic processes for the homogeneous transfer hydrogenation catalysed by transition metal complexes. Geldbach *et al* studied ruthenium complexes (Figure 1.8) for the transfer hydrogenation of acetophenone in the absence and presence of an ionic liquid. Catalysts **24** and **25** were found to have been less active than their analogous **22** and **23** when tested in the presence of 2-propanol with 5 mol % KOH and in the absence of an ionic liquid. The 1-butyl-2,3-dimethylimidazolium hexafluorophosphate ionic liquid was introduced with the aim of immobilizing the catalysts and because it also forms a separate phase with 2-propanol and is also stable towards the base. At the start of the reaction, catalysts **24** and **25** were found to be in the ionic liquid phase but as the reaction progressed, leaching occurred and this was accounted to base-induced catalyst degradation. Reducing the amount of base to two equivalents reduced catalyst loss, i.e. from 22 % to 5 %. Catalysts **22** and **23**, however, were found to be present in both phases; even at the beginning of the reaction. Catalyst loss for **22** and **23** is significantly higher than **24** and **25** which demonstrates the positive effect of the imidazolium tag. Geldbach *et al* also noticed that catalyst **24** deactivated quickly and thus the ionic liquid phase could not be re-used while catalyst **25** was stable for up to 72 hours and thus making ionic liquid recycling feasible. However, conversion drops from 80 % to 21 % in the fourth cycle.[37]

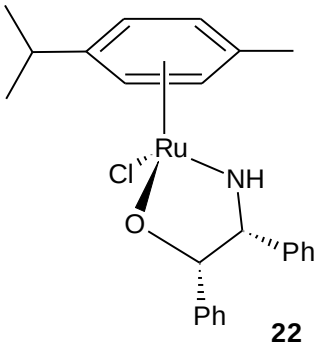

22

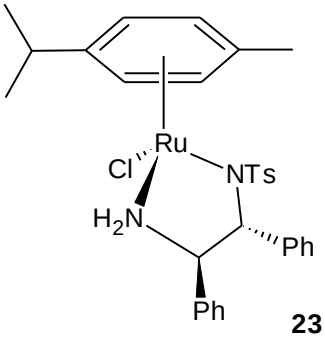

23

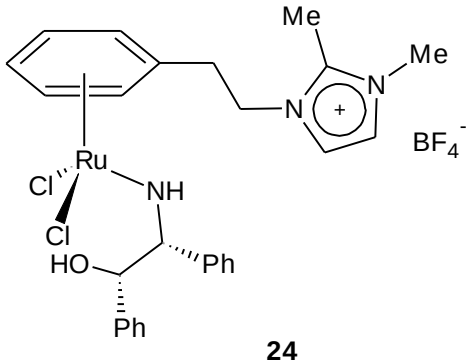

24

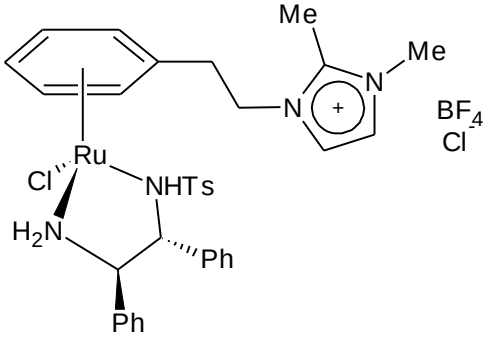

25

Figure 1.8: Ruthenium catalysts applied in transfer hydrogenation in the presence of an ionic liquid.[37]

Two TsDPEN-coordinated Ru (II) complexes were applied in the transfer hydrogenation of ketones in ionic liquids and they were reported to be some of the most effective catalysts that were developed by Noyori, Ikariya and co-workers. The asymmetric transfer hydrogenation of ketone **26** (Figure 1.9 (i)) in the presence of the two catalysts in the [bmim]PF_6 and the [bmim]BF_4 ionic liquids was performed. The ionic liquids were used because of their attractive properties such as the ability to stabilize a variety of transition metal catalysts and they allow for recycling of the catalysts. Catalyst **27** in the [bmim]PF_6 gave 96 % conversion and was also effective in the reduction of other acetophenone derivatives **26a-e** (Figure 1.9 (i)) with conversions >75 %.[44]

(i)

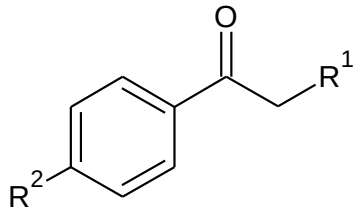

26

a: $R^1 = R^2 = H$

b: $R^1 = H$; $R^2 = CF_3$

c: $R^1 = H$; $R^2 = Me$

d: $R^1 = H$; $R^2 = OMe$

e: $R^1 = Me$; $R^2 = H$

(ii)

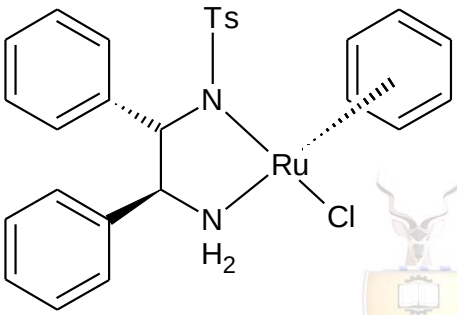

27

Figure 1.9: Structures of (i) acetophenone derivatives converted to secondary alcohols and (ii) TsDPEN-coordinated Ru(II) catalysts **27**.[44]

An imidazolium salt was then attached to the TsDPEN unit in order to investigate the reactivity of **27** (Figure 1.9 (ii)) in the recyclable transfer hydrogenation of ketones with a formic acid-triethylamine azeotropic mixture as the hydrogen source. The design of the ionic liquid **28** is shown in Scheme 1.6. The recyclability of acetophenone **26a** was tested with **27** and **28** in the presence of $[RuCl_2(benzene)]_2$ (**28**-*Ru*) in [bmim]PF_6 and they both gave good conversions. Catalyst **27** showed good conversion and enantioselectivity to the third cycle but the activity decreased from the fourth cycle while the ionic catalyst **28**-*Ru* showed better results than catalyst **27**. The reason for this is accounted to the immobilization of the imidazolium moiety in the ionic liquid phase. Both catalysts were found to be soluble in the

ionic liquid and they were easily recovered after extracting 1-phenylethanol by adding *n*-hexane and the ionic liquid phase was recycled and reused for the next reaction.[44]

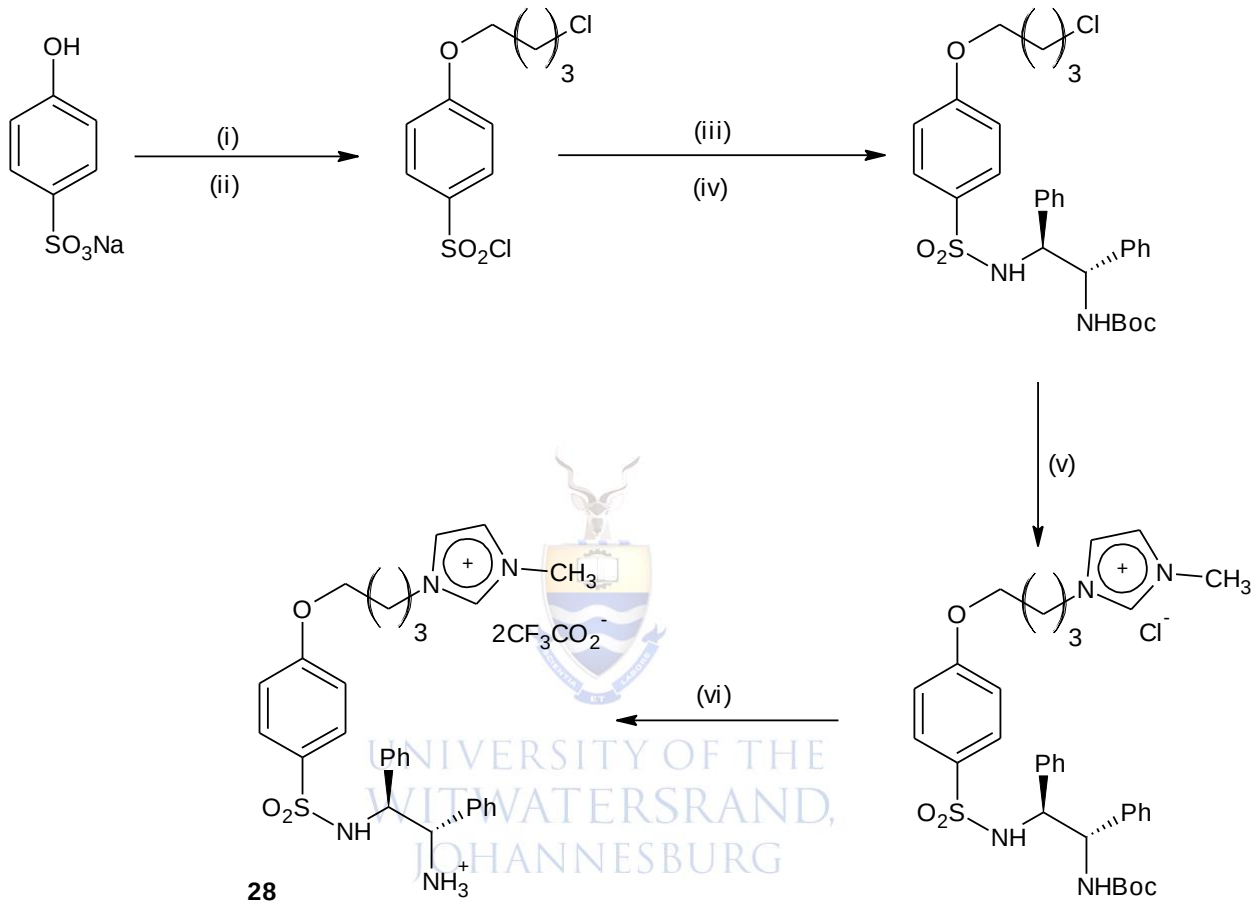

Reaction conditions:

(i) NaH, $Br(CH_2)_4$, DMF, 100 °C

(ii) $SOCl_2$, DMF, 90 °C, 54%

(iii) (1*S*, 2*S*) - 1,2 - diphenylethylenediamine, Et_3N, DCM, rt

(iv) $(Boc)_2O$, Et_3N, DCM, rt, 70%

(v) 1-methylimidazole, 80 °C, 95%

(vi) TFA, 0 °C, 97%

Scheme 1.6: The synthesis of the ionic liquid **28**.[44]

1.3 Aim and objectives of this study

The aim of this project was to study the catalytic activity of the Ru(II) and Co(II) salicylaldiminato metal complexes for the transfer hydrogenation of acetophenone using 2-propanol as the hydrogen source. Another aim was to investigate the recyclability of these complexes by immobilizing the catalyst in an ionic liquid while products and reactants are in an organic phase. The catalytic performance of these complexes will be compared to determine if the nature of the solvent medium has an effect on the activity of the catalysts.

The objectives of this study were to:

1. synthesise and characterize salicylaldimine ligands.
2. synthesise and characterize cobalt and ruthenium salicylaldiminato complexes.
3. evaluate the performance of the metal complexes in the transfer hydrogenation of acetophenone.
4. investigate the performance of active complexes in an ionic liquid – organic biphasic system.

1.3 References

1. C. Coperet, M. Chabanas, R.P. Saint-Arroman and J.-M. Basset, *Angew. Chem. Int. Ed.*, 2003, **42**, 156-181.
2. R.A. Sheldon, I.W.C. Arends and U. Hanefeld, *Gr. Chem. Cat.*, WILEY-VCH Verlag GmbH & Co. KGaA, Weinheim, Germany, 2007.
3. P.T. Anastas and J.C. Warner, *Gr. Chem.: Theory and Practice*, Oxford University Press, New York, 1998, 30.
4. G.W. Parshall and R.E. Putscher, *J. Chem. Edu.*, 1986, **63**, 189.
5. J. Dupont, R.F. de Souza and P.A.Z. Suarez, *Chem. Rev.*, 2002, **102**, 3667-3692.
6. E. Farnetti, R. Di Monte and J. Kaspar, *Inorg. Bio-Inorg. Chem.*, **2**, 1-10.
7. N. Malumbazo and S.F. Mapolie, *J. Mol. Cat. A:Chem.*, 2009, **312**, 70-77.
8. C.W. Kohlpaintner, R.W. Fischer and B. Cornils, *App. Cat. A: Gen.*, 2001, **221**, 219-225.
9. N.A. Cortez, C.Z. Flores-Lopez, R. Rodriguez-Apodaca, L.Z. Flores-Lopez, M. Parra-Hake and R. Somanathan, *Arkivoc*, 2005, **vi**, 162-171.
10. R.L. Chowdhury and J-E. Backvall, *J. Chem. Soc., Chem. Comm.*, 1991, 1063-1064.
11. G. Brieger and T.J. Nestrick, *Chem. Rev.*, 1974, **74**, 567-580.
12. R. Noyori and S. Hashiguchi, *Acc. Chem. Res.*, 1997, **30**, 97-102.
13. S. Gladiali and E. Alberico, *Chem. Soc. Rev.*, 2006, **35**, 226-236.
14. M. Zhao, Z. Yu, S. Yan and Y. Li, *Tetr. Lett.*, 2009, **50**, 4624-4628.
15. M. Rueping, E. Sugiono, C. Azap, T. Theissmann and M. Bolte, *Org. Lett.*, 2005, **7**, 3781-3783.
16. Y. Ma, H. Liu, L. Chen, X. Cui, J. Zhu and J. Deng, *Org. Lett.*, 2003, **5**, 2103-2106.
17. C. Liu, Y. Shan, X. Yang, X. Ye and Y. Wu, *J. Cat.*, 1997, **168**, 35-41.
18. J.S.M. Samec, J-E. Backvall, P.G. Andersson and P. Brandt, *Chem. Soc. Rev.*, 2006, **35**, 237-248.

19. R. Cohen, C. R. Graves, S. T. Nguyen, J. M. L. Martin and M. A. Ratner, *J. Am. Chem. Soc.*, 2004, **126**, 14796–14803.
20. S. Hashiguchi, A. Fujii, J. Takehara, T. Ikariya and R. Noyori, *J. Am. Chem. Soc.*, 1995, **117**, 7562-7563.
21. J.B. Aberg, *Mechanistic Studies on Ruthenium-Catalyzed Hydrogen Transfer Reactions*, 'Doctor of Philosophy Thesis', Stockholm University, 2009.
22. A. Stradi, M. Molnar, P. Szakal, G. Dibo, D. Gaspar and L.T. Mika, *RSC Adv.*, 2015, **5**, 72529-72535.
23. A. Aupoix, C. Bournaud and G. Vo-Thanh, *Eur. J. Org. Chem.*, 2011, 2772-2779.
24. M. Aydemir, N. Meric, A. Baysal, Y. Turgut, C. Kayan, S. Seker, M. Togrul and B. Gumgum, *J. Organomet. Chem.*, 2011, **696**, 1541-1546.
25. T. Ikariya and A.J. Blacker, *Acc.Chem. Res.*, 2007, **40**, 1300-1308.
26. R. Malacea, R. Poli and E. Manoury, *Coord. Chem. Rev.*, 2010, **254**, 729-752.
27. S. Sakaguchi, T. Yamaga and Y. Ishii, *J. Organomet. Chem.*, 2001, **66**, 4710-4712.
28. M. Aydemir, N. Meric, C. Kayan and A. Baysal, *Inorg. Chimi. Act.*, 2013, **398**, 1-10.
29. D.A. Evans, S.G. Nelson, M.R. Gagneʹ, A.R. Muci, *J. Am. Chem. Soc.*, 1993, **115**, 9800.
30. K. Ohno, Y. Kataoka and K. Mashima, *Org. Lett.*, 2004, **6**, 695-4697.
31. C. Ahmet and D. Osman, *Chin. J. Chem.*, 2009, **27**, 978-982.
32. P.O. Lagaditis, A.J. Lough and R.H. Morris, *Inorg. Chem.*, 2010, **49**, 10057-10066.
33. R.H. Morris, *Chem. Soc. Rev.*, 2009, **38**, 2282-2291.
34. A.N. Ajjou and J.-L. Pinet, *J. Mol. Cat. A: Chem.*, 2004, **214**, 203-206.
35. A.H. Gemeay, A.B. Zaki, M.Y. El-Sheikh and H.F. El-Saied, *Trans. Met. Chem.*, 2003, **28**, 625-631.

36. A.K.S. Alhmaideen, *Synthesis, Immobilization, and Applications of Solvent Stabilized Transition Metal Cations with Weakly Coordinating Anions*, 'Doctor of Philosophy Thesis', Technische Universitat Munchen, 2008.
37. T.J. Geldbach and P.J. Dyson, *J. Am. Chem. Soc.*, 2004, **126**, 8114-8115.
38. A.J. Sandee, D.G.I. Petra, J.N.H. Reek, P.C.J. Kamer and P.W.N.M. van Leeuwen, *Chem. Eur. J.*, 2001, **7**, 1202-1208.
39. P.N. Liu, P.M. Gu, F. Wang and Y.Q. Tu, *Org. Lett.*, 2004, **6**, 169-172.
40. D.E. Bergbreiter, B.L. Case, Y.-S. Liu and J.W. Caraway, *Macromolecules*, 1998, **31**, 6053-6062.
41. B. Clapham, T.S. Reger and K.D. Janda, *Tetrahedron*, 2001, **57**, 4637-4662.
42. N. Kann, *Macromolecules*, 2010, **15**, 6306-6331.
43. T. Mizugaki, Y. Kanayama, K. Ebitani and K. Kaneda, *J. Org. Chem.*, 1998, **63**, 2378-2381.
44. I. Kawasaki, K. Tsunoda, T. Tsuji, T. Yamaguchi, H. Shibuta, N. Uchida, M. Yamashita and S. Ohta, *Chem. Comm.*, 2005, 2134-2136.

CHAPTER 2

SYNTHESIS AND CHARACTERISATION OF SALICYLALDIMINE LIGANDS AND THEIR RESPECTIVE COBALT AND RUTHENIUM COMPLEXES

2.1. Introduction

Schiff bases are a class of ligands that are formed by the condensation of an active carbonyl group (either an aldehyde or ketone) and a primary amine. The condensation reaction results in an azomethine (-RC=N) functionality.[1-5] These compounds fall in the class of ligands known as the salicylaldimines which are N, O- donors.[6]

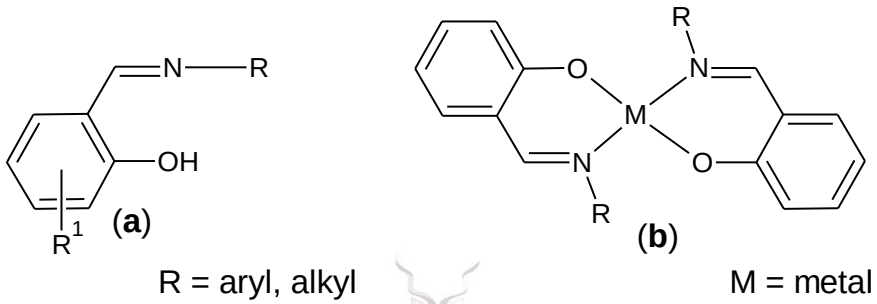

Figure 2.1: General structure of (a) a salicylaldimine ligand and (b) a tetracoordinate metal complex derived from a salicylaldimine ligand.

Salicylaldimine ligands (Figure 2.1 (a)) are readily synthesised and therefore their steric and electronic properties can be tuned easily by an appropriate choice of substituents.[7] For example, by varying the R group on the azomethine functionality and by adding substituents (R^1) on the phenolic ring. The chemistry of salicylaldimine ligands is important in coordination chemistry due to their ability to form stable complexes with a variety of transition metals and can be applied in different fields.[8] The coordination sites of the ligands involve the phenolic oxygen and the imine nitrogen forming a six-membered chelate ring.[9]

Salicylaldimine metal complexes (Figure 2.1 (b)) are well known for their easy synthesis, wide application, and their stability.[10] The backbone substituents on the ligands play an important role in improving the catalytic behaviour and they allow altering of the salicylaldimine metal complex properties.[7, 11] Metal complexes of manganese, copper, nickel,

ruthenium, zinc and chromium with a variety of salicylaldimine ligands can be used as catalysts for hydrogenation,[8] epoxidation,[12] carbonylation[8] and hydroformylation[8] reactions. Salicylaldiminato metal complexes have also shown significant biological applications.[2-3]

This chapter focuses on the synthesis of salicylaldimine ligands and their Co(II) and Ru(II) metal complexes. The ligands and the metal complexes were characterized using a variety of techniques such as NMR spectroscopy, FTIR spectroscopy, mass spectrometry, elemental analysis and TGA.

2.2 Experimental

2.2.1 Materials and instrumentation

All chemicals were of reagent grade and were used without further purification. All solvents were dried over the appropriate drying agent and distilled prior to use. The $[RuCl_2(\eta^6\text{-}p\text{-cymene})]_2$ was prepared according to a literature procedure.[13] ^{1}H-NMR and $\{^1H\}$ ^{13}C-NMR spectra of the compounds in $CDCl_3$ were obtained using a Bruker 300 MHz Ultrashield spectrophotometer, using tetramethylsilane as an internal standard. Infrared spectra were recorded on a Bruker Tensor 27 spectrophotometer. Elemental analysis was performed at the University of Johannesburg using a Thermoscientific Flash 2000 organic elemental analyser with an oven temperature of 65 ^oC and a reactor tube temperature of 900 ^oC with oxygen and helium being the carrier gasses. Thermogravimetric analysis (TGA) of the complexes was performed using a Pyris Stat 4000 analyzer with nitrogen and air as the purge gasses with a flow rate of 20 ml/min.

2.2.2 General procedure for the synthesis of salicylaldimine ligands

The salicylaldimine ligands **L1 - L4** were prepared using a modified literature procedure by Bhunora and co-workers.[14] The methodology is described using **L1** as an example.

To a schlenck tube flushed with nitrogen gas was added salicylaldehyde (1.278 ml, 12.00 mmol), formic acid (0.5000 ml), dry methanol (15.00 ml) and aniline (1.458 ml, 16.00 mmol). The resulting orange-yellow solution was stirred at room temperature for approximately 15 h. After the elapsed time the solvent was evaporated using a rotary evaporator. The resulting orange-yellow oil was re-dissolved in dichloromethane (DCM) and sodium hydrogen carbonate was added to neutralize the formic acid. The sodium hydrogen carbonate was removed by filtration and the solvent of the filtrate was evaporated by using a rotary evaporator. The resulting oil was dried under reduced pressure which resulted in a yellow solid. The salicylaldimine ligands were obtained as yellow to orange solids with average yields of 70 - 93%.

2.2.3 General procedure for the synthesis of cobalt complexes Co1 - Co4

The cobalt (II) complexes **Co1 – Co4** were prepared as previously described in literature by van Wyk and co-workers.[15] The synthetic procedure is described using **Co1** as an example.

Salicylaldimine ligand **L1** (0.1972 g, 1 mmol), NaOH (0.04 g, 1 mmol) and dry methanol (20 ml) were placed in a round-bottomed flask. The resulting yellow mixture was heated at 50 ^{o}C with stirring for approximately 30 minutes. $Co(OAc)_2.4H_2O$ (0.1245 g, 0.5 mmol) was added and the resulting red-brown mixture was stirred at 50 ^{o}C for approximately 4 h during which a brown solid precipitated out. The reaction flask was placed in ice for approximately 15 minutes to cool down the reaction mixture and the solid was isolated from the solution. The brown solid was dissolved in DCM in order to remove any salt present and the precipitated

salt was separated from the mixture by filtration and DCM was distilled by rotary evaporation. The resulting brown solid was dried under reduced pressure. The cobalt (II) complexes were obtained as brown solids with average yields of 60 - 66%.

2.2.4 General procedure for the synthesis of ruthenium complexes Ru1 - Ru4

The ruthenium (II) complexes **Ru1 – Ru4** were prepared as previously described in literature by Rath and co-workers.[16] The synthetic procedure is described using **Ru1** as an example.

To a round-bottomed flask was added the $[RuCl_2(\eta^6\text{-}p\text{-cymene})]_2$ (0.2028 g, 0.3312 mmol), ligand **L1** (0.1828 g, 0.9269 mmol), Na_2CO_3 (0.1671 g, 1.577 mmol) and DCM (15.00 ml). The red-brown mixture was stirred at room temperature under a nitrogen atmosphere for 24 h. After 24 h, the salt was filtered and the DCM was distilled by rotary evaporation. The red-brown residue was concentrated in DCM and an excess amount of hexane was added upon which precipitation occurred. The mixture was filtered and the red-brown solid was dried under reduced pressure. The Ru (II) complexes were obtained as red-brown to orange-brown solids with average yields of 90 - 97%.

2.3 Results and discussion

2.3.1 Synthesis and characterisation of salicylaldimine ligands

The ligands were prepared by Schiff base condensation using salicylaldehyde and an appropriate aromatic amine in the presence of formic acid as the catalyst as depicted in Scheme 2.1. Ligands **L1**, **L3**, and **L4** were isolated as yellow to orange solids. This observation confirms literature observation.[14] However, ligand **L2** was isolated as an orange

oil but was observed as a solid in literature. The yields ranged from 70 - 93%. These ligands were found to show good solubility in a range of organic solvents.

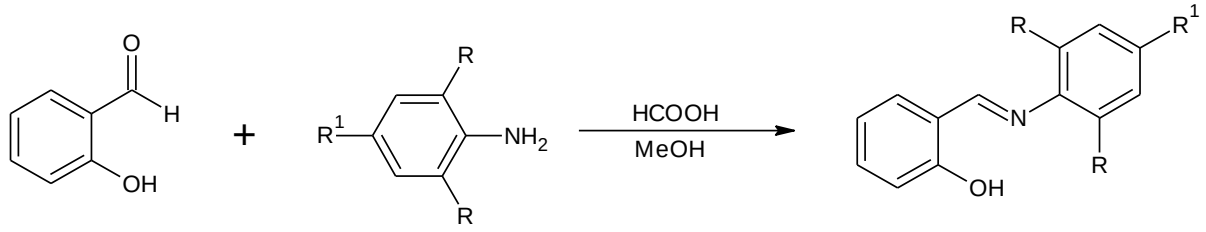

L1: R = H, R^1 = H

L2: R = CH_3, R^1 = H

L3: R = $CH(CH_3)_2$, R^1 = H

L4: R = H, R^1 = $N(CH_2CH_3)_2$

Scheme 2.1: Synthesis of salicylaldimine ligands.[14]

2.3.1.1 ^{1}H-NMR spectroscopy studies of the salicylaldimine ligands

The ^{1}H-NMR data of the ligands are summarised in Table 2.1. For all the ligands, the **H**C=N proton was observed as a singlet in the range δ8.33 - 8.63 ppm which confirmed the condensation between salicylaldehyde and the amine. The aromatic protons of the phenolic moiety and the imine ring were observed as multiplets in the range δ6.52 - 7.53 ppm. The ^{1}H-NMR spectrum for **L3** containing the isopropyl moiety showed a doublet at δ1.18 ppm for the C**H**$_3$ protons and a septet in the range δ2.93 - 3.07 ppm for the C**H** protons. The methyl substituent of **L2** was observed in the ^{1}H-NMR spectrum as a singlet at δ2.20 ppm. For **L4**, the N-diethyl substituent displayed a triplet at δ1.19 ppm for the C**H**$_3$ protons and a quartet at δ3.39 ppm for the C**H**$_2$ protons. For all the ligands the O**H** proton was observed as a singlet

in the range δ13.09 - 13.83 ppm. The data obtained for the salicylaldimine ligands are in agreement with the NMR data observed for published ligands.[14]

2.3.1.2 {^{1}H} ^{13}C-NMR studies of the salicylaldimine ligands

The {^{1}H} ^{13}C-NMR results for the salicylaldimine ligands are summarised in Table 2.2. For all the ligands, the signal for the carbon of the imine moiety was observed in the range δ160 - 166 ppm and the aromatic protons were observed in the range δ112 - 148 ppm. The signal for the carbon attached to the hydroxyl group was observed in the range δ156 - 163 ppm. The spectrum for the ligand containing the isopropyl moiety (**L3**) showed a signal at δ23 ppm for the **C**H$_3$ carbons and a signal at δ28 ppm for the **C**H carbons. The spectrum for the ligand with the methyl moiety (**L2**) showed a signal at δ18 ppm for the **C**H$_3$ carbons. The spectrum with the N-diethyl moiety (**L4**) showed a signal at δ12 ppm for the **C**H$_3$ carbons and a signal at δ44 ppm for the **C**H$_2$ protons.

2.3.1.3 Infrared spectroscopy, elemental analysis and mass spectrometry studies of the ligands

The IR results for the ligands are summarised in Table 2.3. Infrared spectroscopy showed a band at 2900 - 3000 cm^{-1} for all the ligands due to the O-H vibrational stretching which is in agreement to that observed by van Wyk *et al.*[15] The ν(C=N) stretch was observed at a frequency range of 1612 - 1623 cm^{-1} for all the ligands. The presence of this band is confirmation that condensation between the aldehyde and the amine took place as was also observed in literature.[15] The ν(C-O) stretch for the ligands was observed in the range 1268 - 1279 cm^{-1}.[15]

The elemental analysis and mass spectrometry results are summarised in Table 2.3. The elemental analysis data obtained for the ligands (**L1, L3 - L4**) were in agreement with the calculated values as depicted by the formulations in Scheme 2.1. The carbon composition for **L2** had a difference of 7.83 %. The found value was lower than the expected value. The reason for the huge difference can be attributed to the fact that this ligand was obtained as an oil whereas it was reported as a solid in literature.[15] The mass spectra of the ligands were obtained using ESI - MS. For **L1** the parent ion peak was not observed, however, a fragment due to $[M - H]^+$ is observed at m/z 196.3, **L2** was observed as M^+ at m/z 225.1, **L3** was observed as M^+ at m/z 281.4 and **L4** was observed as $[M + H]^+$ at m/z 269.5.

The melting point of the solidified ligands was also investigated to confirm the purity of these ligands. **L1** had a melting point of 50 – 52 ^oC and **L3** had a melting point of 52 – 54 ^oC which are in agreement with literature.[15] **L4** had a melting point of 101 – 105 ^oC.[17]

Table 2.1: ^{1}H-NMR[a] chemical shifts δ (ppm) for the salicylaldimine ligands **L1 - L4**.

	L1	**L2**	**L3**	**L4**
O<u>H</u>	13.18 (br s, 1H)	13.01 (br s, 1H)	13.08 (br s, 1H)	13.84 (br s, 1H)
<u>H</u>C=N	8.56 (s, 1H)	8.25 (s, 1H)	8.23 (s, 1H)	8.63 (s, 1H)
Ar-<u>H</u>	6.85-6.90 (td, 1H) 6.95-6.98 (dd, 1H) 7.19-7.21 (td, 1H) 7.22-7.24 (td, 2H) 7.27-7.35 (dd, 1H) 7.36-7.37 (dd, 1H) 7.38-7.39 (td, 2H)	6.84-6.90 (td, 1H) 6.91-6.99 (m, 1H) 6.96-6.99 (dd, 1H) 7.02 (d, 2H) 7.24-7.27 (dd, 1H) 7.29-7.35 (td, 1H)	6.88-6.93 (td, 1H) 7.00-7.03 (dd, 1H) 7.12-7.13 (m, 1H) 7.16 (d, 2H) 7.27-7.28 (dd, 1H) 7.30-7.39 (td, 1H)	6.62-6.64 (dd, 2H) 6.82-6.85 (td, 1H) 6.91-6.93 (dd, 1H) 7.22 (d, 1H) 7.23-7.23 (dd, 1H) 7.25-7.28 (m, 2H)
Ar-C<u>H</u>$_3$	-	2.12 (s, 6H)	-	-
C<u>H</u>(CH$_3$)$_2$	-	-	2.88-2.97 (m, 2H)	-
CH(C<u>H</u>$_3$)$_2$	-	-	1.10 (d, 12H)	-
N(C<u>H</u>$_2$CH$_3$)$_2$	-	-	-	3.38-3.45 (q, 4H)
N(CH$_2$C<u>H</u>$_3$)$_2$	-	-	-	1.20 (t, 6H)

[a] Spectra obtained in $CDCl_3$; br s = broad singlet; d = doublet; t = triplet; m = multiplet; q = quartet; dd = doublet of doublets; td = triplet of doublets

Table 2.2: {^{1}H} ^{13}C-NMR[a] chemical shifts δ (ppm) for the salicylaldimine ligands **L1 - L4**.

	L1	**L2**	**L3**	**L4**
H<u>C</u>=N	162.68	166.78	166.63	160.89
Ar-<u>C</u>	117.27, 119.07, 119.22,121.16,126.90, 129.41, 132.28, 133.16	117.36, 118.03, 118.83, 119.01, 121.71, 124.98, 128.27, 128.31, 128.38, 132.20, 133.22, 148.22	123.29, 125.50, 133.29, 138.74	112.02, 117.02, 118.78, 122.48, 131.40, 131.85, 156.88
Ar-<u>C</u>H$_3$	-	18.51	-	-
<u>C</u>H(CH$_3$)$_2$	-	-	28.15	-
CH(<u>C</u>H$_3$)$_2$	-	-	23.56	-
N(<u>C</u>H$_2$CH$_3$)$_2$	-	-	-	44.59
N(CH$_2$<u>C</u>H$_3$)$_2$	-	-	-	12.62

[a] Spectra obtained in $CDCl_3$

Table 2.3: Elemental analysis, mass spectrometry and FTIR data for the salicylaldimine ligands **L1 - L4**.

Ligand	m.p. (°C)	FTIR assignment (cm^{-1})		Elemental analysis Obtained (Calculated)			M^+ (m/z) (calculated)	Yield
		ν(C=N)	ν(C-O)	%C	%H	%N		
L1	50 - 52	1616	1276	78.76 (79.16)	5.73 (5.62)	7.15 (7.10)	196.3[a] (197.23)	93%
L2	-	1623	1279	72.14 (79.97)	6.60 (6.71)	6.16 (6.22)	225.1 (225.28)	91%
L3	53 - 55	1622	1277	81.59 (81.10)	8.72 (8.24)	4.94 (4.98)	281.4 (281.38)	75%
L4	101-105	1612	1268	76.54 (76.08)	7.37 (7.51)	9.98 (10.44)	269.5[b] (268.35)	70%

[a] Represents m/z for the fragment $[M - H]^+$

[b] Represents m/z for the fragment $[M + H]^+$

2.3.2 Synthesis and characterisation of cobalt salicylaldiminato complexes

These complexes were prepared according to a literature procedure by reacting the salicylaldimine ligands with cobalt acetate tetrahydrate (Scheme 2.2) in a 2:1 mole ratio.[15] The presence of sodium hydroxide in the reaction aids in the deprotonation of the salicylaldimine ligand to assist coordination to the metal centre.[15] The cobalt salicylaldiminato complexes were isolated as brown solids with yields in the range of 60 – 66 %. The complexes were air and moisture stable and were found to be soluble in DCM and toluene as was observed for similar compounds reported by van Wyk *et al.*[15] Complexes **Co1** and **Co2** were also found to be soluble in methanol.

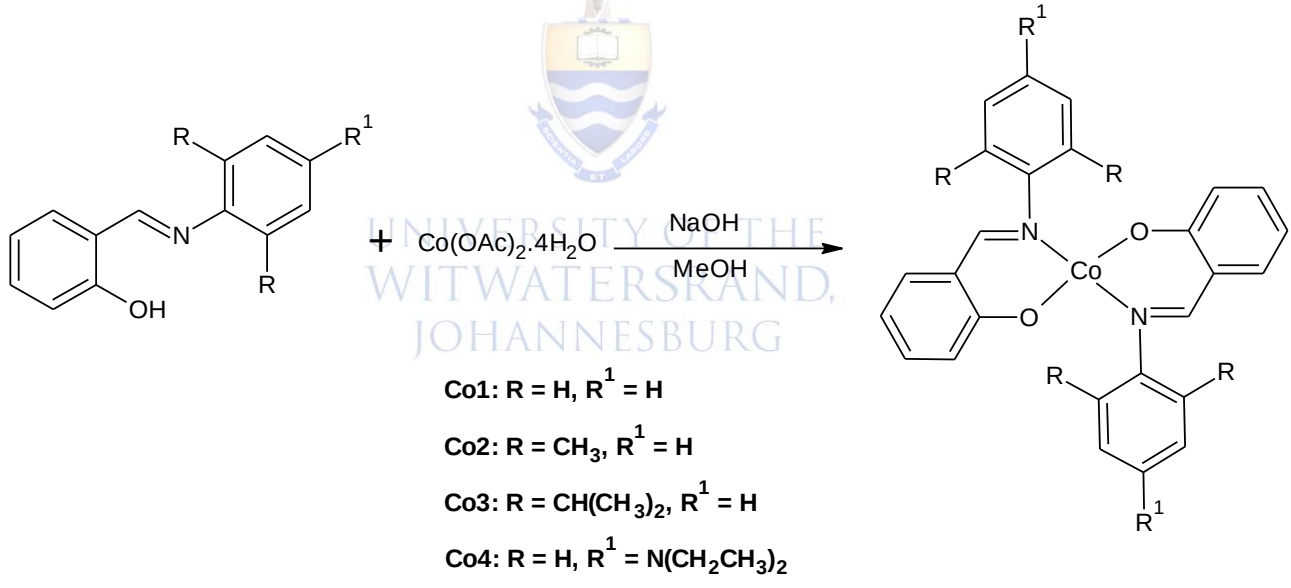

Co1: R = H, R^1 = H

Co2: R = CH_3, R^1 = H

Co3: R = $CH(CH_3)_2$, R^1 = H

Co4: R = H, R^1 = $N(CH_2CH_3)_2$

Scheme 2.2: Synthesis of Co(II) salicylaldiminato complexes.[15]

2.3.2.1 FTIR, mass spectrometry and elemental studies of the cobalt salicylaldiminato complexes

The infrared spectroscopy results were compared to those of the ligands. In principle, coordination of the ligand to the metal centre occurs via the azomethine nitrogen and the phenolic oxygen.[15] According to literature, if coordination did occur then the ν(C=N) stretch shifts to a lower frequency (an M - N bond has been formed) and the ν(C-O) stretch shifts to a higher frequency (an M - O bond has been formed).[15] Tas and co-workers went on to explain that coordination through the azomethine nitrogen is expected to reduce the electron density in C=N bond and thus lower the ν(C=N) bond.[8] This is what was observed in the IR spectra of the cobalt (II) complexes. The ν(C=N) and ν(C-O) bands in the IR spectra of the free ligands was observed in the range of 1612 - 1623 cm^{-1} and 1268 - 1279 cm^{-1}, respectively. Upon coordination to Co(II), the ν(C=N) band in the IR spectra of the complexes shifted to the region 1602 - 1607 cm^{-1} and the ν(C-O) band shifted to the region 1314 - 1324 cm^{-1}. The IR data of the cobalt (II) salicylaldiminato complexes are summarised in Table 2.4.

The mass spectra of the complexes were obtained using ESI - MS. The parent ions of these complexes were observed as M^+. For **Co1** the parent ion peak was observed at m/z 451, **Co2** at m/z 507, **Co3** at m/z 619 and **Co4** at m/z 593. A fragment due to the free ligand at m/z 269 was also observed in the mass spectra of the **Co4** complex. The elemental analysis data obtained for the complexes were in agreement with the calculated values as depicted by the formulations in Scheme 2.2. The mass spectrometry and elemental analysis results are summarised in Table 2.4.

Table 2.4: Elemental analysis, mass spectrometry and FTIR data for the cobalt complexes **Co1 - Co4**.

Complex	**m.p. (^{o}C)**	**FTIR assignment (cm^{-1})**		**Elemental analysis Obtained (Calculated)**			**M^{+} (m/z) (calculated)**	**Yield**
		ν(C=N)	**ν(C-O)**	**%C**	**%H**	**%N**		
Co1	160 - 165	1606	1324	69.25 (69.18)	4.48 (4.47)	6.12 (6.21)	451.08 (451.38)	60%
Co2	215 - 219	1605	1321	70.86 (71.00)	5.99 (5.56)	5.35 (5.52)	507.14 (507.49)	60%
Co3	240 - 243	1602	1314	73.37 (73.65)	7.16 (7.16)	4.51 (4.52)	619.27 (619.70)	66%
Co4	260 - 265	1607	1323	68.74 (68.79)	6.53 (6.45)	9.64 (9.44)	593.2 (593.62)	65%

2.3.2.2 TGA studies of the cobalt salicylaldiminato complexes

Thermogravimetric analysis was performed to study the thermal stability of the cobalt complexes **Co1 - Co4** (Figure 2.2). The decomposition profiles of these complexes were fairly similar. For the complex **Co1**, two steps were observed in the decomposition profile. The first stage of decomposition occurred at 100 ^{o}C with a mass loss of approximately 5 %. This loss is most likely due to the presence of water in the complex. The second stage of decomposition occurred at 300 – 480 ^{o}C with a mass loss of approximately 80 %. This loss is probably due to the loss of the ligands attached to the metal centre. **Co2** had a two-step decomposition profile. The first stage of decomposition occurred at 100 ^{o}C with a mass loss of 10 %. This could have been due to the presence of two water molecules. The second stage of decomposition was observed at 300 – 480 ^{o}C with a mass loss of approximately 80 % which could be due to the loss of the ligands.

For complex **Co3**, only one decomposition profile was observed at 300 – 460 ^{o}C with a mass loss of 95 % which is due to the loss of the ligands in the complex. Complex **Co4** had three decomposition profiles. The first stage of decomposition was observed at 100 ^{o}C with approximately 5 % mass loss which is due to the presence of water in the complex. The second stage of decomposition occurred at 300 – 400 ^{o}C with a mass loss of 40 % which is due to the loss of one ligand but the N and O remain attached to the metal. The third stage of decomposition occurred at 410 – 490 ^{o}C with a mass loss of 45 % which is due to the loss of the remaining ligand.

From Figure 2.2, it can be seen that **Co3** and **Co2** are slightly more stable than **Co4** and **Co1** is also slightly more stable than **Co4**. **Co1** appears to be the most stable of the cobalt complexes while **Co4** is the least stable.

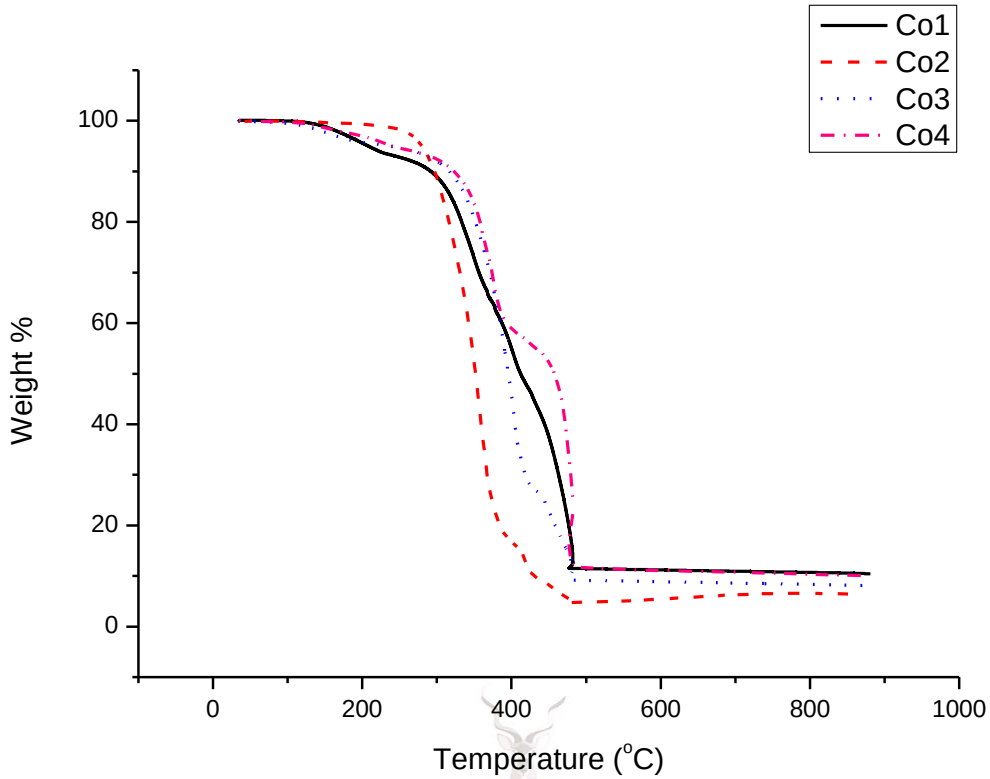

Figure 2.2: Thermogram of the TGA results of the cobalt complexes **Co1 - Co4**.

2.3.3 Synthesis of ruthenium salicylaldiminato complexes

These complexes were prepared according to a literature procedure by reacting the salicylaldimine ligand and the $[(\eta^6\text{-}p\text{-cymene})RuCl_2]_2$ (Scheme 2.3) in a 2:1 mole ratio.[16] The ruthenium salicylaldiminato complexes were isolated as red-brown to orange-brown solids with yields in the range 90 – 97 %. They were characterized using techniques such as ^{1}H-NMR and $\{^1H\}$ ^{13}C-NMR spectroscopy, mass spectrometry, FTIR spectroscopy, elemental analysis and TGA. These characterization techniques proved that the desired compounds were obtained. A solubility study was also performed and these complexes were observed to be soluble in general organic solvents like DCM.

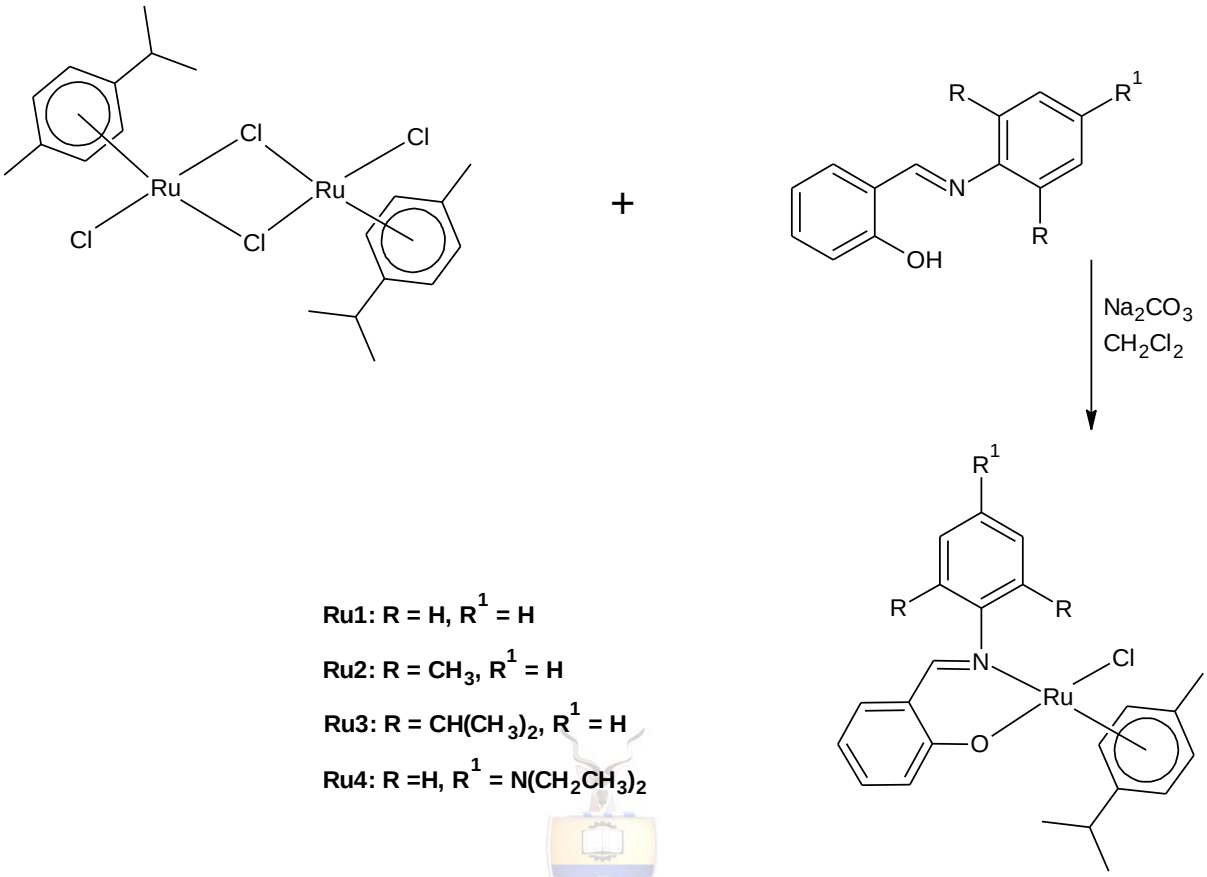

Ru1: R = H, R^1 = H

Ru2: R = CH_3, R^1 = H

Ru3: R = $CH(CH_3)_2$, R^1 = H

Ru4: R =H, R^1 = $N(CH_2CH_3)_2$

Scheme 2.3: Synthesis of reduced Ru(II) salicylaldiminato complexes.[16]

2.3.3.1 ^{1}H-NMR spectroscopy studies of the ruthenium salicylaldiminato complexes

Complexation of the ruthenium dimer to the ligand to form the ruthenium complex was confirmed by proton NMR. Coordination of the *N, O*-chelating ligands to the metal centre is confirmed by the disappearance of the OH proton and the shift in the **H**C=N proton of the imine moiety.[17] The **H**C=N proton of these complexes was observed as a singlet in the range δ7.348 - 7.694 ppm compared to the ligand which is observed in the range δ8.33 - 8.63 ppm and the aromatic protons for the ligands were observed in the range 6.62 – 7.39 ppm and were observed in the range 6.31 – 7.29 ppm. In Figure 2.3 below, (a) is the spectrum for ligand **L1** where the **H**C=N proton was observed as a sharp singlet at 8.55 ppm and (b) is the spectrum for the ruthenium complex **Ru1** where the **H**C=N proton shifted to 7.68 ppm from

8.55 ppm of the ligand as a result of complexation. This change in chemical shift is a confirmation of complexation. The aromatic protons of the free ligand (Figure 2.3 (a)) were observed to form combined multiplets but upon complexation, the multiplicity of these protons can be distinguished (Figure 2.3 (b)).

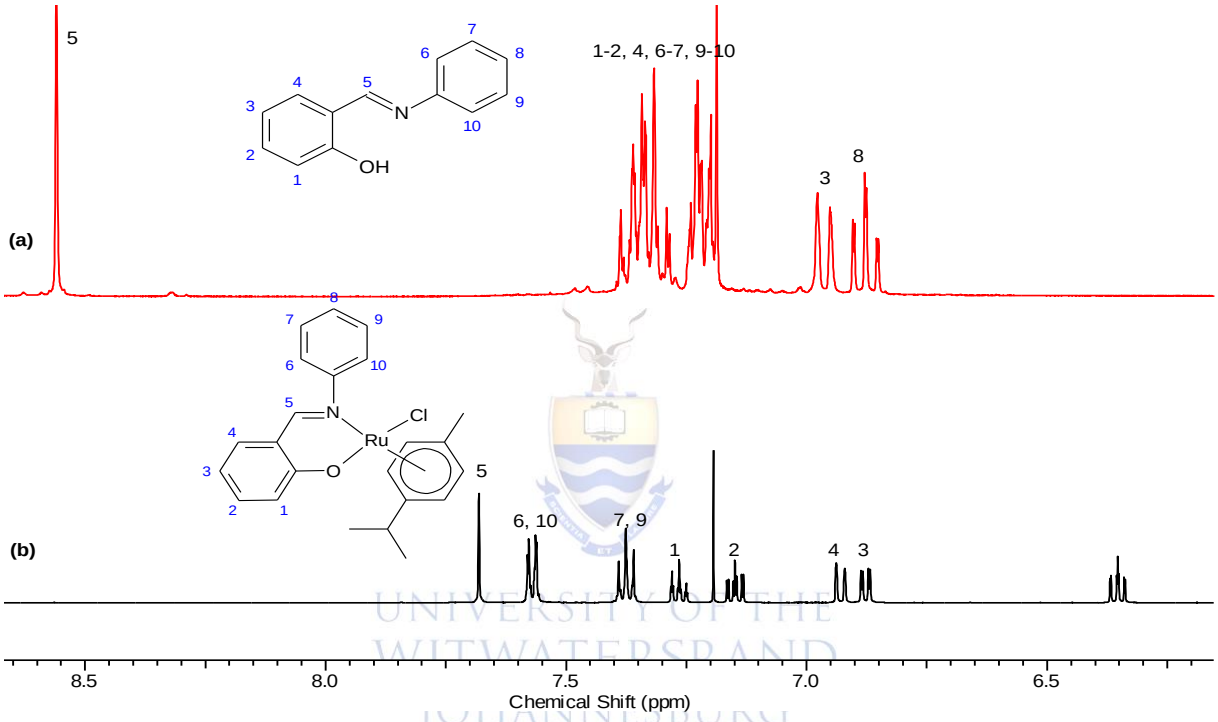

Figure 2.3: ^{1}H-NMR spectra of (a) **L1** and (b) **Ru1** displaying the aromatic region and the chemical shift of **H**C=N for both compounds.

For the dimer $[(\eta^6\text{-}p\text{-cymene})RuCl_2]_2$, the cymene ring protons were observed as two doublets in the range δ5.34 – 5.48 ppm as shown in Figure 2.4 (a). Upon complexation of $[(\eta^6\text{-}p\text{-cymene})RuCl_2]_2$ with the ligand, the cymene ring protons were observed as four doublets in the range δ4.12 - 5.35 ppm as observed in Figure 2.4 (b). Rath and co-workers also observed this and they attributed it to the fact that the complexes are unstable in the solution phase.[16]

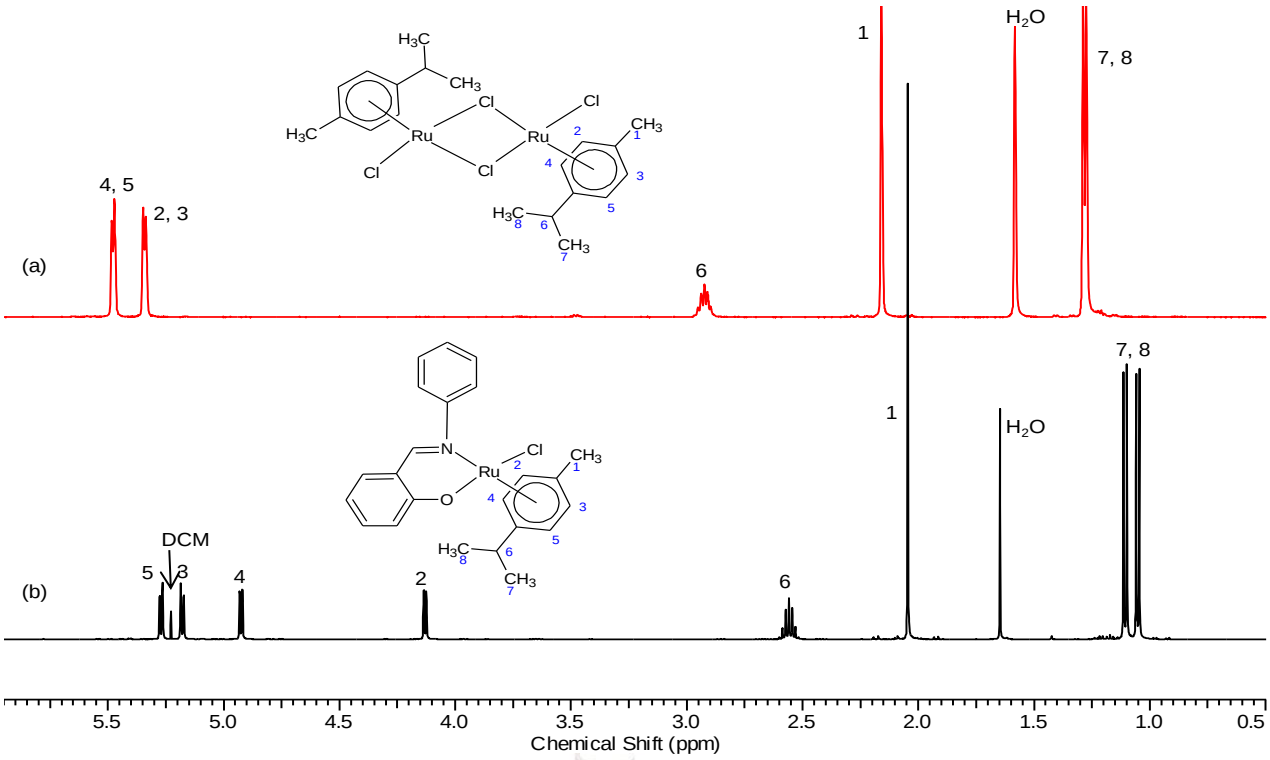

Figure 2.4: ^{1}H-NMR spectrum of the protons on the cymene ring in (a) the [(η^6-*p*-cymene)$RuCl_2$]$_2$ and (b) **Ru1** compounds.

For complex **Ru2** the protons of the two methyl substituents appeared as two different signals at 2.20 and 2.50 ppm compared to the free ligand. On the free ligand (**L2**), the protons of the di-methyl groups appeared as one signal at 2.12 ppm. The (C**H**$(CH_3)_2)_2$ on **Ru3** also appeared as two individual multiplets in the range 3.06 - 3.15 ppm and 4.10-4.15 ppm. However, for the free ligand **L3**, the protons appeared as one multiplet in the range 2.88 - 2.97 ppm. The (CH(C**H**$_3)_2)_2$ on the same complex appeared as two individual doublet of doublets at 0.93 - 0.98 ppm and 1.28 - 1.31 ppm while for the free ligand they appeared as one doublet at 1.10 ppm. ^{1}H-NMR results of the ruthenium salicylaldiminato complexes are summarised in Table 2.5.

2.3.3.2 {^{1}H} ^{13}C-NMR spectroscopy studies of ruthenium salicylaldiminato complexes

The carbon of the imine moiety (C=N) was observed at δ163 - 165 ppm and the aromatic protons were observed at δ111 - 158 ppm. The carbon attached to the oxygen (C-O) was observed at δ164 - 167 ppm which shifted from δ156 – 163 ppm for the free ligand. The alkenes from the cymene ring gave signals at δ80 - 81 ppm and the alkyls gave signals in the region δ12 - 44 ppm. When comparing the protons on the cymene ring for [(η^6-*p*-cymene)$RuCl_2$]$_2$ and **Ru1**, a similar was observed as with ^{1}H-NMR. Magnetic equivalence was observed in [(η^6-*p*-cymene)$RuCl_2$]$_2$ because four signals rising from the cymene carbons were observed but for the complex, six different carbon signals were observed which confirms magnetic non-equivalence as was also observed in the ^{1}H-NMR. Figure 2.5 shows the regions for the cymene carbons. The {^{1}H} ^{13}C-NMR results are summarised in Table 2.6.

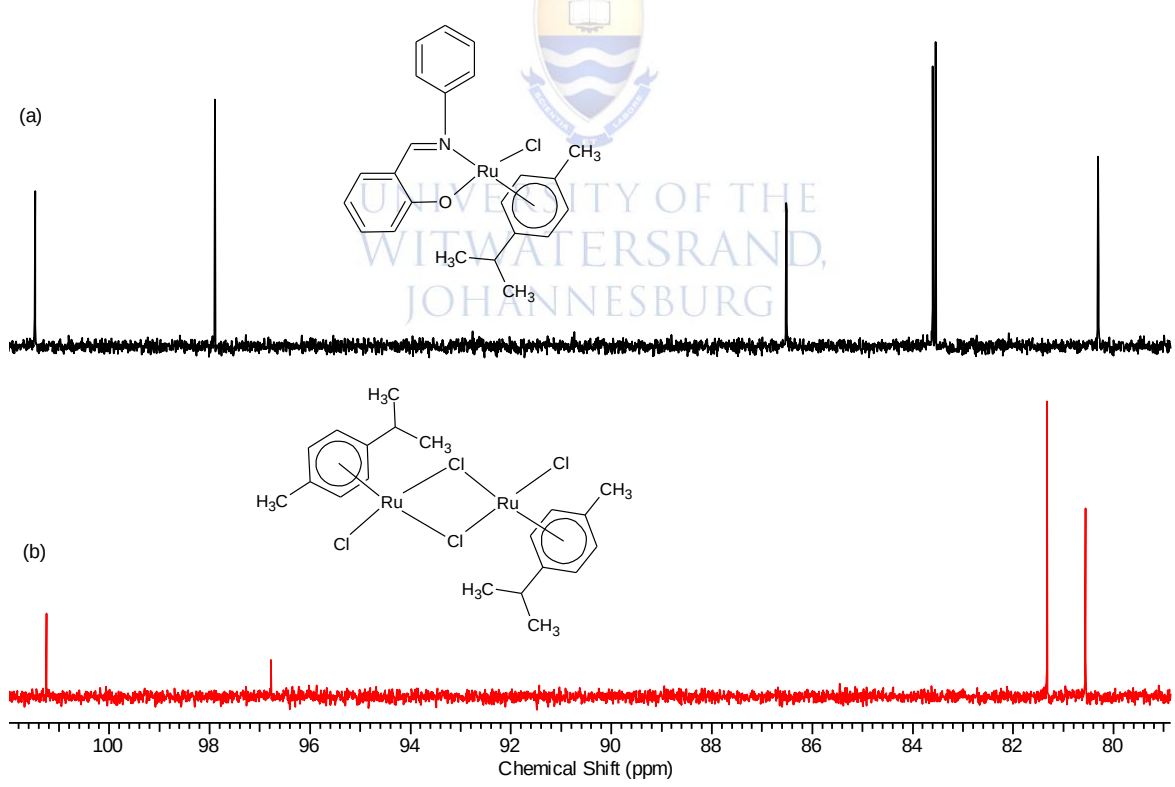

Figure 2.5: {^{1}H} ^{13}C-NMR spectrum of the cymene ring carbon signals on (a) the **Ru1** complex and (b) the [(η^6-*p*-cymene)$RuCl_2$]$_2$ dimer.

Table 2.5: [1]H-NMR[a] chemical shift δ (ppm) for the ruthenium complexes **Ru1 - Ru4**.

	Ru1	**Ru2**	**Ru3**	**Ru4**
HC=N	7.35 (s, 1H)	7. 35 (s, 1H)	7. 39 (s, 1H)	7.68 (s, 1H)
Ar-**H**	6.33-6.38 (td, 1H), 6.87, 6.90 (m, 1H), 6.92 (d, 1H), 7.13-7.15 (td, 1H), 7.24, 7.25 (dd, 1H), 7.26-7.28 (td, 2H), 7.29-7.30 (td, 2H)	6.33-6.36 (td, 1H), 6.80-6.81 (dd, 1H), 6.87-6.88 (dd, 1H), 7.08-7.10 (dd, 1H), 7.11-7.13 (td, 2H), 7.14-7.16 (dd, 1H)	6.33-6.36 (td, 1H), 6.74-6.77 (dd, 1H), 6.87 (d, 1H), 7.08-7.14 (td, 2H), 7.21-7.23 (td, 1H), 7.24-7.27 (dd, 1H)	5.25-5.27 (d, 1H), 6.31-6.36 (td, 2H), 6.58 (d, 1H), 6.84-6.87 (m, 1H), 6.91-6.93 (dd, 1H), 7.10-7.15 (td, 2H)
Ar-C**H**$_3$	-	2.20 (s, 3H), 2.50 (s, 3H)	-	-
C**H**(CH$_3$)$_2$	-	-	3.06-3.15 (m, 1H), 4.10-4.15 (m, 1H)	-
(CH(C**H**$_3$)$_2$)$_2$	-	-	0.93-0.89 (dd, 6H), 1.28-1.31 (dd, 6H)	-
N(C**H**$_2$CH$_3$)$_2$	-	-	-	3.31-3.38 (q, 4H)
N(CH$_2$C**H**$_3$)$_2$	-	-	-	1.13 (t, 6H)
Cy-**H**	4.12 (d, 1H), 4.92 (d, 1H), 5.17 (d, 1H), 5.26 (d, 1H)	4.12 (d, 1H), 4.87 (d, 1H), 5.06 (d, 1H), 5.29 (d, 1H)	4.16 (d, 1H), 4.85 (d, 1H), 5.20 (d, 1H), 5.34 (d, 1H)	4.24 (d, 1H), 4.92 (d, 1H), 5.19 (d, 1H), 5.25 (d, 1H)
Cy-C**H**$_3$	2.05 (s, 3H)	1.91 (s, 3H)	1.88 (s, 3H)	2.10 (s, 3H)
Cy-C**H**(CH$_3$)$_2$	2.52-2.61 (m, 1H)	2.66-2.71 (m, 1H)	2.68-2.79 (m, 1H)	2.54-2.6 (m, 1H)
Cy-CH(C**H**$_3$)$_2$	1.04 (d, 3H), 1.09 (d, 3H)	1.19 (d, 3H), 1.23 (d, 3H)	1.19 (d, 3H), 1.38 (d, 3H)	1.03 (d, 3H), 1.10 (d, 3H)

[a] Spectra obtained in $CDCl_3$; s = singlet; d = doublet; q = quartet; m = multiplet; dd = doublet of doublets; td = triplet of doublet

Table 2.6: $\{^1H\}$ ^{13}C-NMR[a] chemical shift δ (ppm) for the $[(\eta^6\text{-}p\text{-cymene})RuCl_2]_2$ and ruthenium complexes, **Ru1 - Ru4**.

	Ru1	**Ru2**	**Ru3**	**Ru4**
HC=N	165.25	167.08	166.24	164.92
C-O	164.23	165.62	165.56	163.28
CH_3	17.42, 22.34	17.42, 18.70, 19.71, 22.14, 22.34	16.69, 20.44, 20.96, 21.50, 22.22, 25.07, 25.69	12.59, 14.21, 18.62, 21.06, 21.73
CH_2	-	-	-	22.82, 30.38
CH	30.63	30.63	26.43, 26.85, 29.57	44.55
Ar-C	118.16, 122.70, 123.73, 126.93, 128.84, 135.37, 135.53, 158.58	119.96, 122.02, 126.59, 127.95, 129.20, 130.58, 132.27, 134.96, 135.35, 155.02	118.29, 120.92, 122.30, 123.29, 124.28, 126.44, 127.20, 128.02, 133.91, 134.39, 140.58, 141.64, 151.58	113.99, 118.56, 122.51, 124.52, 134.91, 135.11, 146.63, 148.66
Cy-C	80.30, 83.54, 86.51, 97.89, 101.4, 114.23	81.51, 85.82, 87.80, 93.73, 105.37, 114.39	80.67, 83.64, 86.63, 93.26, 103.64, 113.47	81.00, 83.41, 86.68, 98.03, 100.87, 111.10

[a] Spectra obtained in $CDCl_3$

2.3.3.3 FTIR, mass spectrometry and elemental analysis studies of the ruthenium salicylaldiminato complexes

As observed for the cobalt salicylaldiminato complexes, the same shifts in the bands due to the functional groups were observed. The results obtained for the ruthenium complexes were in agreement with what was reported by Matsinha and co-workers.[18] The ν(C=N) and ν(C-O) bands in the IR spectra of the free ligands was observed at frequencies of 1612 - 1623 cm^{-1} and 1268 - 1279 cm^{-1}, respectively. Upon coordination to Ru(II), the ν(C=N) band in the IR spectra of the complexes shifted to the region 1606 - 1608 cm^{-1} and the ν(C-O) band shifted to the region 1323 - 1330 cm^{-1}. The FTIR results for the ruthenium complexes are summarised in Table 2.7.

The mass spectra of the complexes were obtained using ESI - MS. The parent ion for **Ru1** was observed as M^+ at m/z 466.4. For **Ru2**, the parent ion peak was not observed but a fragment due to $[M - H]^+$ was observed at m/z 494.5. The parent ion for **Ru3** was observed as M^+ at m/z 551.6 and **Ru4** was observed as $[M + H]^+$ at m/z 539.4. Fragments due to the free ligands were also observed in the mass spectra of these complexes as was observed with the cobalt salicylaldiminato complexes. The results are summarised in Table 2.7.

The elemental analysis data obtained for the complexes were in agreement with the calculated values as depicted by the formulations in Scheme 2.3. The agreement in values observed between the found and calculated values depict the purity of the complex. The results are summarised in Table 2.7.

Table 2.7: Elemental analysis, mass spectrometry and FTIR data for the ruthenium complexes **Ru1 - Ru4**.

Complex	m.p. (^{o}C)	FTIR assignment (cm^{-1})		Elemental analysis Obtained (Calculated)			M^{+} (m/z) (calculated)	Yield
		ν(C=N)	ν(C-O)	%C	%H	%N		
Ru1	220 - 225	1607	1330	59.08 (59.15)	4.98 (5.18)	3.57 (3.00)	466.4 (466.97)	90%
Ru2	220 - 224	1607	1323	60.22 (60.70)	5.56 (5.70)	3.28 (2.83)	494.5 (495.02)	97%
Ru3	235 - 237	1608	1323	62.76 (63.20)	6.23 (6.58)	2.24 (2.54)	551.6 (551.13)	94%
Ru4	195 - 200	1606	1330	60.10 (60.26)	6.08 (6.18)	5.47 (5.21)	539.4 (538.09)	95%

2.3.3.4 TGA studies of the ruthenium salicylaldiminato complexes

Thermogravimetric analysis (TGA) was also performed on the ruthenium complexes **Ru1 - Ru4**. These complexes have similar decomposition profiles. The complex **Ru1** had two decomposition profiles. The first stage of decomposition occurred at 200 ^{o}C with a mass loss of approximately 25 %. This mass loss could probably be due to the loss of the cymene ring. The second stage of decomposition was observed at 320 – 380 ^{o}C with a mass loss of approximately 45 % which is most probably due to the loss of the ligand. **Ru2** had three decomposition profiles. The first stage of decomposition occurred at 100 ^{o}C with a mass loss of approximately 5 % which is due to the loss of a water molecule in the complex. The second stage of decomposition occurred at 200 – 300 ^{o}C with a mass loss of approximately 5 % which is most probably due to the loss of the ligand and the third stage of decomposition occurred at 400 ^{o}C with a mass loss of 30 % due to the loss of the cymene ring.

Complex **Ru3** had two decomposition profiles. The first stage of decomposition occurred at 280 – 300 ^{o}C with a mass loss of 50 % which is due to the loss of the ligand and the second stage of decomposition occurred at 300 – 410 ^{o}C with a mass loss of 25 % which is due to the loss of the cymene ring. The complex **Ru4** had three decomposition profiles. The first stage of decomposition occurred at 250 – 260 ^{o}C with a mass loss of 25 % which is due to the loss of the cymene ring, the second stage of decomposition occurred at 300 ^{o}C with a mass loss of 10 % which is probably due to the loss of the diethyl moiety of the ligand and the third stage of decomposition occurred at 430 ^{o}C with a mass loss of 35 % which is due to the loss of the remainder of the ligand.

From Figure 2.6 it can be observed that **Ru1** is the most stable of these ruthenium complexes and **Ru2** is the least stable of these ruthenium complexes. It is also observed that **Ru3** is more stable than **Ru4**.

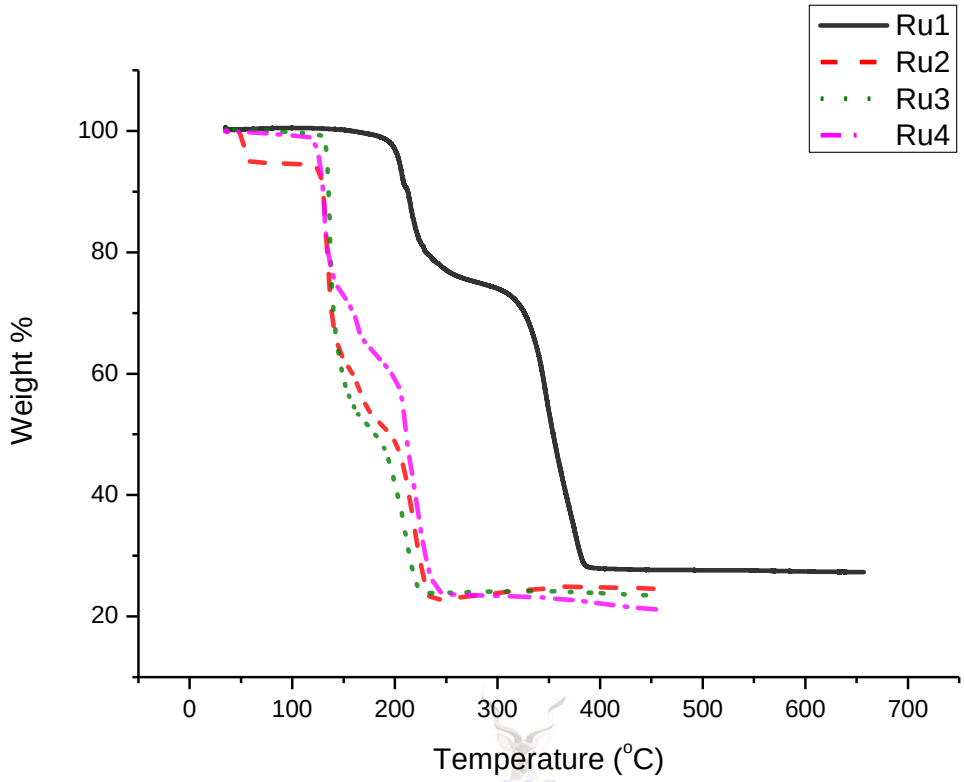

Figure 2.6: Thermogram of the TGA data of the ruthenium complexes **Ru1 - Ru4**.

2.4 Conclusion

The salicylaldimine ligands were successfully prepared by the condensation of salicylaldehyde and aniline, 2,6 – dimethylaniline, 2,6 – diisopropylaniline, and N,N-diethyl-p-phenylenediamine to give the ligands **L1** – **L4**. These ligands were obtained as yellow – orange solids with yields in the range 70 – 93 %. **L2**, however, was obtained as an oil instead of a solid. NMR spectroscopy, FTIR spectroscopy, ESI mass spectrometry and CHN elemental analysis were used to confirm that the desired ligands were obtained.

The cobalt complexes were obtained by reacting the salicylaldimine ligands with $Co(OAc)_2.4H_2O$ to give **Co1** – **Co4**. These complexes were obtained as stable brown solids with yields in the range 60 – 66 % and FTIR spectroscopy confirmed coordination of the

ligand and cobalt acetate. The ruthenium complexes were also obtained by reacting the salicylaldimine ligands with $[(\eta^6\text{-}p\text{-cymene})RuCl_2]_2$ to afford **Ru1** – **Ru4**. These complexes were obtained as red-brown to orange-brown solid with excellent yields in the range 90 – 97 %. ^{1}H-NMR spectroscopy confirmed the coordination of the ligands and $[(\eta^6\text{-}p\text{-cymene})RuCl_2]_2$ by observing a change in chemical shift of the **H**C=N when compared to the free ligand. FTIR spectroscopy also confirmed the formation of the ligand. Other techniques used to characterise the cobalt and ruthenium complexes include ESI mass spectrometry, CHN elemental analysis and TGA.

2.5 References

1. M.M.H. Khalil, E.H. Ismail, G.G. Mohamed, E.M. Zayed and A. Badr, *J. Inorg. Chem.*, 2012, **2**, 13-21.
2. E. Yousif, A. Majeed, K. Al-Sammarrae, N. Salih, J. Salimon and B. Abdullah, *Ar. J. Chem.*, 2013, 1-6.
3. M.S. Refat, M.Y. El-Sayed and A.M.A. Adam, *J. Mol. Struc.*, 2013, **1038**, 62-72.
4. N.A.I. Hisham, H. Khaledi, H.M. Ali and H.A. Hadi, *J. Coord. Chem.*, 2012, **65**, 2992-3006.
5. B. Li, Y.Q. Li and M.Y. Zhou, *Arkivoc*, 2009, **xi**, 165-171.
6. E. Farnetti, R. Di Monte and J. Kaspar, *Inorg. Bio-Inorg. Chem.*, **2**, 1-10.
7. R. Drozdzak, B. Ailaert, N. Ledoux, I. Dragutan, V. Dragutan and F. Verpoort, *Adv. Synth. Cat.*, 2005, **347**, 1721-1743.
8. E. Tas, A. Kilic, N. Konak and I. Yilmaz, *Polyhedron*, 2008, **27**, 1024-1032.

9. C.M. da Silva, D.L. da Silva, L.V. Modolo, R.B. Alves, M.A. de Resende, C.V.B. Martins and A. de Fatima, *J. Adv. Res.*, 2011, **2**, 1-8.
10. G.G. Mohamed, M.M. Omar and A.M. Hindy, *Turk. J. Chem.*, 2006, **30**, 361-382.
11. F.S. Liu, Y.T. Huang, C. Lu, D.S. Shen and T. Cheng, *Appl. Organomet. Chem.*, 2012, **26**, 425-429.
12. R.M. Ahmed, E.I. Yousif, H.A. Hasan and M.J. Al-Jeboori, *The Sci. Wor. J.*, 2013, **2013**, 2-8.
13. M.A. Bennett, T.N. Huang, T.W. Matheson, A.K. Smith, S. Ittel and W. Nickerson, *Inorg. Syn.*, 1982, **XXI**, 74-78.
14. S. Bhunora, J. Mugo, A. Bhaw-Luximon,S. Mapolie, J.L. Van Wyk, J. Darkwa and E. Nordlander, *Appl. Organanomet. Chem.*, 2011, **25**, 133-145.
15. J.L. van Wyk, S.F. Mapolie, A. Lennartson, M. Hakansson and S. Jagner, *Inorg. Chim. Acta*, 2008, **361**, 2094-2100.
16. R.K. Rath, M. Nethaji and A.R. Chakravarty, *Polyhedron*, 2001, **20**, 2735-2739.
17. Y. Nagao, T. Kaneko and K. Kozawa, *J. Jap. Soc. Col. Mat.*, 2006, **79**, 2-9.
18. L.C. Matsinha, S.F. Mapolie and G.S. Smith, *Polyhedron*, 2013, **53**, 56-61.

CHAPTER 3

CATALYTIC EVALUATION OF Co(II) AND Ru(II) SALICYLALDIMINATO COMPLEXES AS CATALYSTS IN TRANSFER HYDROGENATION OF ACETOPHENONE

3.1 Introduction

Many ruthenium complexes have been reported to be efficient catalysts in the transfer hydrogenation of ketones and imines in the presence of 2-propanol and a base.[1-2] Some examples of these complexes include the work done by Rath *et al* and Venkatachalam *et al*. Rath and co-workers reported on half-sandwich (η^6-arene) ruthenium (II) complexes bearing an N, O-donor chelating Schiff base auxiliary ligand[5] (Figure 3.1) and they concluded that the (arene) ruthenium (II) Schiff base complexes were active in the transfer hydrogenation of acetophenone. They also observed that introducing bulky substituents on the ligand backbone increased the activity of the catalyst to give conversions >90 %.[1]

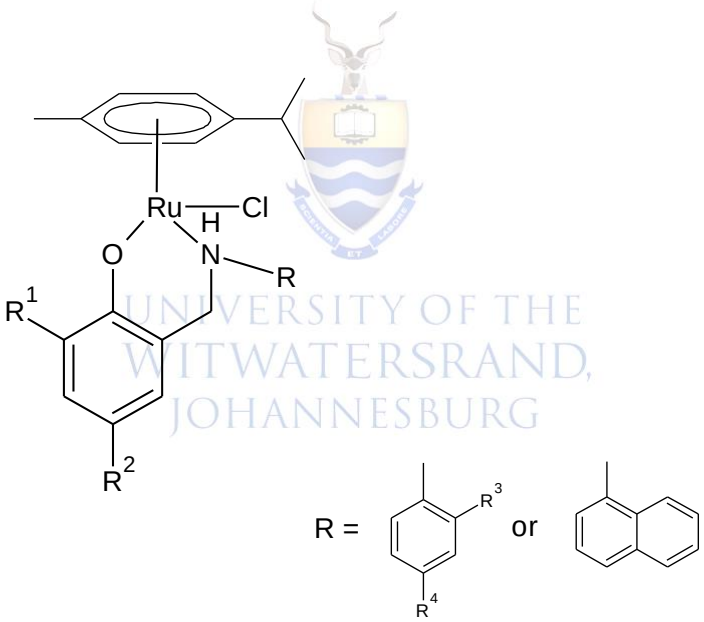

Figure 3.1: The (η^6-Arene) ruthenium (II) complex used for the transfer hydrogenation of acetophenone.[1]

Similarly, Venkatachalam and co-workers reported on the ruthenium complexes bearing N_2O_2 Schiff base ligands[2] (Figure 3.2) and they concluded that the complex [RuCl(PPh3)(DHAphen)] performed efficiently in the transfer hydrogenation of a variety of ketones and gave moderate to good yields. Excellent conversions with this catalyst were

observed for five and six membered cyclic ketones, i.e. cyclopentanol gave 92% conversion and cyclohexanol gave 90 % conversion.[2]

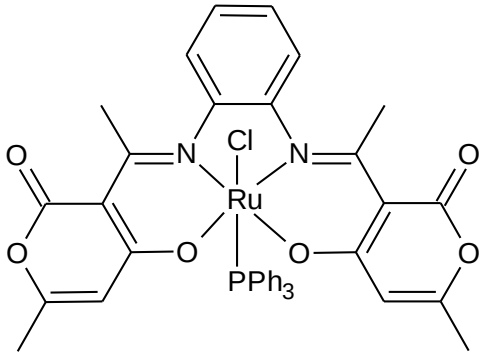

Figure 3.2: Representation of the [RuCl(PPh3)(DHAphen)] complex.[2]

One of the objectives of this project is to investigate the activity of cobalt complexes in the transfer hydrogenation process. Only a few cobalt systems have been reported for the transfer hydrogenation process. However, an example of the work done on cobalt complexes is reported by Wang *et al*. They reported on the use of cobalt complexes as catalyst precursors in the hydrogenation of ketones, aldehydes, imines, and α,β – unsaturated carbonyl compounds. One such example is the cobalt catalysts illustrated in Figure 3.3. Wang *et al* reported that this catalyst produced alcohol and imine products in good yields, under mild reaction conditions.[3] It was also noted that when converting compounds like trans-4-phenyl-3-buten-2-one and cinnamaldehyde, this catalyst reduced both the C=C and C=O bonds to the corresponding alcohols with yields >90 %. The mechanistic study of this catalyst in transfer hydrogenation was further investigated and it was observed that the cobalt–ligand cooperativity was not required for catalysis conducted by a cobalt-monohydride intermediate.[3]

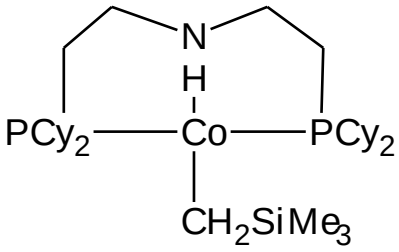

Figure 3.3: Cobalt complex that showed excellent catalytic activity in the hydrogenation of ketones, aldehydes, and imines with good yields.[3]

Transfer hydrogenation is a homogeneous process which makes separating products from the reaction mixture a problem.[4] It has, however, been established that the use of two-phase catalysis in water or high polar organic solvents is one approach to solving this problem.[5] Attempts have been made in developing biphasic processes for the homogeneous hydrogenation catalysed by transition metal complexes. According to Zhao and co-workers, aqueous – organic biphasic systems have been developed as a means to achieve product and catalyst separation.[6] However, water as a solvent was observed to have some limitations and thus the disadvantages of the aqueous – organic biphasic system are that the ligands have to be modified in order to introduce water solubility of the catalyst, some of the organic substrates are immiscible in water thus resulting in low reaction rates and in most cases water has been found to be reactive with organometallic catalysts.[6] However, introducing an ionic liquid to form an ionic liquid – biphasic system required no further modification of the catalyst system. Ionic liquids are also advantageous because of their favourable properties.[4, 6-8]

One of the objectives of this study is to investigate the use of an ionic liquid – organic biphasic system as a means to achieve separation of the catalyst and products from the reaction mixture. Ionic liquids have also been described as suitable reaction mediums in two-phase catalysis because of their favourable properties.[6-7] Suarez and co-workers reported on

the application of 1-n-butyl-3-methylimidazolium cations in the two-phase catalytic hydrogenation of cyclohexene with rhodium complexes. The product was easily removed from the reaction mixture by simple decantation while 98 % of the rhodium complexes was reported to remain retained in the ionic liquid.[5]

In this chapter, the catalytic activity of the cobalt (II) and ruthenium (II) salicylaldiminato complexes is investigated for the transfer hydrogenation of acetophenone. The activity of these complexes is also investigated in the ionic liquid 1-butyl-3-methylimidazolium ([BMIM] BF_4). Reaction parameters for preliminary study were also performed to see if the reaction parameters had an effect on the performance of the catalysts.

3.2 Experimental

3.2.1 Materials and instrumentation

All chemicals were of reagent grade and were used without further purification. All solvents were dried over the appropriate drying agent and distilled prior to use. [BMIM]BF_4 was prepared according to a literature procedure.[9] ^{1}H-NMR and {^{1}H} ^{13}C-NMR spectra of the compounds in $CDCl_3$ were obtained using a Bruker 300 MHz Ultrashield spectrophotometer, using tetramethylsilane as an internal standard. GC-MS analysis was performed using an Agilent 7890 Gas Chromatograph with helium as the carrier gas. GC-MS conditions: oven temperature 40-120-130^{o}C, flow rate 1.40 mL/min.

3.2.2. General procedure for the transfer hydrogenation of acetophenone

To a round-bottomed flask was added the complex (0.05 mmol), KOH (0.125 mmol), acetophenone (5 mmol, 0.6 ml) and isopropanol (5 ml). The resulting brown mixture was stirred at the appropriate temperature under an inert atmosphere for the specified time. The reaction mixture was cooled and the catalyst precipitated from solution by the addition of petroleum ether (b.p = 30-60^{o}C) (15 ml). An aliquot (5 ml) of the mixture was syringe-filtered and 10 µl aliquot of the mixture was diluted with MeOH to a total volume of 40 ml. A 2 ml aliquot of this dilution was analysed with GC-MS. The remaining mixture was filtered by gravity filtration and the solution was neutralised using 1M HCl. The HCl layer was decanted and the petroleum ether layer was dried using anhydrous magnesium sulphate ($MgSO_4$). The petroleum ether was distilled by rotary evaporation which resulted in a dark brown oily residue which was analysed with ^{1}H-NMR using $CDCl_3$.

3.2.3 The development of a biphasic system for the transfer hydrogenation of acetophenone

In a round-bottomed flask was added [BMIM]BF_4 (5 ml), the catalyst precursor (0.05 mmol) and KOH (0.125 mmol). The mixture was stirred under an inert atmosphere at 8 2^{o}C for 30 minutes. To this solution was added acetophenone (5 mmol) and 2-propanol (5 ml) dissolved in toluene (10 ml). This resulted in a two-phase system. The mixture was stirred under an inert atmosphere at an appropriate temperature for a specified time. The reaction mixture was allowed to cool to room temperature upon which the two layers separated. The organic layer was decanted from the flask and 10 µl aliquot of the organic layer was diluted with MeOH to a total volume of 40 ml. A 2 ml aliquot of this dilution was analysed by GC-MS.

3.3 Results and discussion

3.3.1 Transfer hydrogenation of acetophenone using Ru(II) and Co(II) salicylaldimine complexes

The transfer hydrogenation of acetophenone was studied using complexes **Ru1 - Ru4** and **Co1 - Co4** (Figure 3.4) as catalyst precursors in the presence of 2-propanol as the solvent and hydrogen source and KOH as the catalyst activator. The catalyst:KOH:acetophenone ratio used was 1:2.5:100 for all the reactions, irrespective of the catalyst precursor used. All the reactions were performed under an inert atmosphere. Preliminary reactions performed with the ruthenium complexes at 82 ^{o}C for 6 h were analysed with ^{1}H-NMR to establish if these complexes were active towards the transfer hydrogenation process. After the elapsed reaction time, petroleum ether (15 ml) was added to the reaction mixture to precipitate the complex. The mixture was gravity-filtered and neutralised with 1M HCl which was then decanted and the petroleum ether layer was dried using $MgSO_4$. The petroleum ether layer was distilled by rotary evaporation to afford a dark brown oily residue which was analysed with ^{1}H-NMR.

The catalytic evaluation was done for all the ruthenium complexes and the ^{1}H-NMR were obtained. A typical ^{1}H-NMR of the reaction mixture after work-up is shown in Figure 3.5. Figure 3.5 (a) shows the spectrum of acetophenone and (b) shows the spectrum obtained after performing the catalytic experiment with **Ru2**. The ^{1}H-NMR spectrum of acetophenone (Figure 3.5 (a)), we observed a signal that arises from the C**H**$_3$ which gave a singlet at 2.42 ppm and we also observed multiplets due to the aromatic protons in the aromatic region. In Figure 3.5 (b), a doublet was observed at 1.42 ppm, a quartet was observed at 4.80 ppm and multiplets due to the aromatic protons were observed in the aromatic region. This observation confirmed the conversion of acetophenone to 1-phenylethanol. However, the spectrum of 1-phenylethanol showed trace amounts of acetophenone. The singlet was observed at 2.51 ppm and the aromatic protons were observed in the aromatic region. This is an indication that not

all of the acetophenone was converted to 1-phenylethanol. This was observed for all the ruthenium complexes.

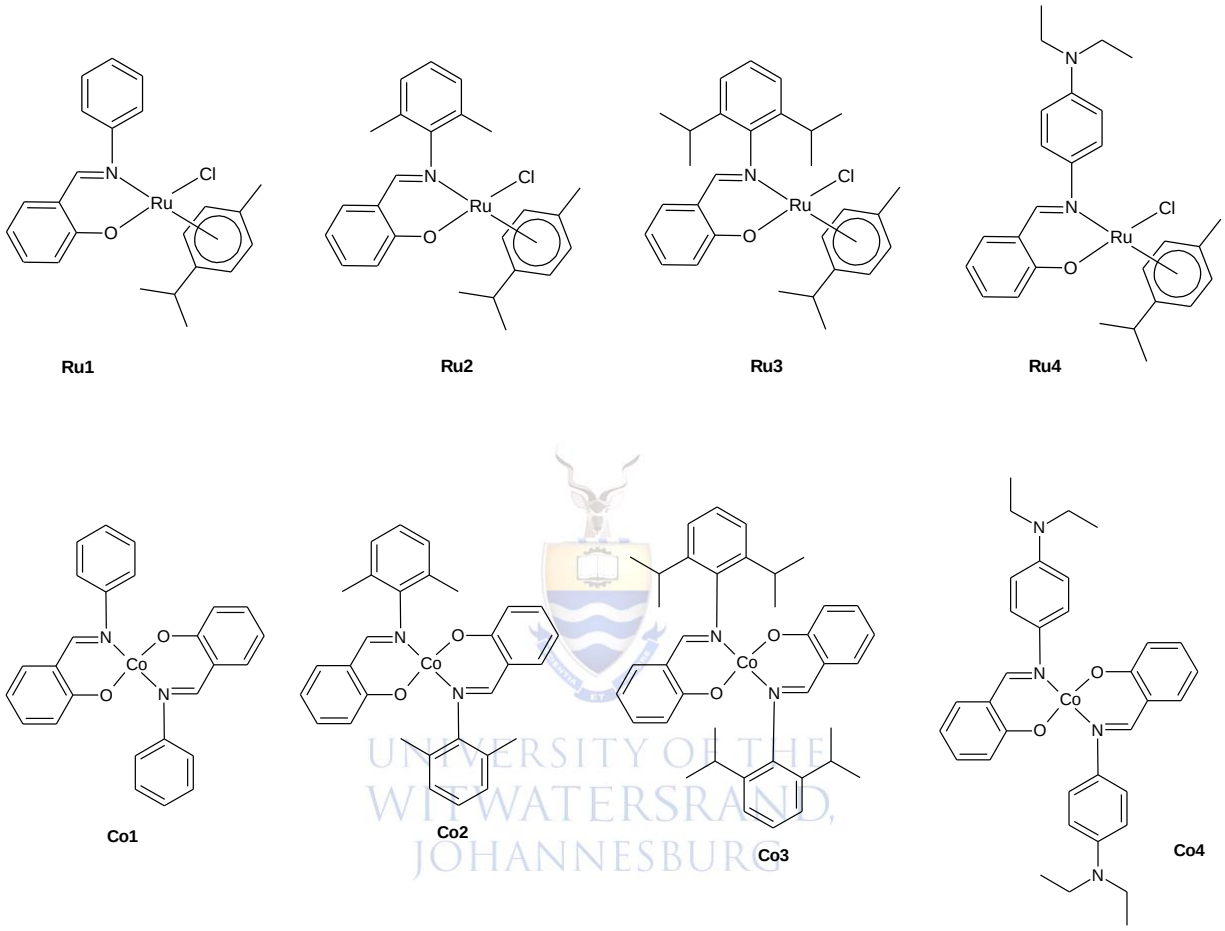

Figure 3.4: The catalyst precursors (**Ru1 - Ru4** and **Co1 - Co4**) used in the conversion of acetophenone to 1-phenylethanol.

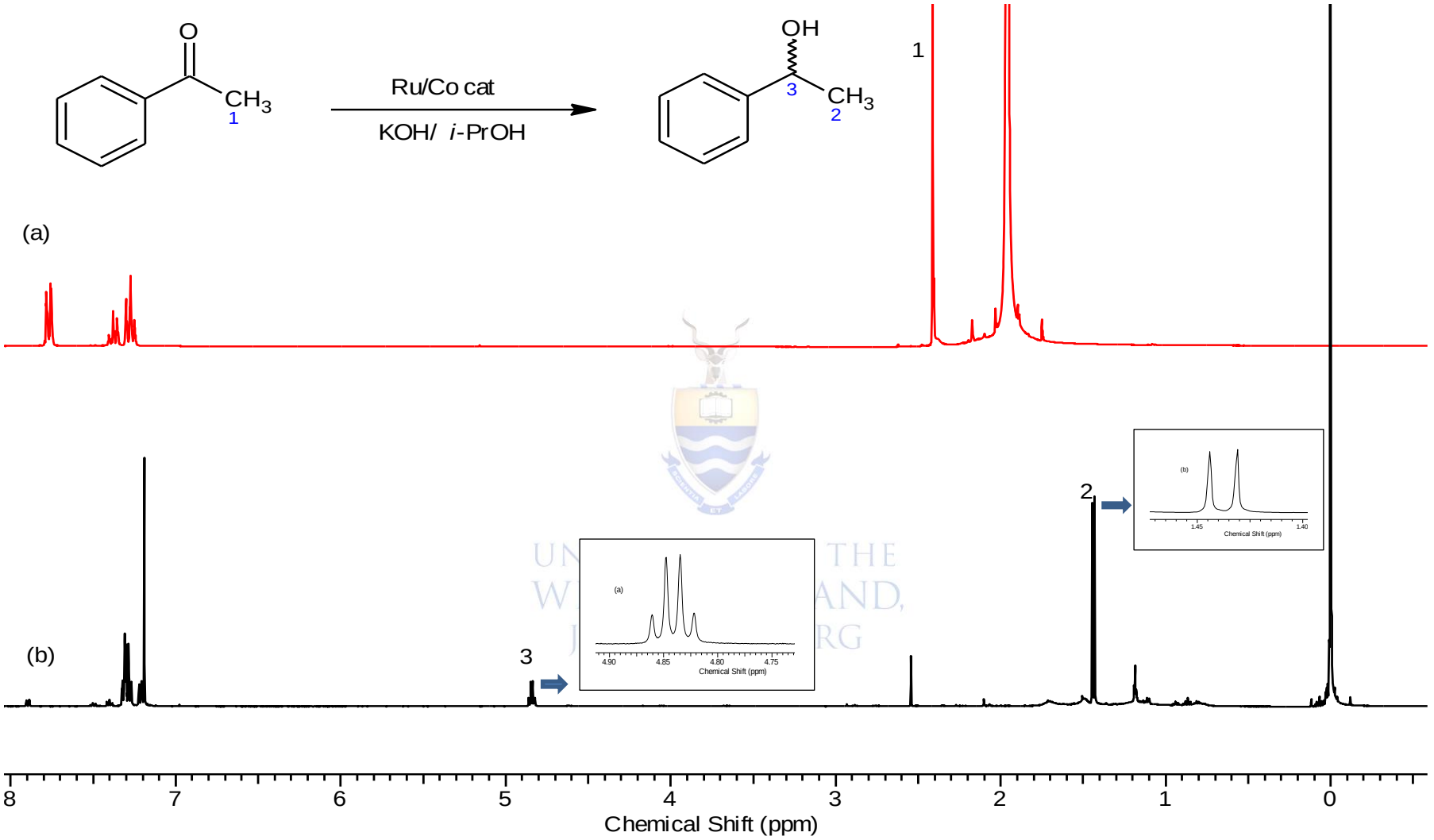

Figure 3.5: ^{1}H-NMR spectrum of (a) acetophenone and (b) reaction residue after using catalyst precursor **Ru2** at 82 ^{o}C for 48 h.

GC-MS was used to quantify conversion of acetophenone in the experiments for all the complexes. An aliquot of the reaction mixture (5 ml) was syringe-filtered from which a 10 µl aliquot was diluted to a total volume of 40 ml using HPLC-grade MeOH. This solution (2 ml) was taken and analysed by GC-MS with an oven temperature range of 40 – 120 – 130 ^{o}C and a flow rate of 1.40 ml/min with helium as the carrier gas. Figure 3.7 shows GC-MS analysis of the reaction mixture obtained with **Ru2**. According to the GC chromatogram in Figure 3.7, (a) is the peak corresponding to 1-phenylethanol and (b) is the peak corresponding to acetophenone based on the GC-MS library as was confirmed by the acetophenone chromatogram. According to the data obtained from the GC, 1-phenylethanol was eluted before acetophenone. Figure 3.6 shows the GC chromatogram of acetophenone and it was observed that acetophenone is eluted at 7:24 (min:sec) as was observed in Figure 3.7. The percentage conversions were determined by calculating the area under the curve. The mass spectra obtained for the two compounds are shown in Figure 3.8 **(A)** and **(B)** and they correlate to what was obtained in the library.

The conversion of acetophenone to 1-phenylethanol produces enantiomers giving the *R* and *S* configurations. The enantioselectivity of the catalyst was not investigated simply because the complexes used are not expected to be enantioselective because these complexes do not have a centre of chirality.

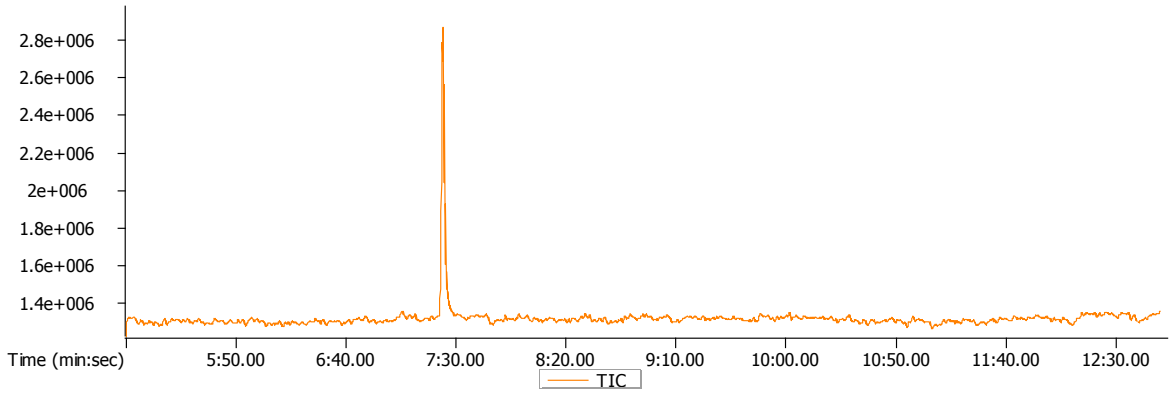

Figure 3.6: GC chromatogram of acetophenone.

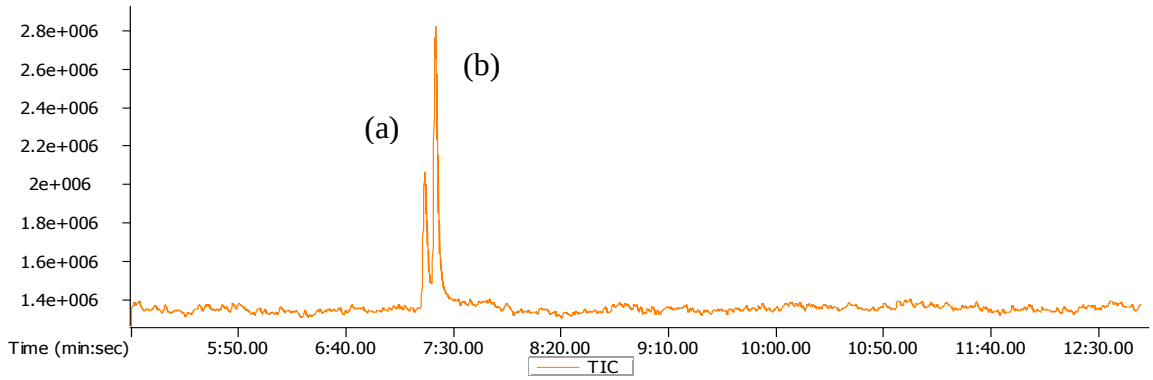

Figure 3.7: GC chromatogram of reaction aliquot when using **Ru2** as the catalyst precursor at 82 ^{o}C for 48 h showing the elution of (a) 1-phenylethanol and (b) acetophenone

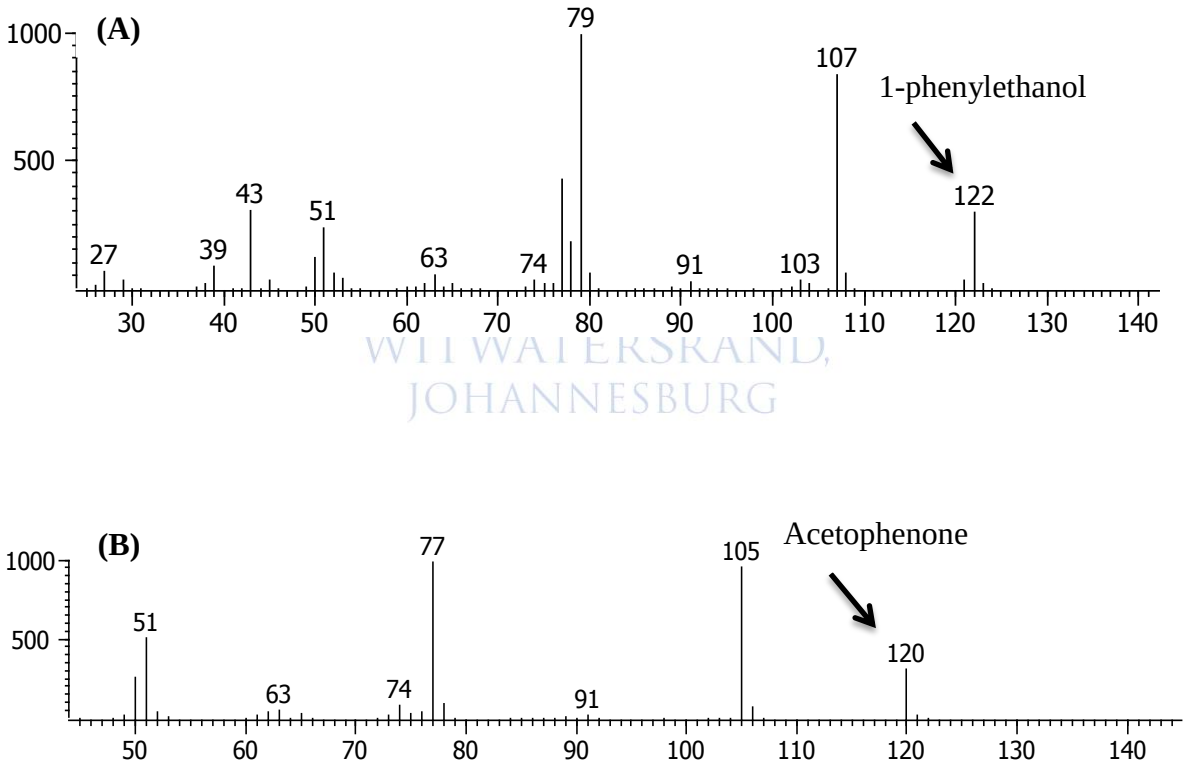

Figure 3.8: Representation of **(A)** the mass spectrum of 1-phenylethanol (molar mass = 122) and **(B)** the mass spectrum of acetophenone (molar mass = 120) from the reaction aliquot when using **Ru2** as the catalyst precursor at 82 ^{o}C for 48 h.

3.3.1.1 Catalytic studies performed with Ru(II) and Co(II) complexes

The catalytic studies for the transfer hydrogenation process were performed with both the ruthenium and cobalt complexes. The data is shown in Table 3.1. The ruthenium complexes were found to be active in the transfer hydrogenation of acetophenone. However, the cobalt complexes were observed to not be active in the transfer hydrogenation of acetophenone. The catalytic experiments for all the complexes were performed for 6 h at 82 ^{o}C. It was observed that only **Ru2** gave significant conversion. Increasing the reaction time to 48 h resulted in improvement in conversion for all the ruthenium complexes. However, **Ru2** still remained the best performing catalyst.

Table 3.1: The catalytic activity of the catalyst precursors in the transfer hydrogenation of acetophenone.

Entry	Complex	Conversion %[a]	
		6 h	48 h
1	**Ru1**	trace	13
2	**Ru2**	30	91
3	**Ru3**	trace	6
4	**Ru4**	trace	19

Reaction conditions: Ru/Co cat (0.05 mmol), acetophenone (5 mmol), *i*-PrOH (5 cm^3), KOH (0.125 mmol)

[a] GC-MS conditions: oven temperature 40-120-130^{o}C, flow rate 1.40 mL/min, carrier gas is helium.

When comparing the performance of the ruthenium complexes to the cobalt complexes (Figure 3.9), it was observed that the ruthenium complexes were active catalyst precursors but the cobalt complexes still remained inactive. This observation was not unexpected since ruthenium complexes have been reported in literature to be active in the transfer

hydrogenation process while the cobalt complexes are rarely reported for this process. The cobalt salicylaldiminato complexes were, however, still tested for transfer hydrogenation with the aim of observing the effect that the salicylaldimine ligands would have on the activity of the cobalt complexes.

Comparing the ruthenium complexes in transfer hydrogenation studied by Rath *et al* and Venkatachalam *et al*, it was observed that the ruthenium complexes prepared in this study had poorer performance. Rath and his co-workers studied the transfer hydrogenation of acetophenone under similar conditions (82 ^{o}C for 6 h) and they observed good conversions in the range 70 – 98 %.[1] Similarly, Venkatachalam and his co-workers studied the transfer hydrogenation catalytic process at 80 ^{o}C for 1 h and they observed conversions in the range 45 – 99%.[2] It can, therefore, be deduced that the ligand backbone plays a significant role in the activity of the ruthenium complexes just as Rath *et al* attributed their percentage conversions to the nature of the ligand backbone.[1]

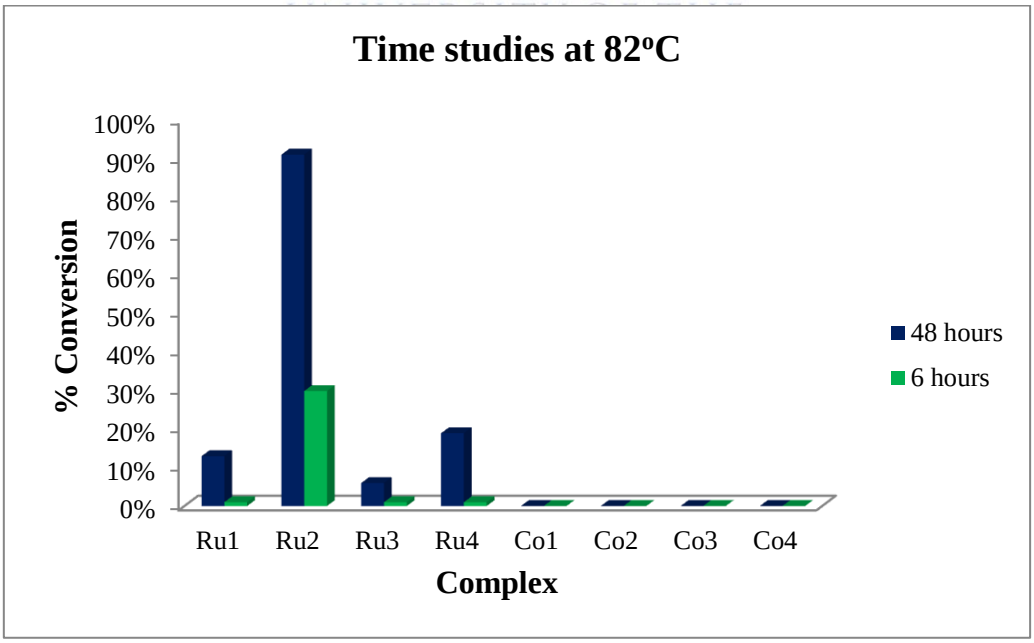

Figure 3.9: The effect of time on the catalytic activity of complexes **Ru1 - Ru4** and **Co1 - Co4**.

3.3.1.2 The effect of temperature on the catalytic performance

The catalytic performance of **Ru2** and **Co3** were studied at various temperatures to determine the effect that temperature has on the performance of these catalysts. The temperature effect was evaluated on **Ru2** because this complex gave the highest catalytic activity. The temperatures investigated were 82 ^{o}C, 90 ^{o}C, 100 ^{o}C, 120 ^{o}C and 140 ^{o}C. The internal temperatures of the reaction mixtures were confirmed by measuring the temperature with a thermometer. These studies were performed for 6 and 48 h. The results obtained are based on single runs. The results are summarised in Table 3.2. The cobalt complex still remained inactive in the transfer hydrogenation of acetophenone.

Table 3.2: Effect of temperature on the catalytic activity of complexes **Ru2** and **Co3**.

Complex	Time (h)	Temperature (^{o}C)	% Conversion[a]
Ru2	6	82	30
		90	32
		100	34
		120	27
		140	27
	48	82	91
		90	94
		100	95
		120	95
		140	67

Reaction conditions: Complex (0.05 mmol), acetophenone (5 mmol), *i*-PrOH (5 cm^{3}), KOH (0.125 mmol)

[a] GC-MS conditions: oven temperature 40-120-130^{o}C, flow rate 1.40 mL/min, carrier gas is helium.

When comparing the effect of temperature on **Ru2**, a dramatic increase in conversion was observed when increasing the reaction time from 6 h to 48 h. When performing the catalysis for 6 h, it was observed that there was a slight increase in conversion for this complex when the temperature was increased from 82 ^{o}C to 100 ^{o}C and then a slight drop in the conversion when increasing the temperature from 120 – 140 ^{o}C. Increasing the reaction time to 48 h, a

slight increase was observed in the activity at when the temperature was increased from 82 – 120 ^{o}C and then a drop in activity after increasing the temperature to 140 ^{o}C. The drop in the conversion of this complex is possibly due to the loss in activity.

Some work reported on evaluating the effect of temperature includes that done by Shingote. This study investigated the effect of temperature on the transfer hydrogenation of acetophenone with $[Ru(benzene)Cl_2]_2$ as the complex and observed that increasing the temperature of reaction resulted in an increase in conversion.[10] Therefore, we expected to observe a similar trend with our complexes but that was not what was observed.

3.3.2. Catalytic studies using an ionic liquid – organic system in the transfer hydrogenation of acetophenone

One of the objectives of this project was to study the possibility of separating the catalyst from the products and the re-use of the catalyst by developing a biphasic system. All the ruthenium complexes were studied in this system because they were observed to be better performing than the cobalt complexes in the transfer hydrogenation of acetophenone.

It was observed that 2-propanol was miscible with the $[BMIM]BF_4$ ionic liquid and did not form a two-phase biphasic system. Therefore, a range of organic solvents was tested with the ionic liquid and it was found that toluene was the only solvent that produced a two-phase system with $[BMIM]BF_4$. The studies were therefore performed with toluene. This then resulted in a biphasic system with the catalyst in the ionic liquid phase and the substrates and products in the organic phase. It was observed after the elapsed reaction time that the organic phase was discoloured to the same colour as the ionic liquid layer meaning that the clear organic phase before the start of the reaction changed to the same colour as the organic layer

in the process of the reaction. This was reasoned to the fact that the catalyst leaches into the organic layer.

The objective of these studies was to determine if we can recycle the catalysts and therefore three cycle experiments were performed. For cycle 1, the catalyst precursor (0.05 mmol) and KOH (0.125 mmol) were dissolved in [BMIM]BF_4 (5ml) by stirring. Meanwhile, 2-propanol (5 ml) and acetophenone (5 mmol) were dissolved in toluene (10 ml). The toluene mixture was added to the ionic liquid mixture and the reaction was performed for 48 h at 82 ^oC. After the elapsed reaction time the organic layer was decanted and analysed with GC-MS. The second cycle was initiated by adding a fresh batch of the toluene mixture to the ionic liquid layer and the reaction was performed for 48 h and the organic phase was decanted and analysed with GC-MS. Cycle 3 was performed similarly to cycle 2. GC-MS analysis was performed by taking an aliquot (10 µl) of the decanted organic layer, diluting it with MeOH to a total volume of 40 ml from which 2 ml was extracted and analysed by GC-MS. The results are summarised in Table 3.3.

Table 3.3: The effect of the ionic liquid on the catalytic activity of **Ru1 - Ru4**

Complex	**% Conversion**		
	Cycle 1	**Cycle 2**	**Cycle 3**
Ru1	17	3	trace
Ru2	42	27	17
Ru3	8	3	2
Ru4	trace	13	61

Reaction conditions: Ru cat (0.05 mmol); acetophenone (5 mmol); *i*-PrOH (5 cm^3); KOH (0.125 mmol); toluene (10 cm^3); [C_4C_1Im] BF_4 (5 cm^3); t=48 h; T=82^oC

The complexes **Ru1** – **Ru3** behaved similarly in these studies. It was observed that the performance of these catalysts decreased from the first cycle to the third cycle. According to a study by Geldbach and co-workers, catalyst recycling was possible with their catalysts but the disadvantage was that it resulted in a decrease in the catalyst activity which was attributed to leaching of the catalyst[11]. In the experiments performed in this study, the decrease in activity of these catalysts with each cycle could be due to catalyst leaching.

Comparing the performance of catalysts **Ru1** and **Ru3** in the ionic liquid – organic biphasic system (Table 3.3) to reactions performed only in the organic solvent system, a slight increase in conversion in the first cycle is observed (Table 3.1). However, for **Ru2** a dramatic decrease in the conversion was observed and this could be due to the nature of the ligand backbone. This, therefore, means that introducing the ionic liquid has an effect on the conversion of these catalysts. This observation is also shown in Figure 3.10.

Catalyst precursor **Ru4**, however, behaved differently from the other ruthenium catalyst precursors because its activity increased with each cycle. This observation could be because the ionic liquid enhances the performance of **Ru4** because of the nitrogen functionality on the ligand backbone as compared to the other complexes. It is possible that the ionic liquid retains the complex with each cycle. However, there is no clear reason for this observation and therefore further investigation will have to be conducted.

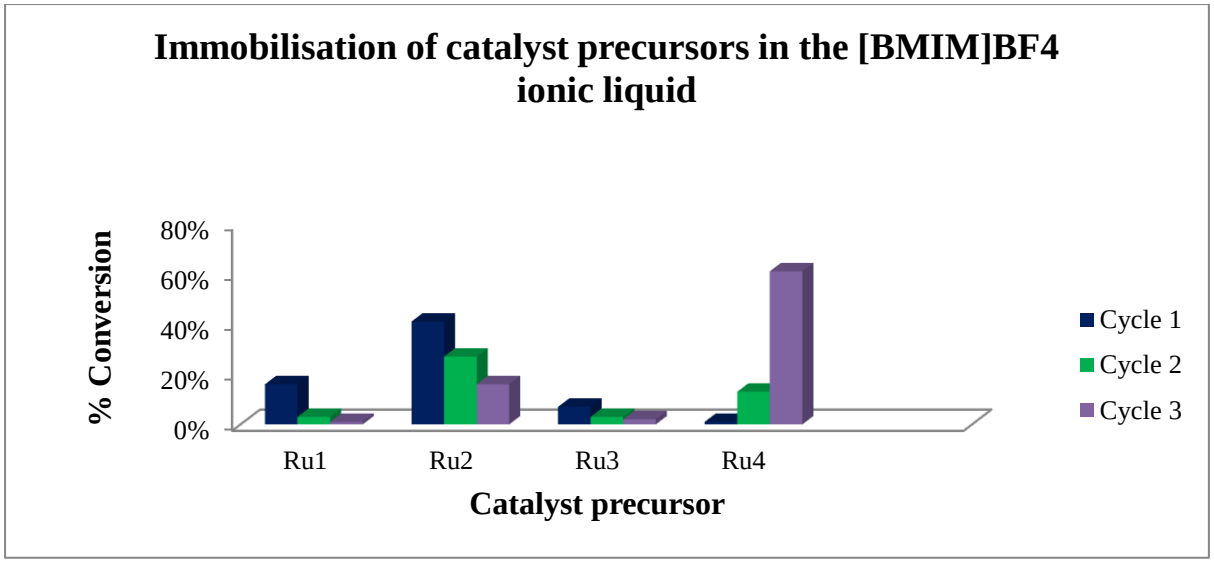

Figure 3.10: The catalytic activity of the catalyst precursors when dissolved in the [BMIM]BF_4 ionic liquid.

3.4 Conclusion

The catalytic activity of the ruthenium (II) and cobalt (II) salicylaldimine complexes was evaluated in the transfer hydrogenation of acetophenone to 1-phenylethanol. Temperature studies were performed to evaluate the effect it has on the performance of the catalyst precursors. It was expected that an increase in temperature would result in an increase in conversion for complexes; however, this expectation was not fulfilled because increasing the temperature did not have the expected effect on the performance of the complexes.

The ruthenium complexes were observed to be active towards the transfer hydrogenation of acetophenone and the cobalt (II) catalysts were observed to have no activity. However, catalyst **Ru2** was observed to have the best activity when compared to the other catalysts prepared in this study.

An ionic liquid – organic biphasic system was investigated where [BMIM]BF_4 ionic liquid was the one phase and toluene was the second phase. Catalyst precursors **Ru1**, **Ru2**, and **Ru3**

were suspected to leach into the organic layer because they were not retained in the ionic liquid. **Ru4**, however, behaved differently when compared to the other catalyst precursors. The reason for this is not clear which therefore needs further investigation.

3.5 References

1. R.K. Rath, M. Nethaji and A.R. Chakeavarty, *Polyhedron*, 2001, **20**, 2735-2739.
2. G. Venkatachalam and R. Ramesh, *Inorg. Chem. Comm.*, 2005, **8**, 1009-1013.
3. D. Wang and D. Astruc, *Chem. Rev.*, 2015, **115**, 6621-6686.
4. T. Welton, *Chem. Rev.*, 1999, **99**, 2071-2083.
5. P.A.Z. Suarez, J.E.L. Dullius, S. Einloft, R.F. de Souza and J. Dupont, *Polyhedron*, 1996, **15 (7)**, 1217-1219.
6. D. Zhao, M. Wu, Y. Khou and E. Min, *Cat. Tod.*, 2002, **74**, 157-189.
7. A.C. Cole, J.L. Jensen, I. Ntai, K.L.T. Tran, K.J. Weaver, D.C. Forbes and J.H. Davis, Jr, *J. Am. Chem. Soc.*, 2002, **124**, 5962-5963.
8. R. Sheldon, *The Roy. Soc. Chem.*, 2001, 2399-2407.
9. C.C. Cassol, G. Ebeling, B. Ferrera and J. Dupont, *Adv. Syn. Cat.*, 2006, **348**, 243-248.
10. S.K. Shingote, *Studies in Catalytic Transfer Hydrogenation Reactions*, 'Doctor of Philosophy Thesis', University of Pune, 2012.
11. T.J. Geldbach and P.J. Dyson, *J. Am. Chem. Soc.*, 2004, **126**, 8114-8115.

CHAPTER 4

Summary

The salicylaldimine ligands (**L1** – **L4**) were successfully synthesised and were obtained in good yields in the range 70 – 93 %. They were obtained as yellow to orange solids; however, **L2** was obtained as an oil instead of a solid as was expected. CHN elemental analysis showed inconsistency in the carbon composition of **L2** which is probably due to the presence of impurities in the compound. The cobalt complexes (**Co1** – **Co4**) were successfully synthesised and they were obtained as stable brown solids with good yields in the range 60 – 66 %. The ruthenium complexes (**Ru1** – **Ru4**) were also successfully synthesised and were obtained as red-brown to orange-brown solids with excellent yields in the range 90 – 97 %. The formation of these complexes was confirmed by ^{1}H-NMR spectroscopy by observing a change in chemical shift of the **H**C=N proton and the disappearance of the O**H** proton. It was also observed that the four cymene ring protons appeared as four doublets in the range δ4.12 – 5.35 ppm for the complexes as compared to $[(\eta^{6}$-*p*-cymene)$RuCl_2]_2$ where the four cymene ring protons were observed as two doublets. The characterisation techniques that were employed in characterising the synthesised ligands and complexes include NMR spectroscopy, FTIR spectroscopy, ESI mass spectrometry, CHN elemental analysis and TGA.

The synthesised cobalt (II) and ruthenium (II) salicylaldiminato complexes were applied as catalyst precursors in the transfer hydrogenation of acetophenone using 2-propanol as the hydrogen source and solvent and KOH as the base. Preliminary reactions with all the synthesised complexes were performed for 6 h at 82 ^{o}C and the crude mixture was analysed with ^{1}H-NMR spectroscopy and GC - MS. Upon increasing the reaction time to 48 h, a dramatic increase in the performance of the ruthenium complexes was observed. The

ruthenium complexes were observed to be active towards the transfer hydrogenation of acetophenone with **Ru2** being the most active while the cobalt complexes were observed to have no activity.

The catalytic performance was also investigated at various temperatures for the complexes **Ru2** and **Co3**. The cobalt complex was still inactive in the transfer hydrogenation of acetophenone even at various temperatures. It was observed that an increase in temperature did not have any significant effect on the performance of the ruthenium complex. When the catalytic reactions were performed for 6 h, it was observed that the conversions of this complex increased when the temperature was increased for 82 – 100 ^{o}C; but increasing the temperature to above 100 ^{o}C resulted in a decrease in the conversion of this complex. When the catalytic reactions were performed for 48 h, the conversions of this complex was observed to increase when the temperature was increased from 82 – 120 ^{o}C; but increasing the temperature to 140 ^{o}C resulted in a decrease in the conversion of this complex. The decrease in conversion of the **Ru2** is attributed to the possibility in the loss of the catalytic activity of the complex.

All the ruthenium complexes (**Ru1** – **Ru4**) were investigated in an ionic liquid – organic biphasic system. It was observed for **Ru1** – **Ru3** that there was an increase in the catalytic performance in the first cycle in comparison to the catalytic activity observed in the absence of the ionic liquid. The catalytic activity of these complexes was observed to have decreased in the second and third cycles. This observation was attributed to the possibility of catalyst leaching. **Ru4**, however, behaved differently from the other complexes. The catalytic performance of this complex was observed to increase with each cycle. This is probably because the ionic liquid enhances the performance of this complex. The performance of this complex, however, still needs to be further investigated.

Future work/recommendations

- Investigate the effect of the ligand backbone on the catalytic activity of the complexes because the nature of the substituents on the backbone can have an effect on the activity of the catalyst precursors.
- Investigate the performance of the complexes at 140 ^{o}C by repeating the reactions and observing if the same results are obtained. If the same results are obtained then further investigation on the drop in catalytic activity should be conducted.
- Investigate the possibility of the catalyst precursors leaching from the ionic liquid phase to the organic phase which would better explain the loss in activity of the catalyst precursors with each cycle.
- Further investigate transfer hydrogenation in the biphasic system and investigate the behaviour of **Ru4** in the presence of the ionic liquid. Investigate why the activity of **Ru4** increases with each cycle.

Appendix

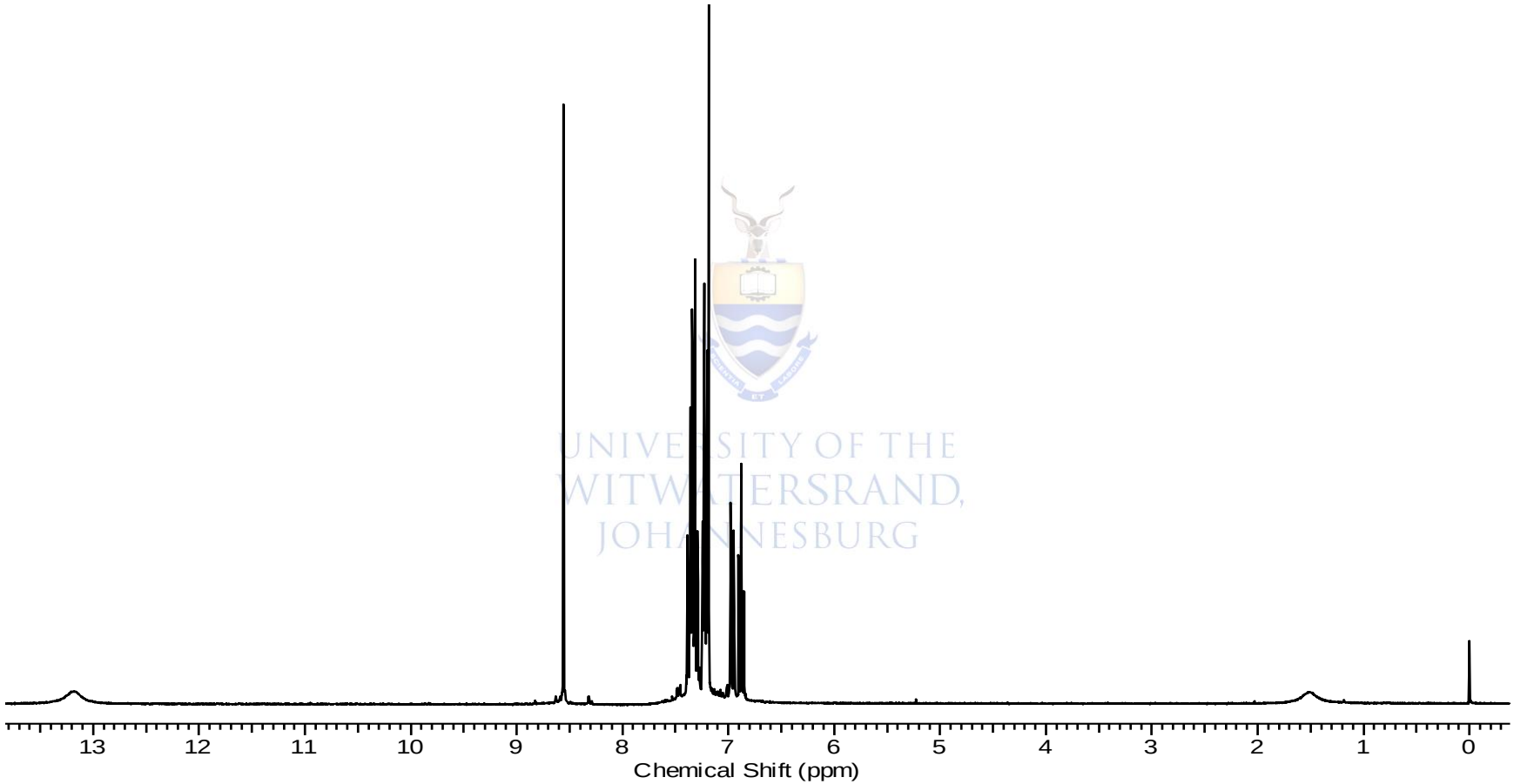

*[1]H-NMR spectrum of salicylaldimine ligand **L1**.*

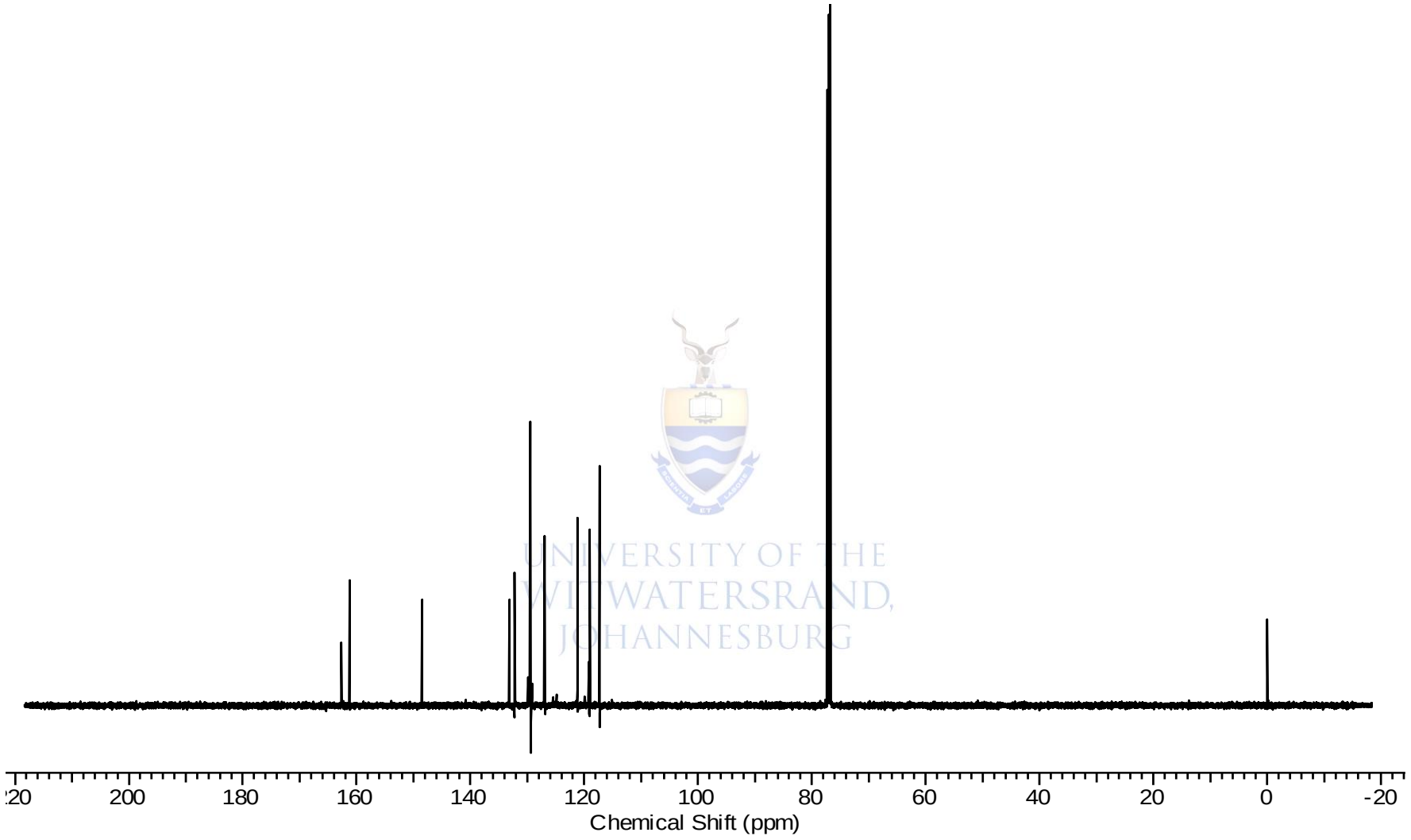

*^{13}C-NMR spectrum of salicylaldimine ligand **L1**.*

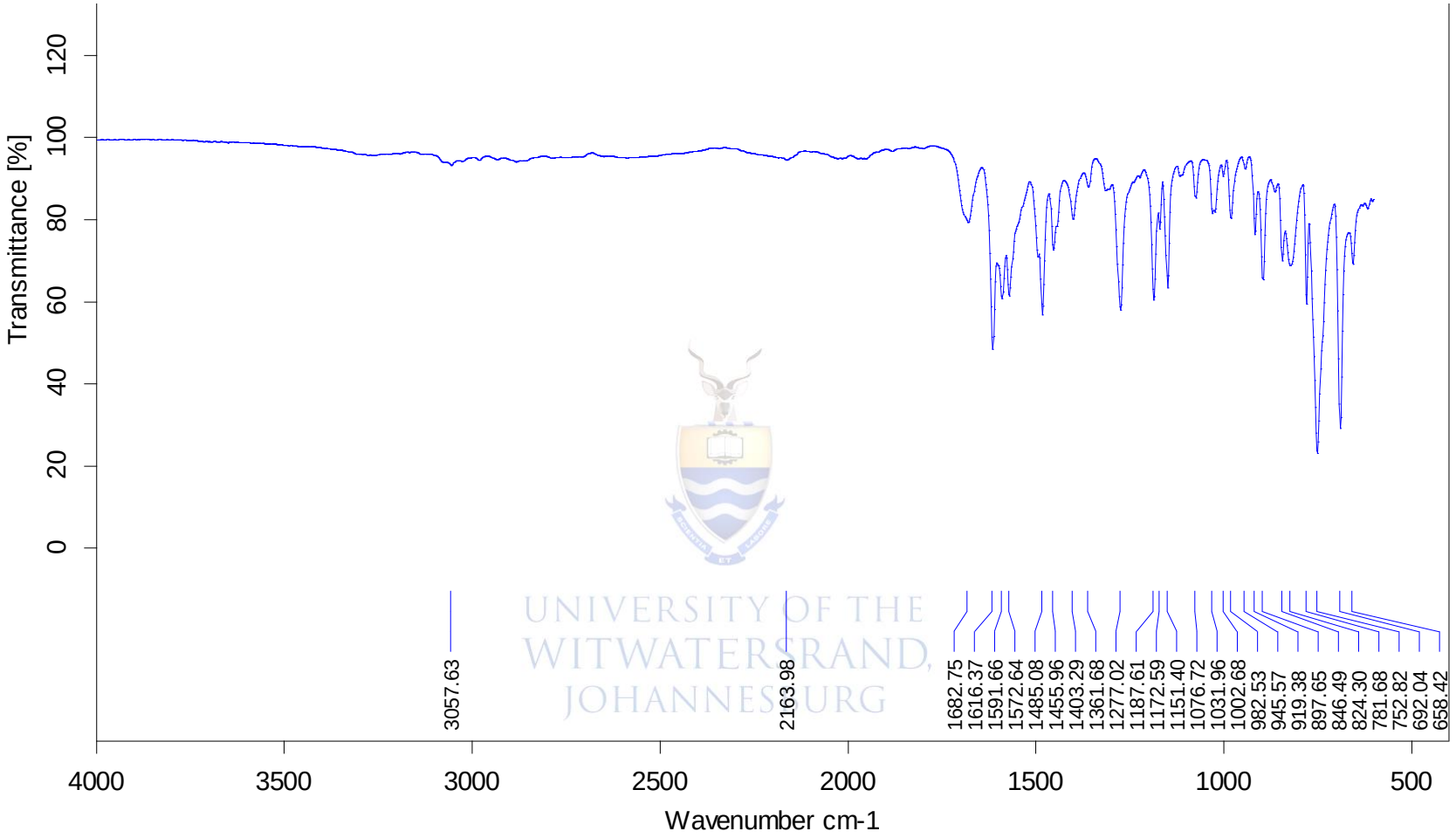

*FTIR spectrum of salicylaldimine ligand **L1**.*

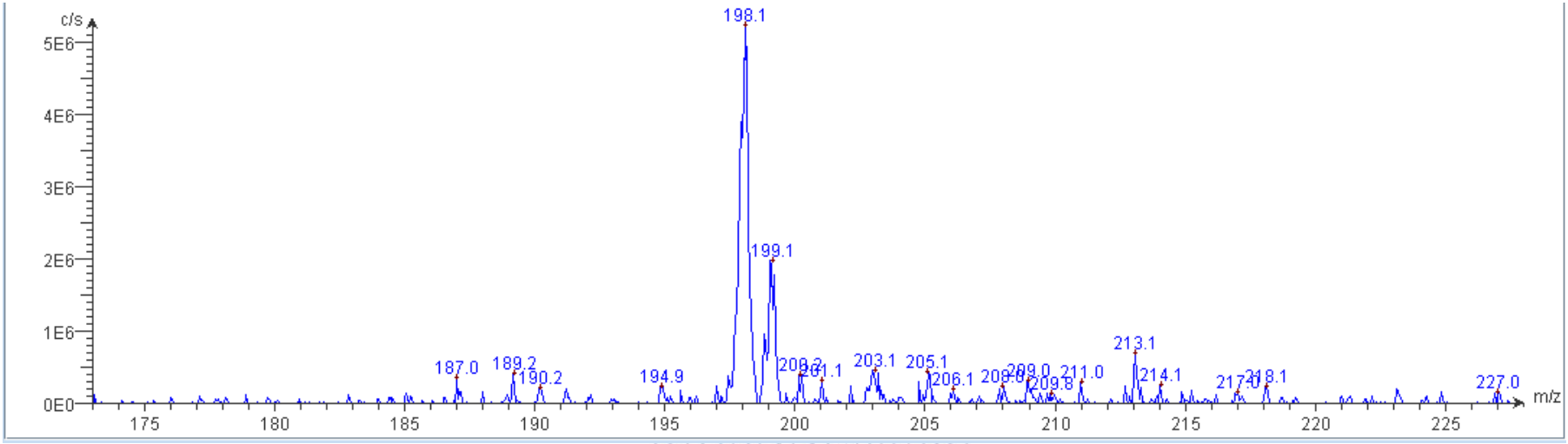

*Mass spectrum of salicylaldimine ligand **L1**.*

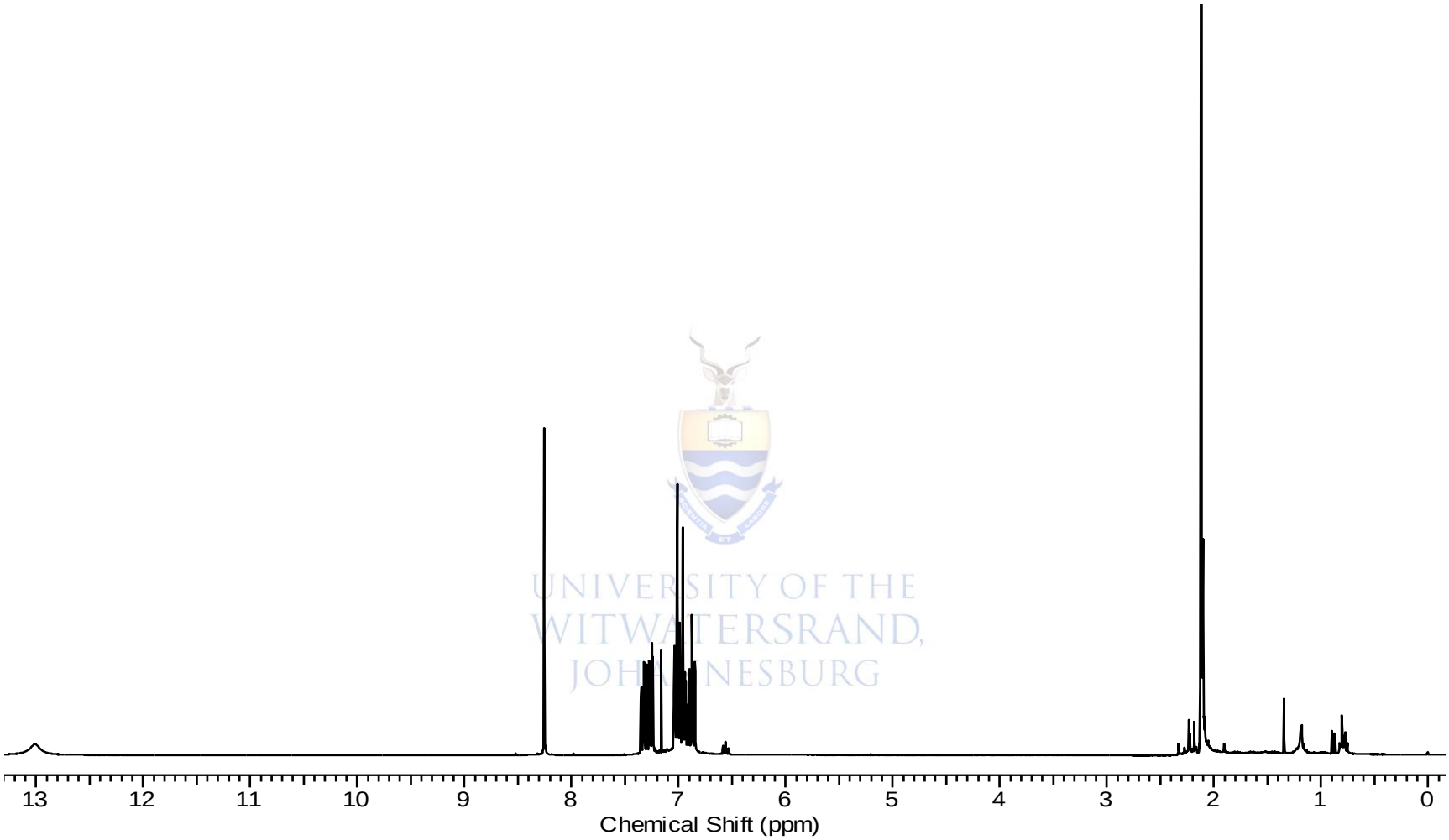

*^{1}H-NMR spectrum of salicylaldimine ligand **L2**.*

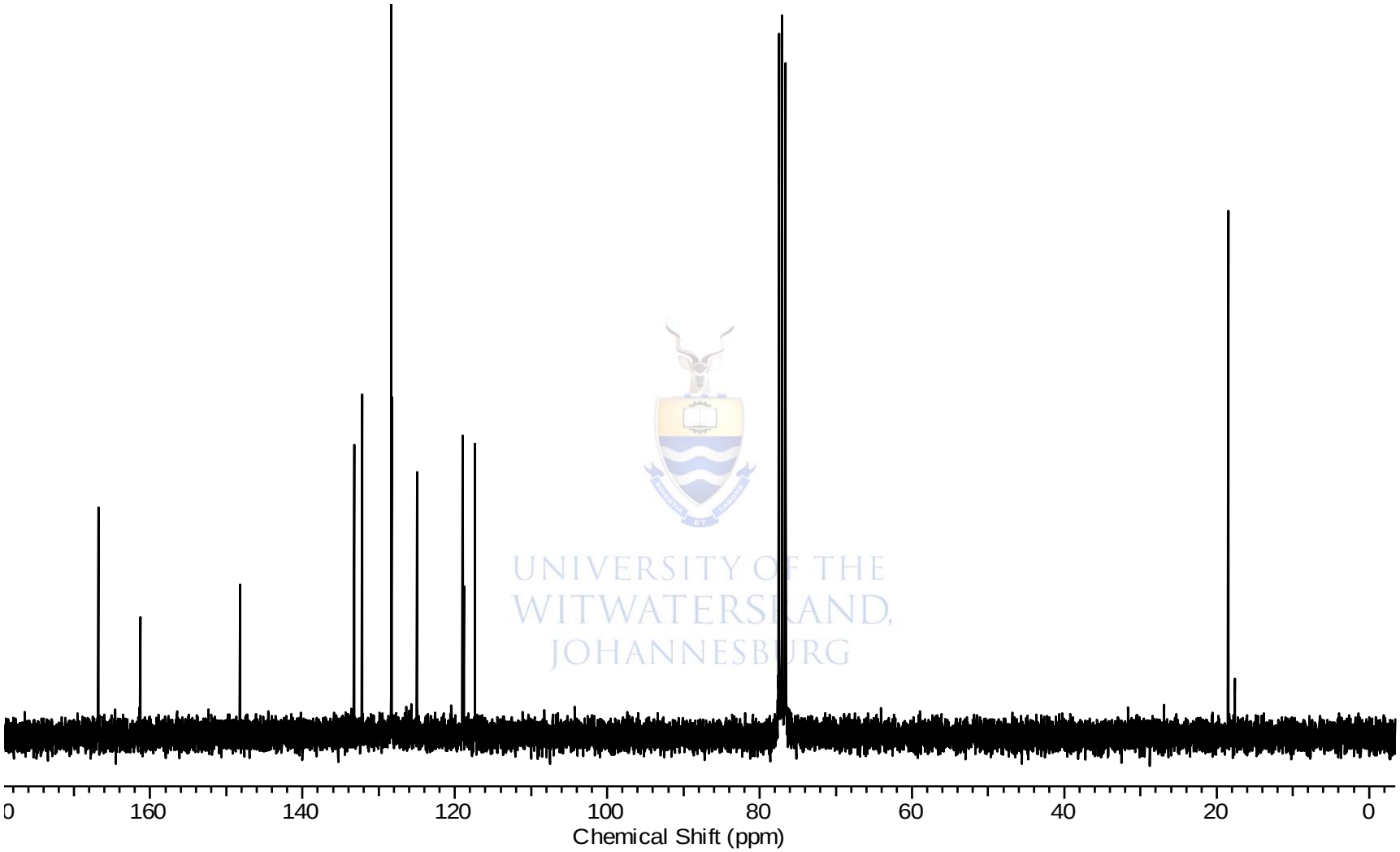

*^{13}C-NMR spectrum of salicylaldimine ligand **L2**.*

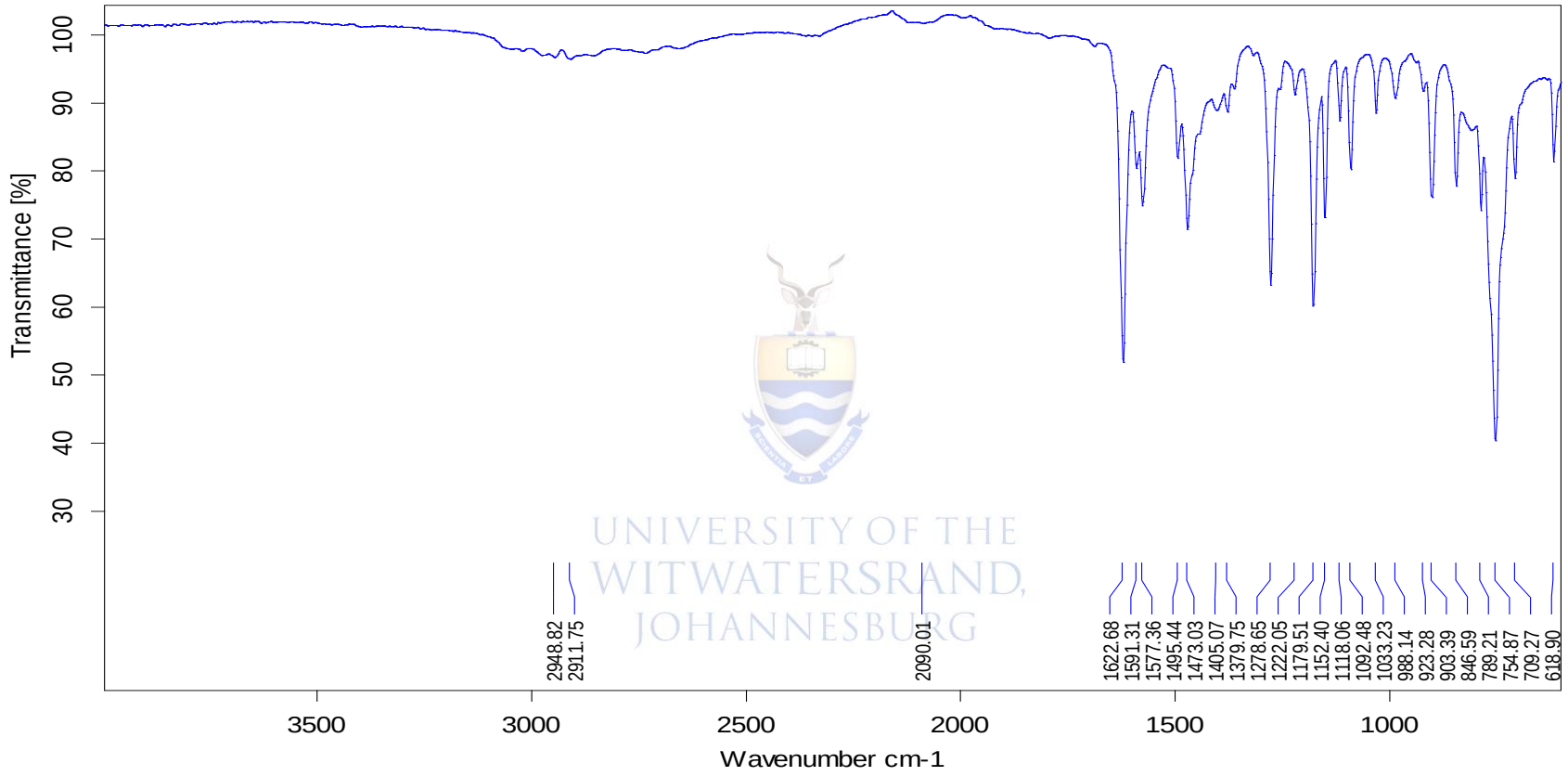

*FTIR spectrum of salicylaldimine ligand **L2**.*

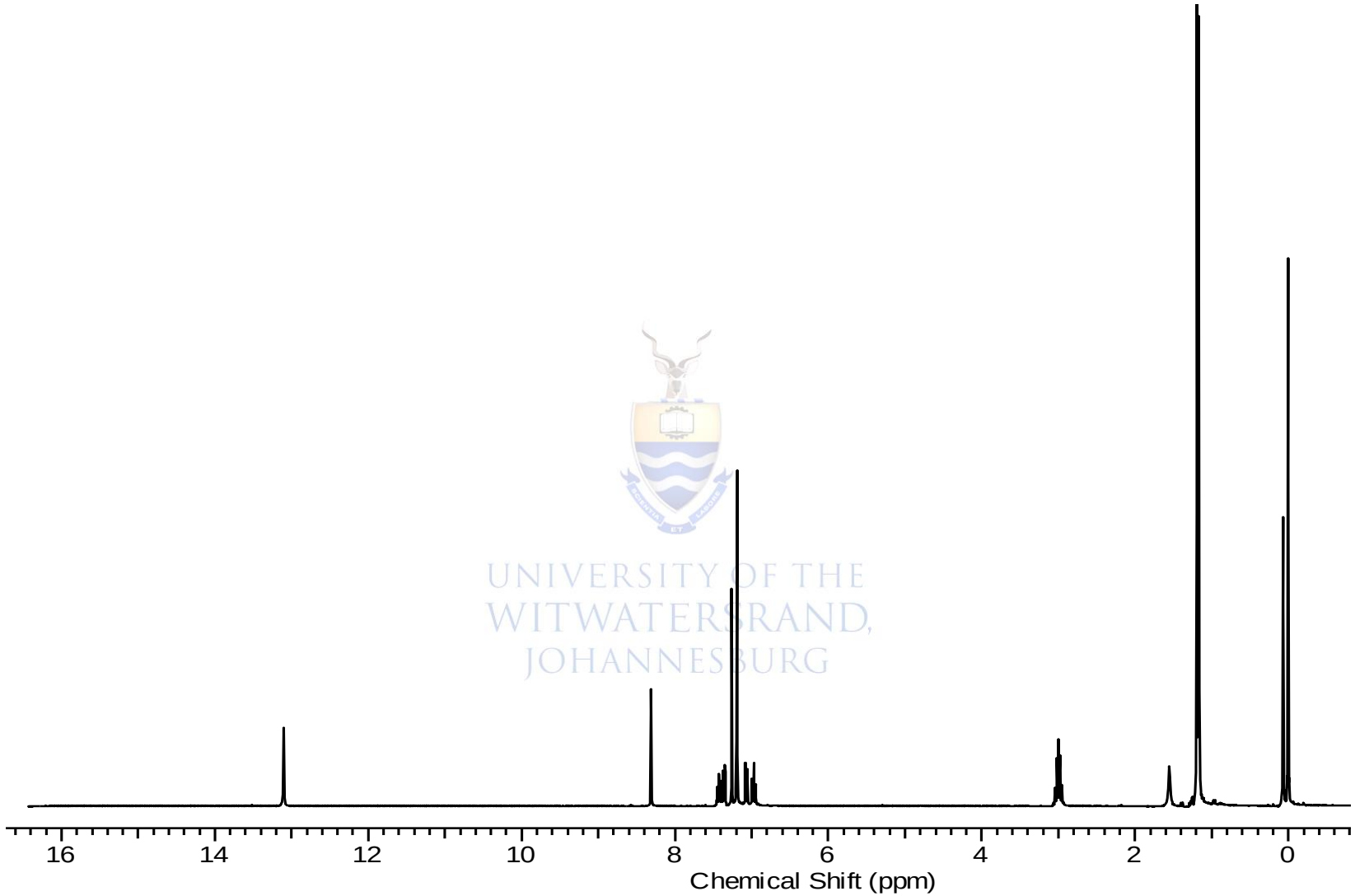

*^{1}H-NMR spectrum of salicylaldimine ligand **L3**.*

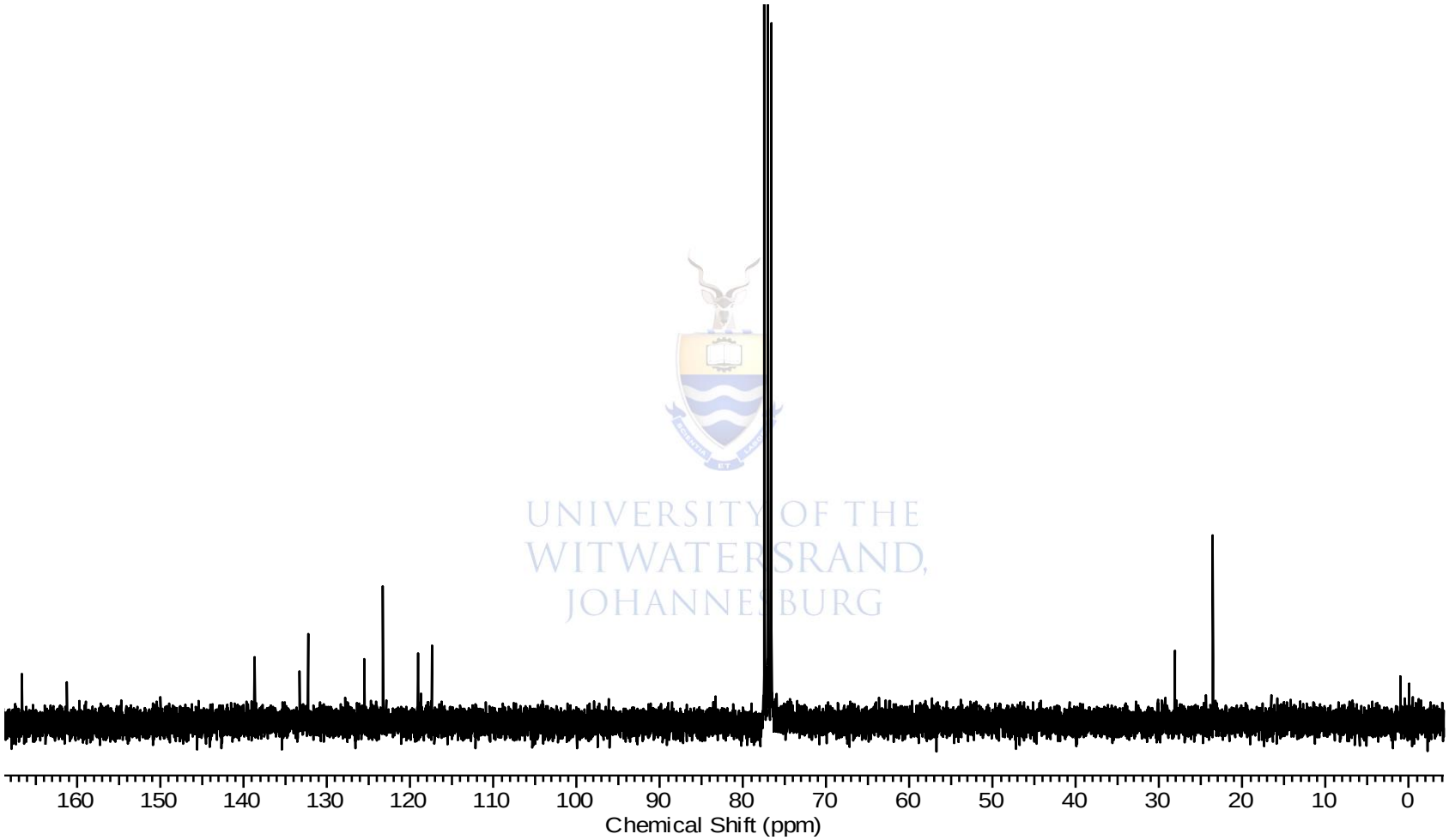

*^{13}C-NMR spectrum of salicylaldimine ligand **L3**.*

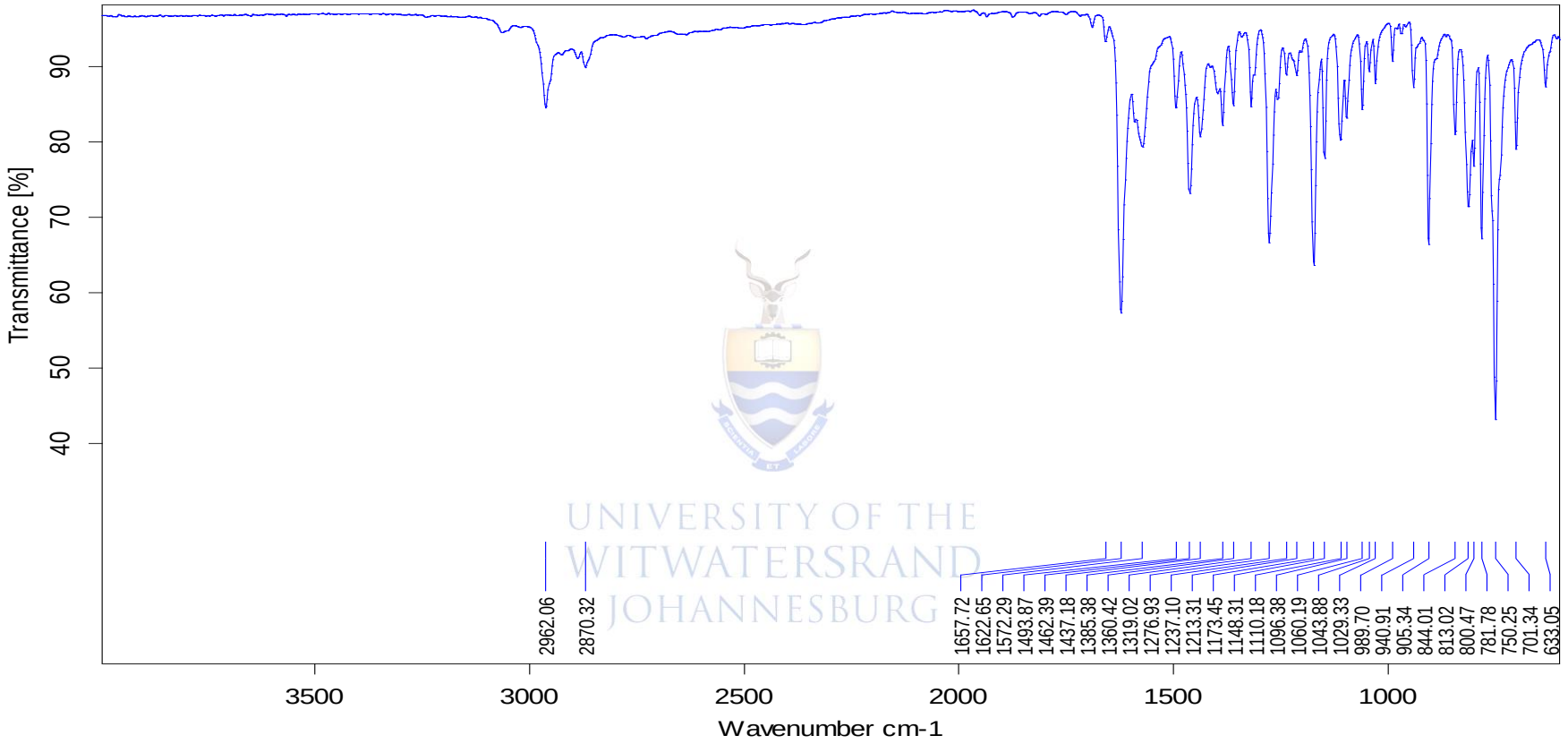

*FTIR spectrum of salicylaldimine ligand **L3**.*

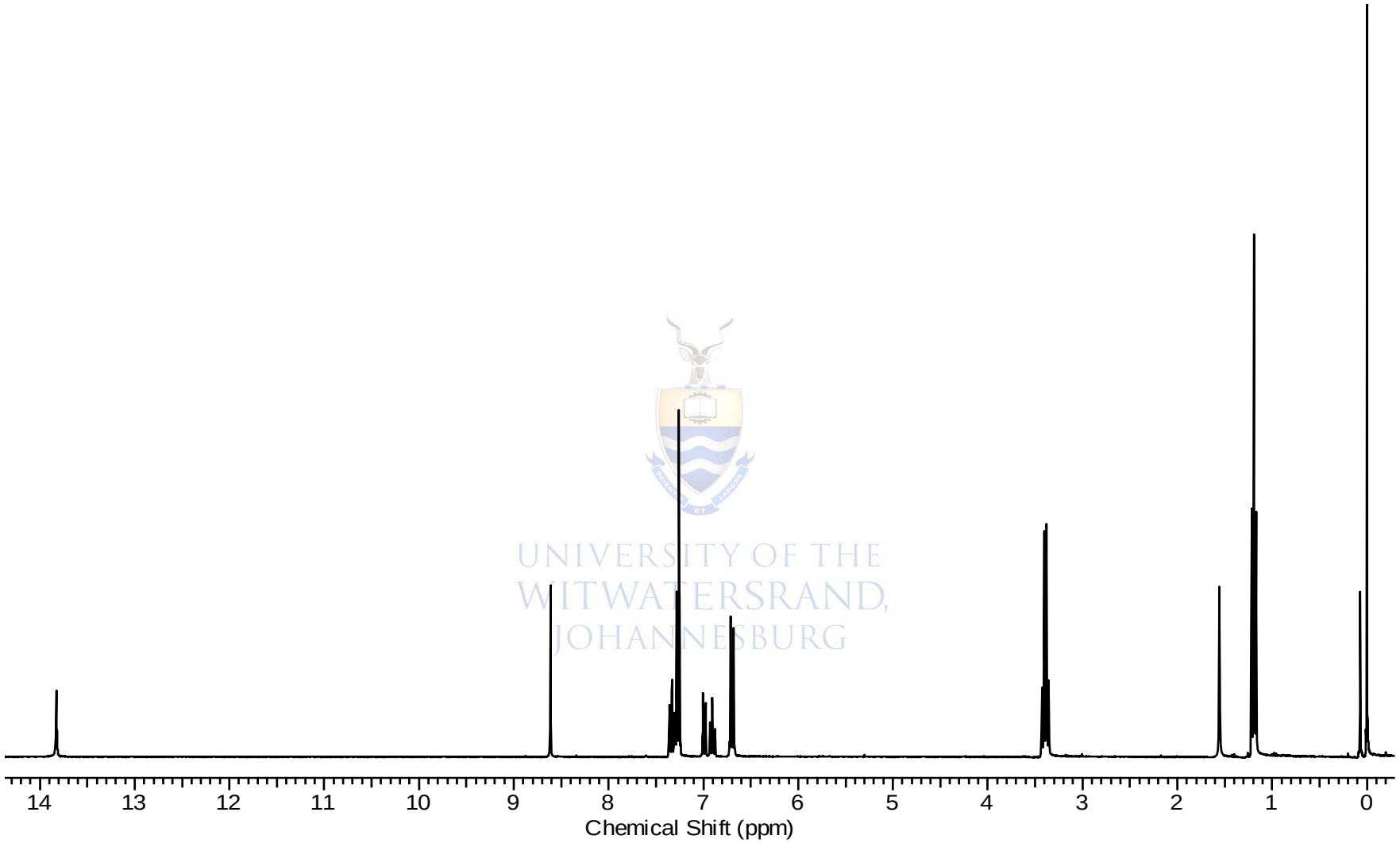

*[1]H-NMR spectrum of salicylaldimine ligand **L4**.*

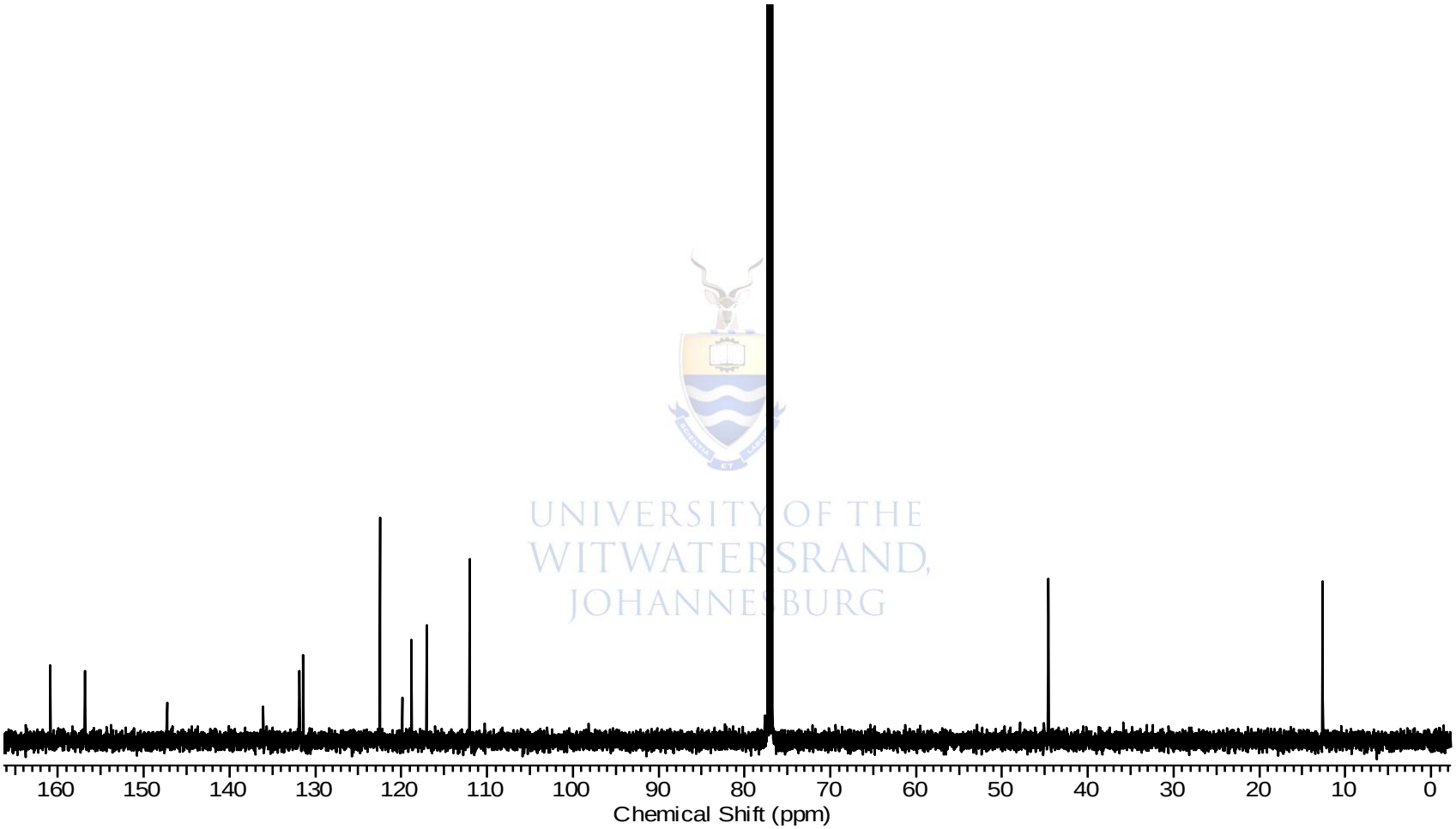

*^{13}C-NMR spectrum of salicylaldimine ligand **L4**.*

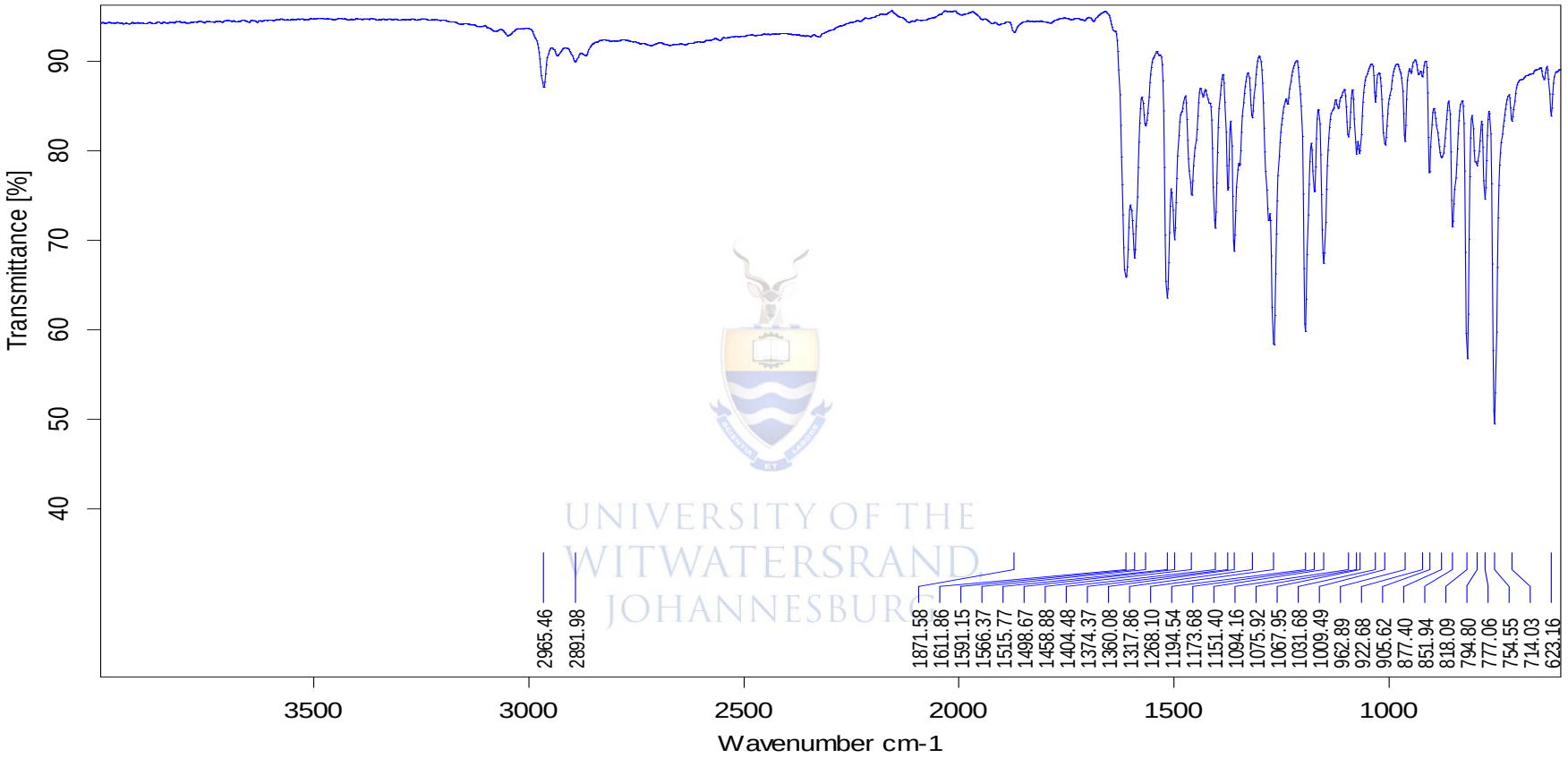

*FTIR spectrum of salicylaldimine ligand **L4**.*

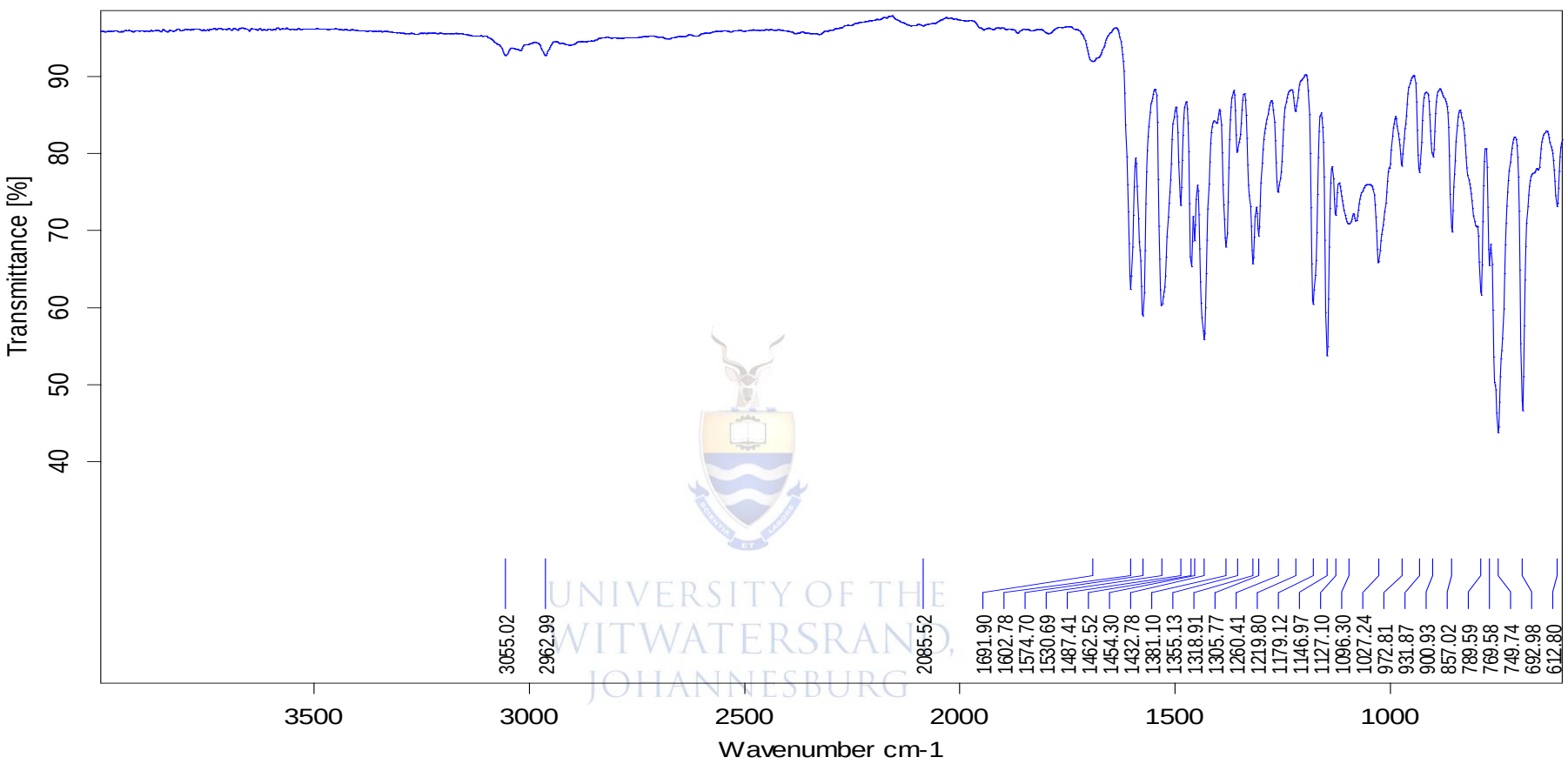

FTIR spectrum of cobalt salicylaldiminato complex ***Co1***.

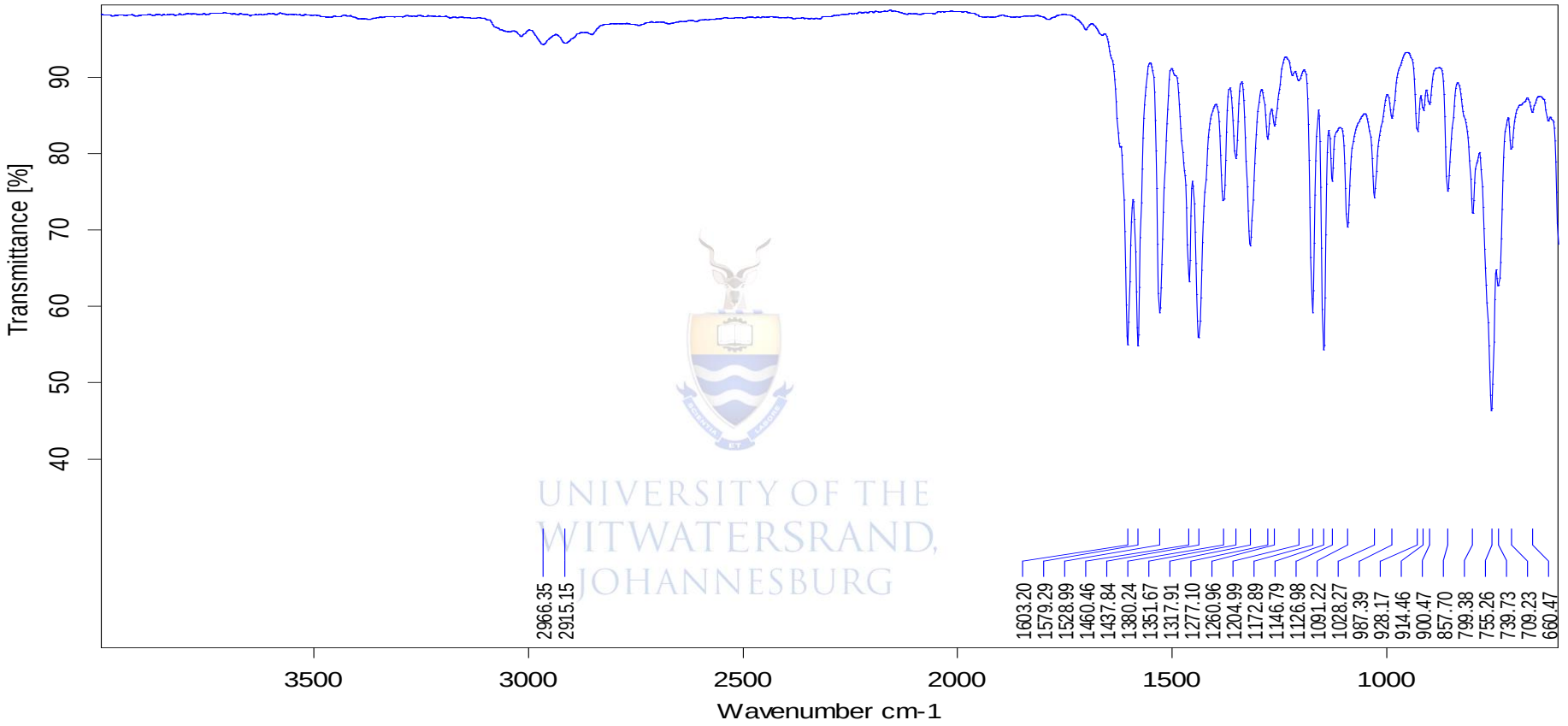

FTIR spectrum of cobalt salicylaldiminato complex ***Co2****.*

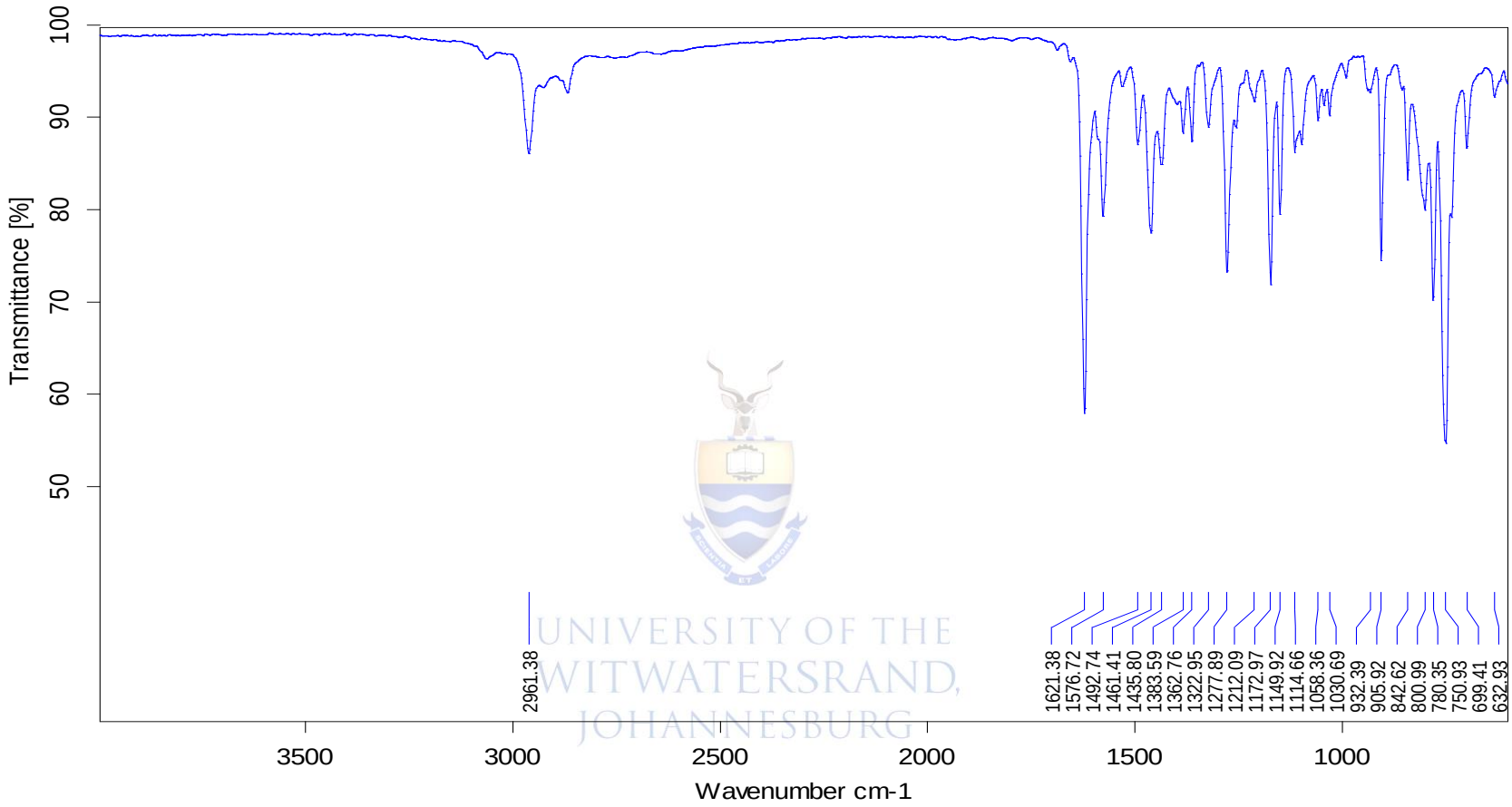

FTIR spectrum of cobalt salicylaldiminato complex ***Co3****.*

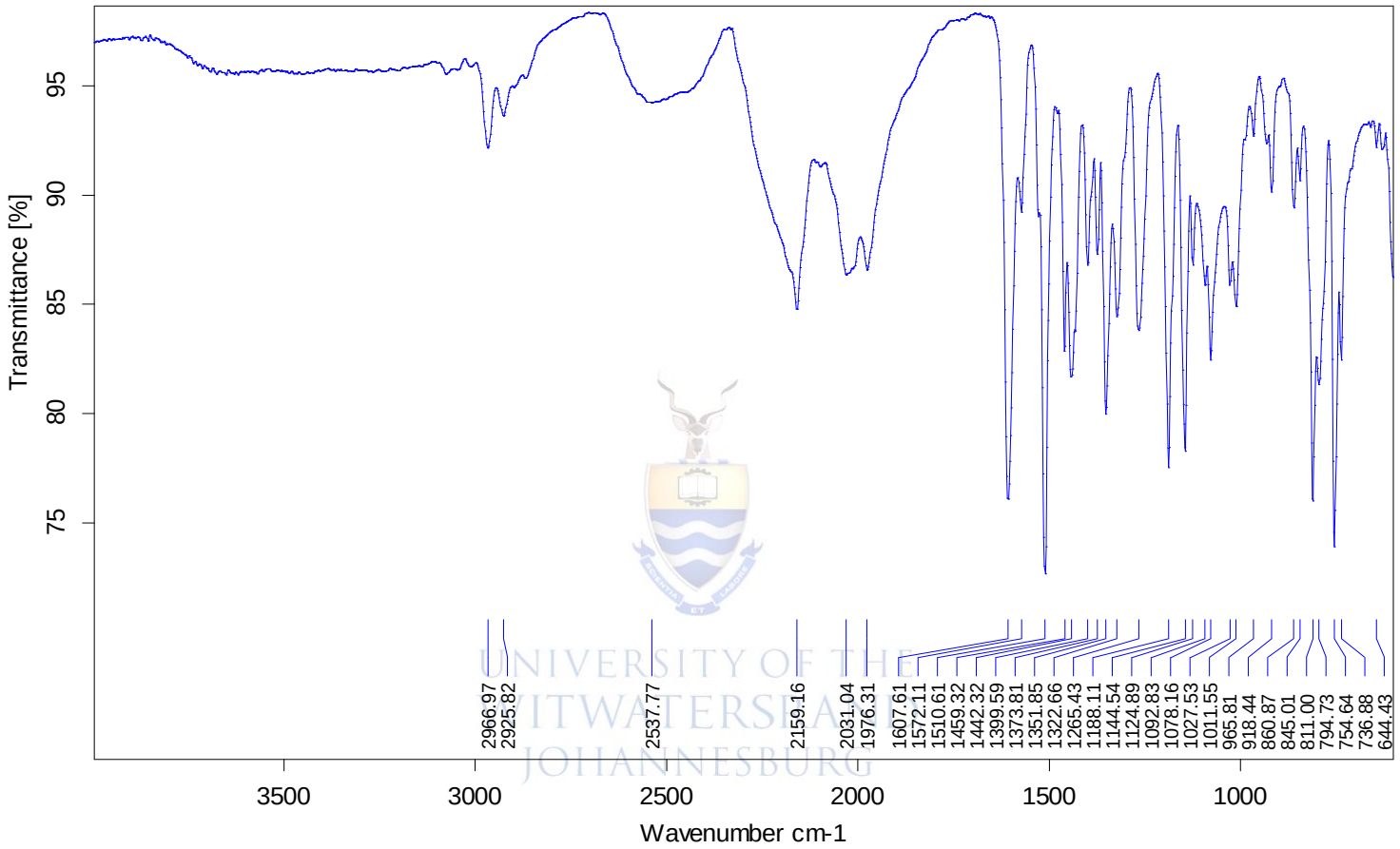

FTIR spectrum of cobalt salicylaldiminato complex ***Co4****.*

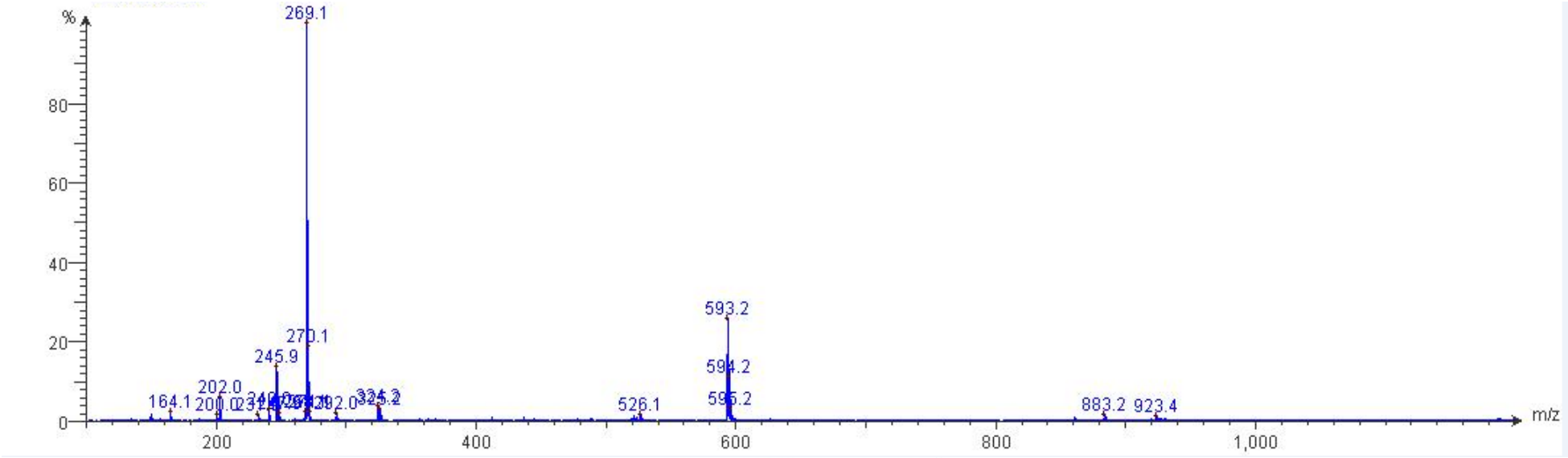

Mass spectrum of cobalt salicylaldiminato complex ***Co4****.*

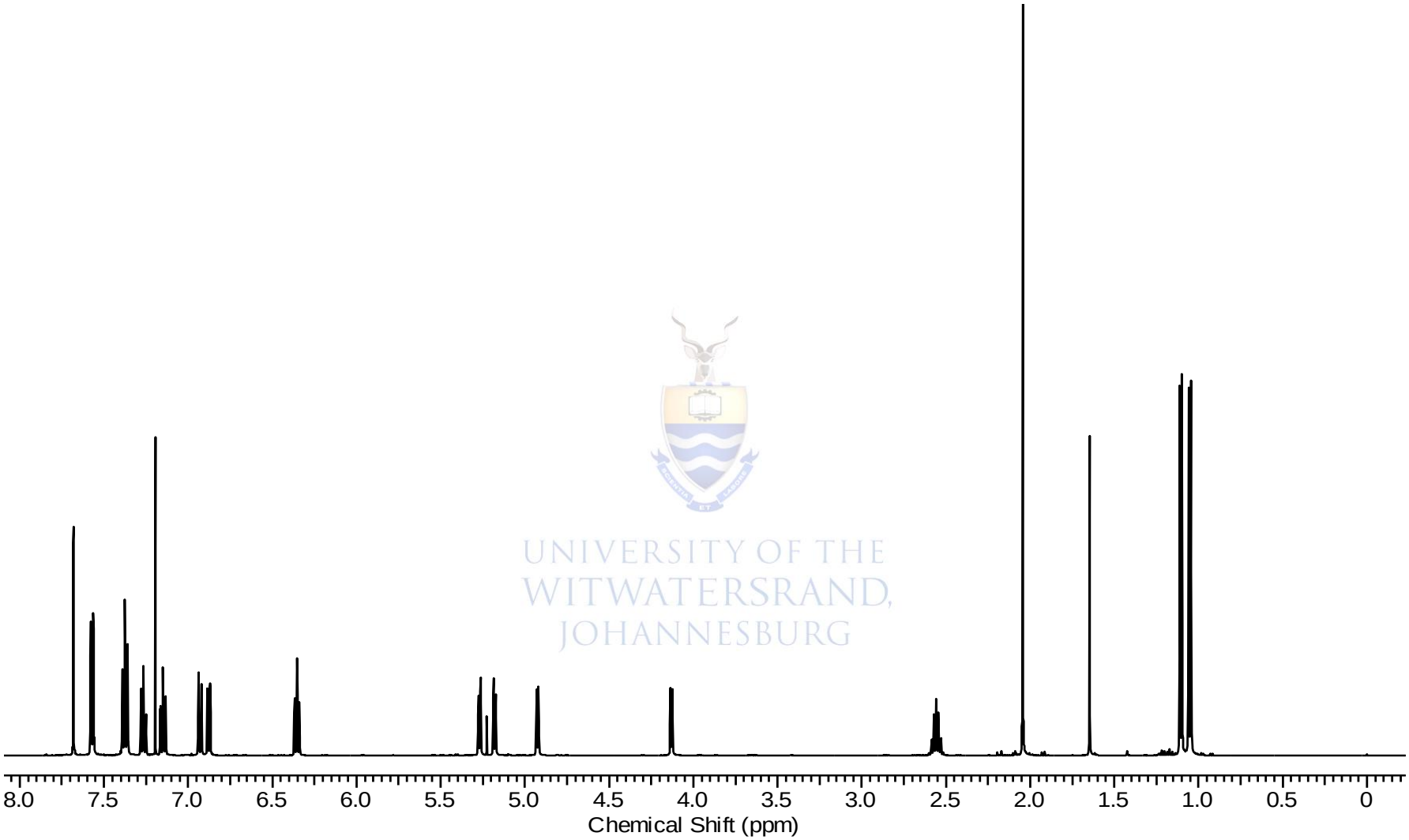

[1]H-NMR spectrum of ruthenium salicylaldimine complex ***Ru1***.

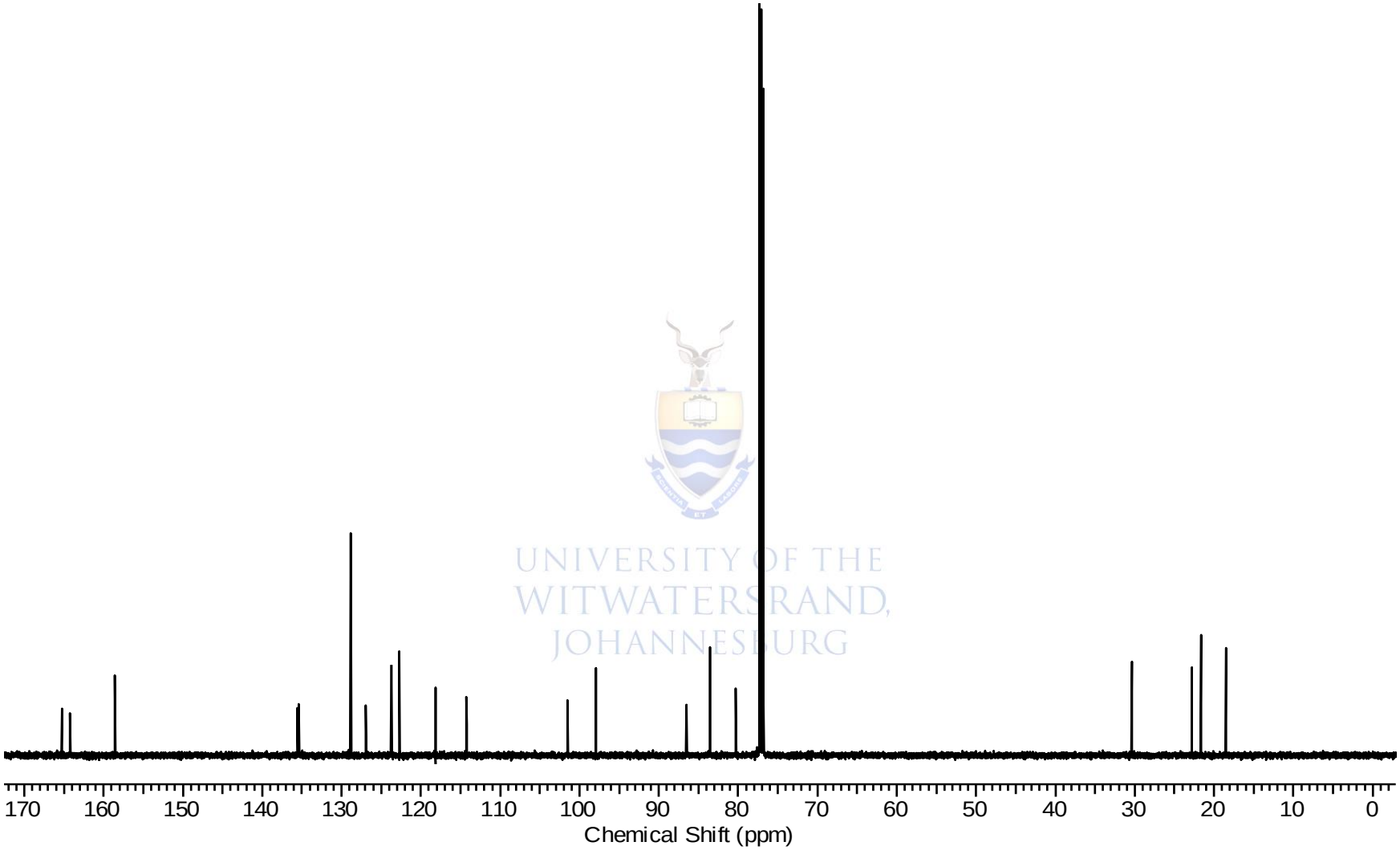

^{13}C-NMR spectrum of ruthenium salicylaldimine complex ***Ru1***.

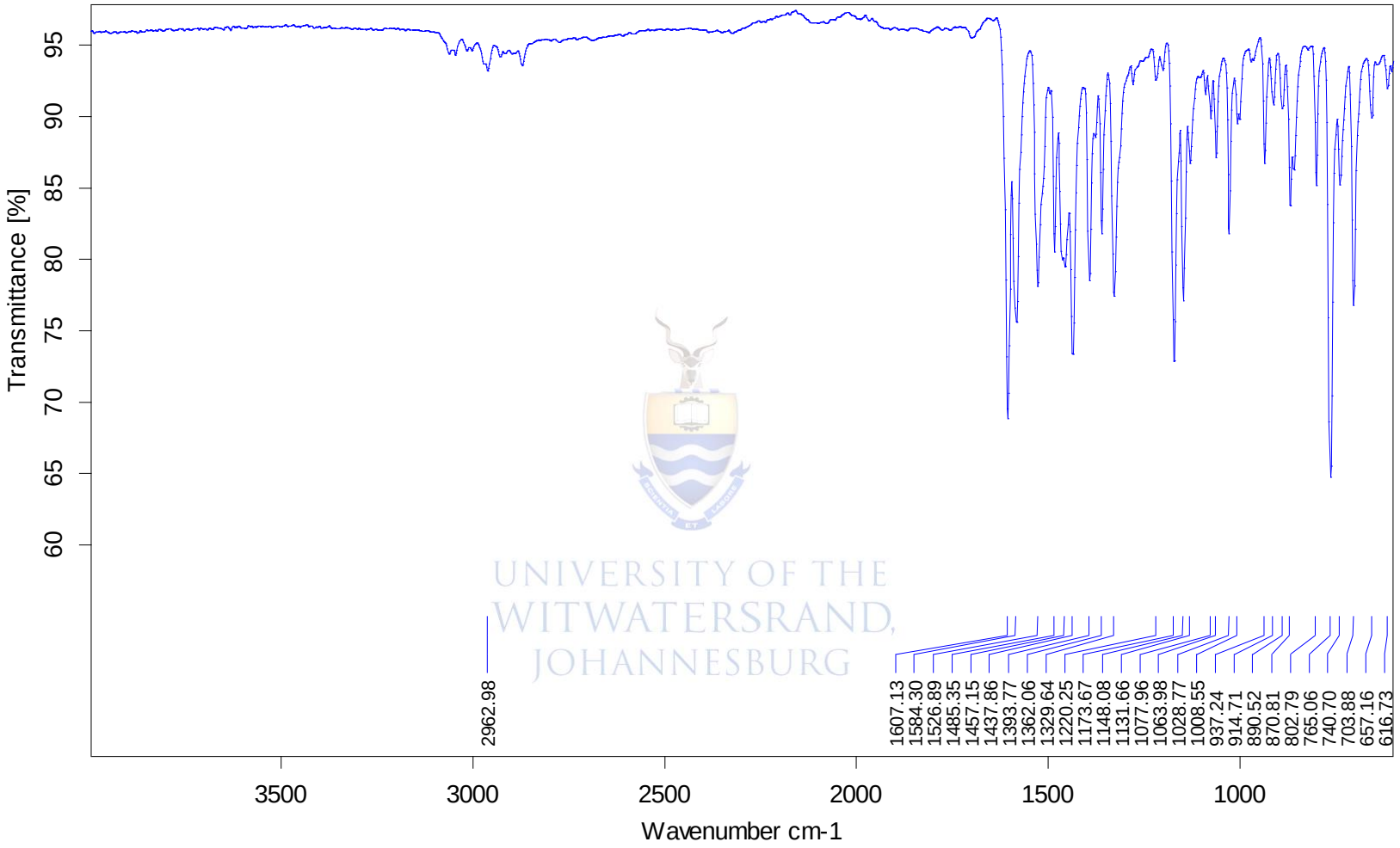

FTIR spectrum of ruthenium salicylaldimine complex ***Ru1***.

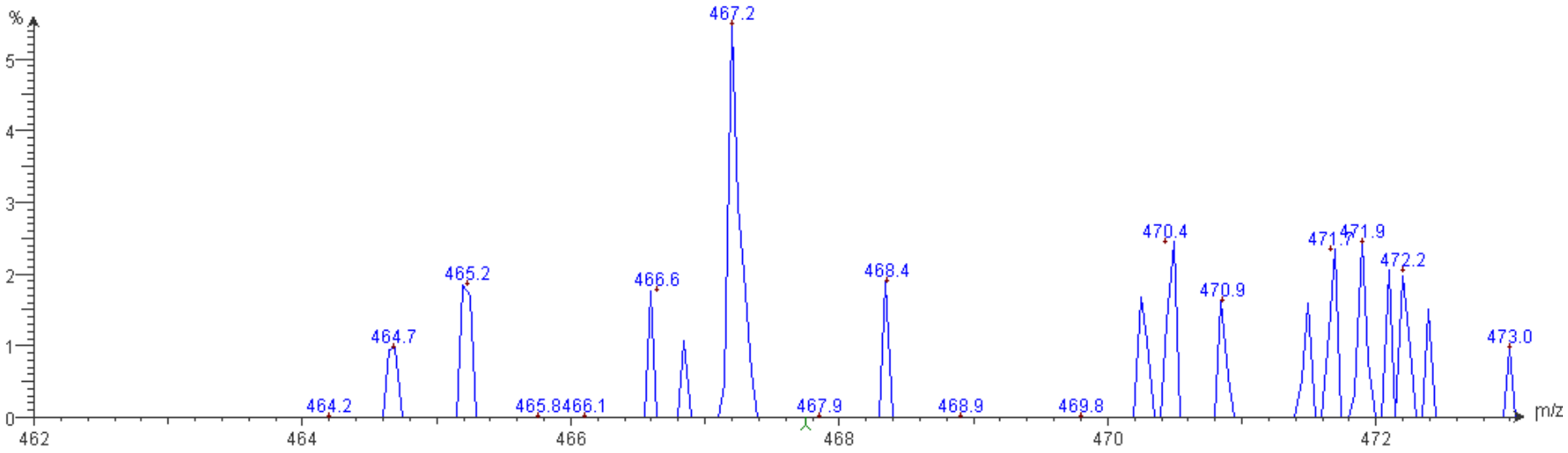

Mass spectrometry of ruthenium salicylaldiminato complex ***Ru1***

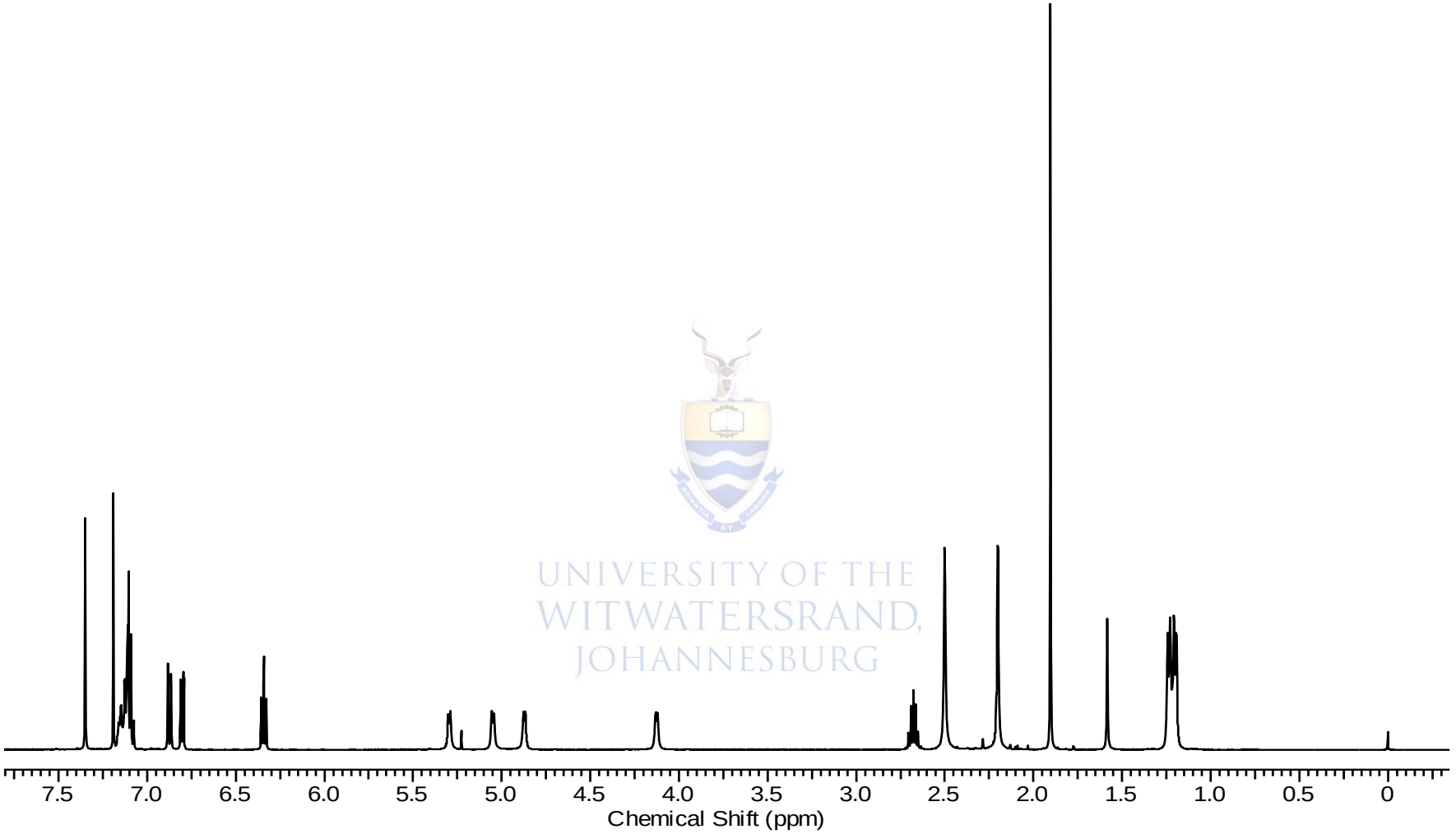

^{1}H-NMR spectrum of ruthenium salicylaldimine complex ***Ru2****.*

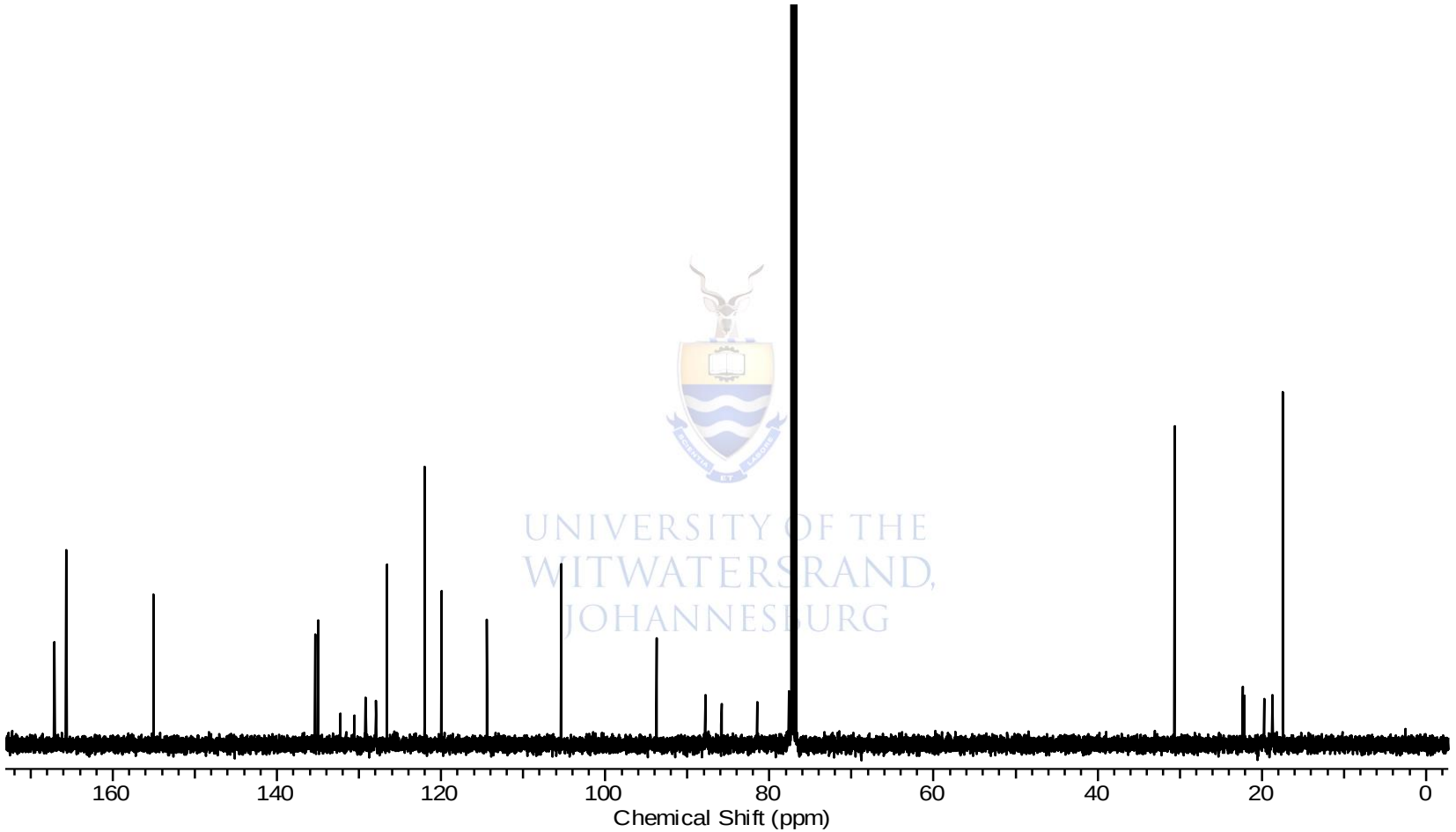

^{13}C-NMR spectrum of ruthenium salicylaldimine complex ***Ru2***.

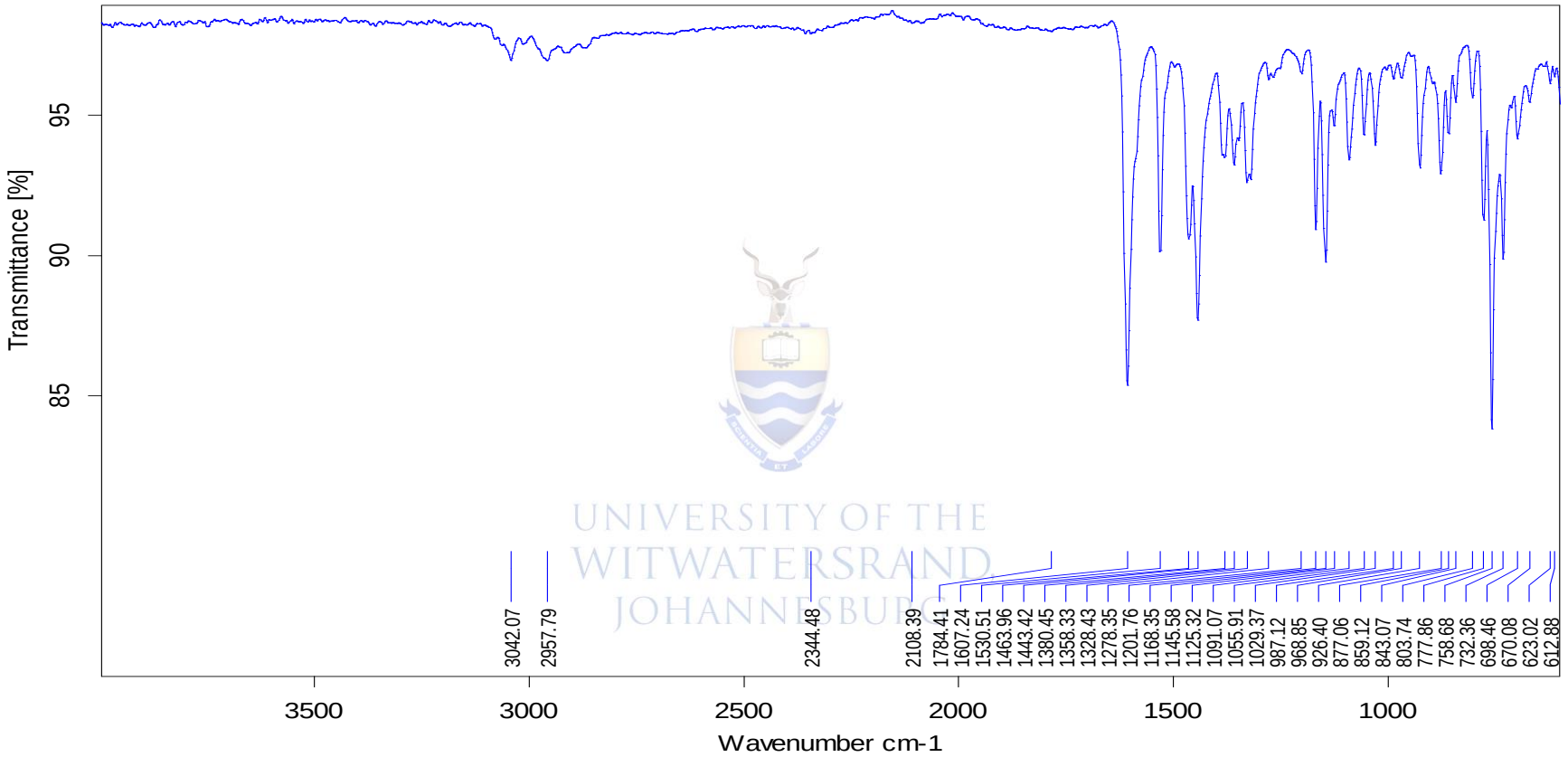

FTIR spectrum of ruthenium salicylaldimine complex ***Ru2***.

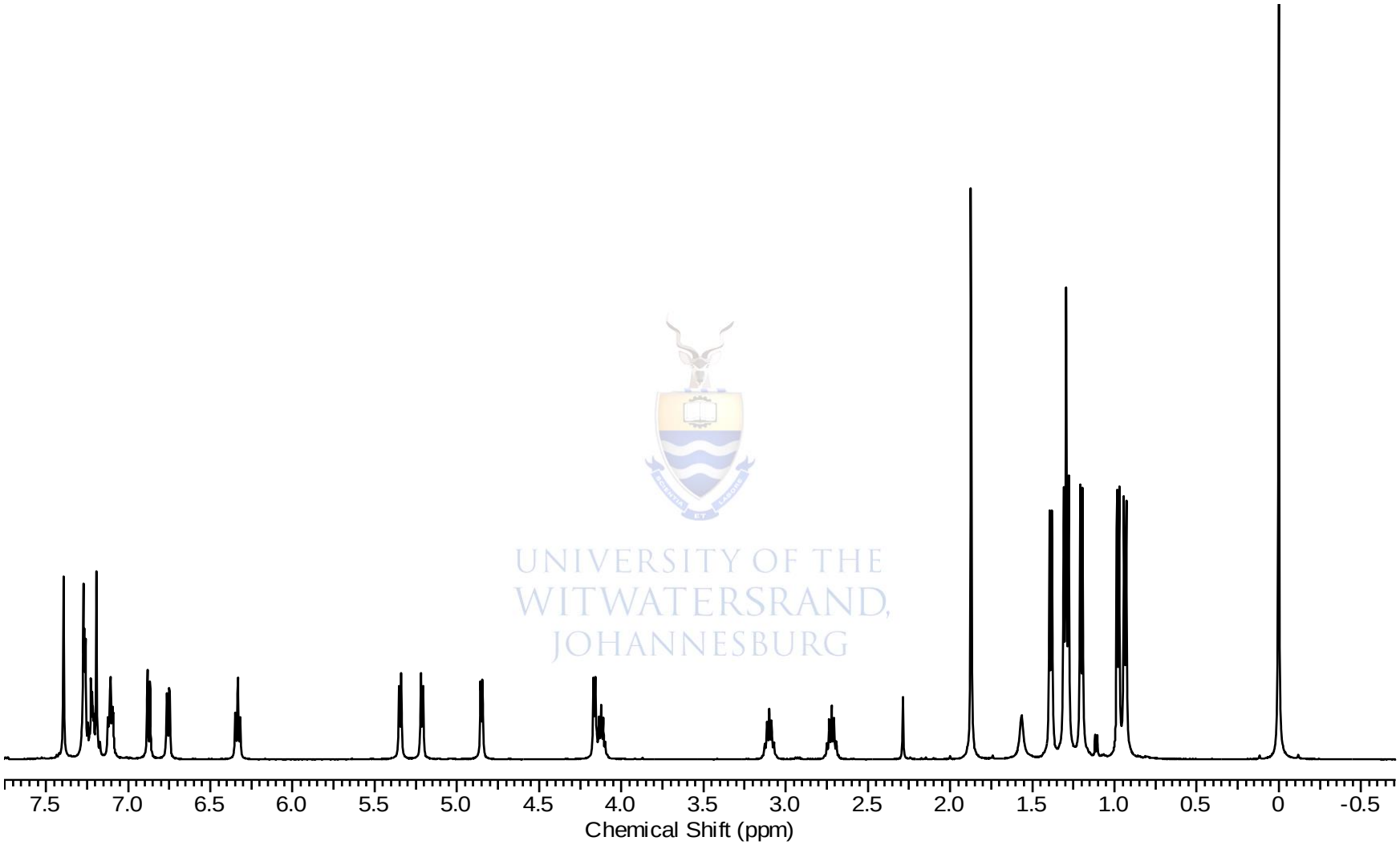

^{1}H-NMR spectrum of ruthenium salicylaldimine complex ***Ru3****.*

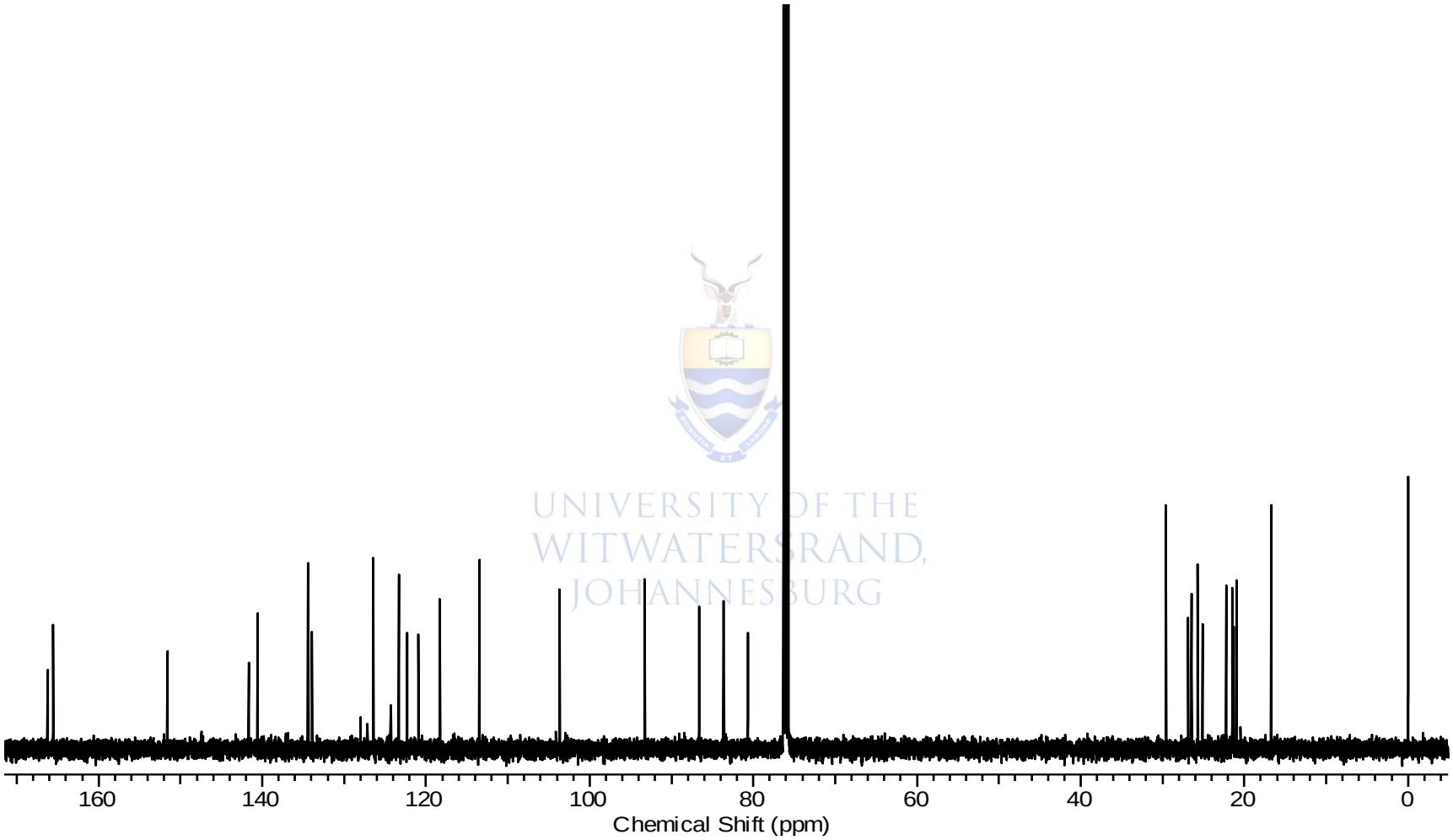

*^{13}C-NMR spectrum of ruthenium salicylaldimine complex **Ru3**.*

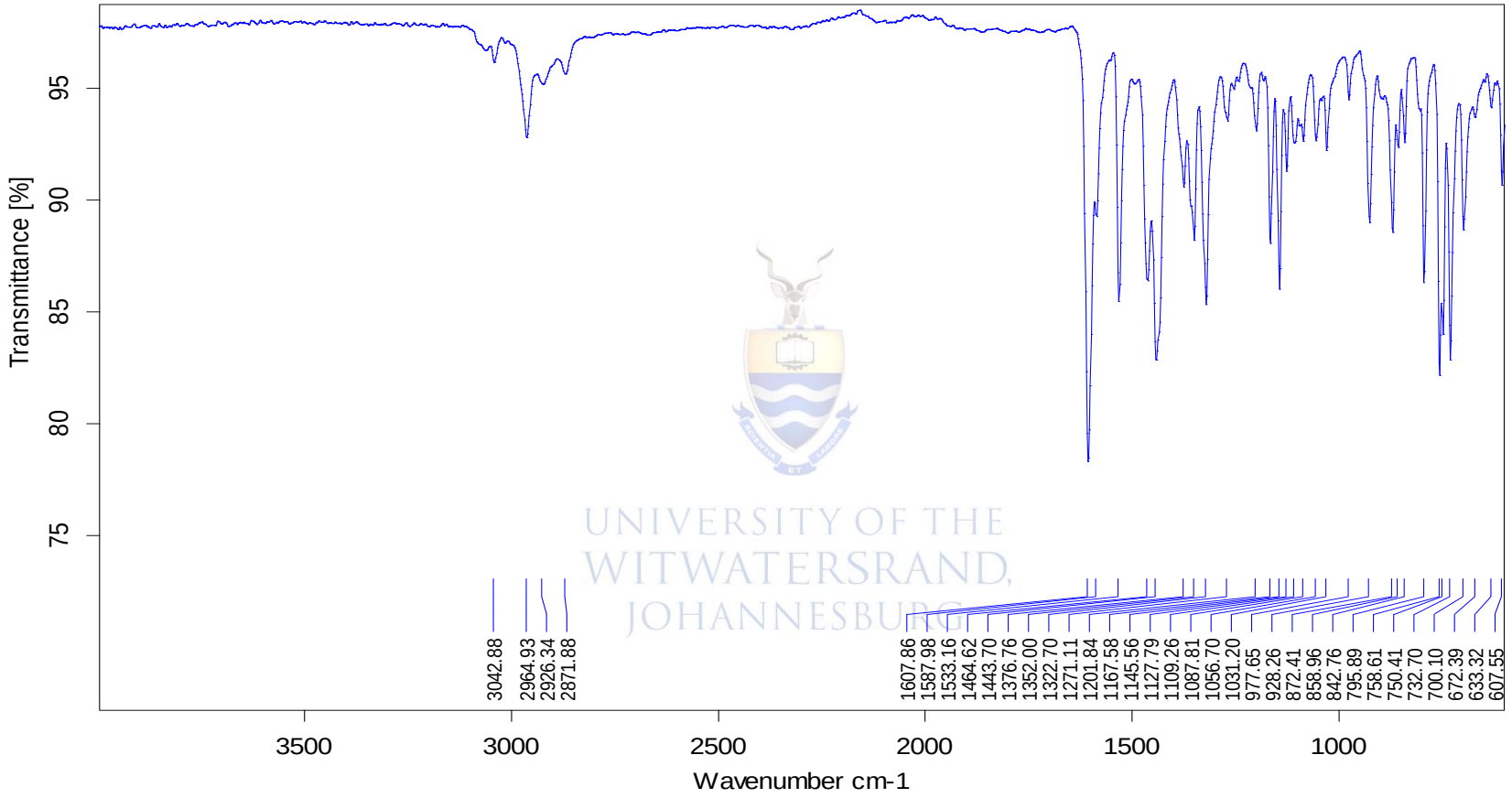

FTIR spectrum of ruthenium salicylaldimine complex ***Ru3*****.**

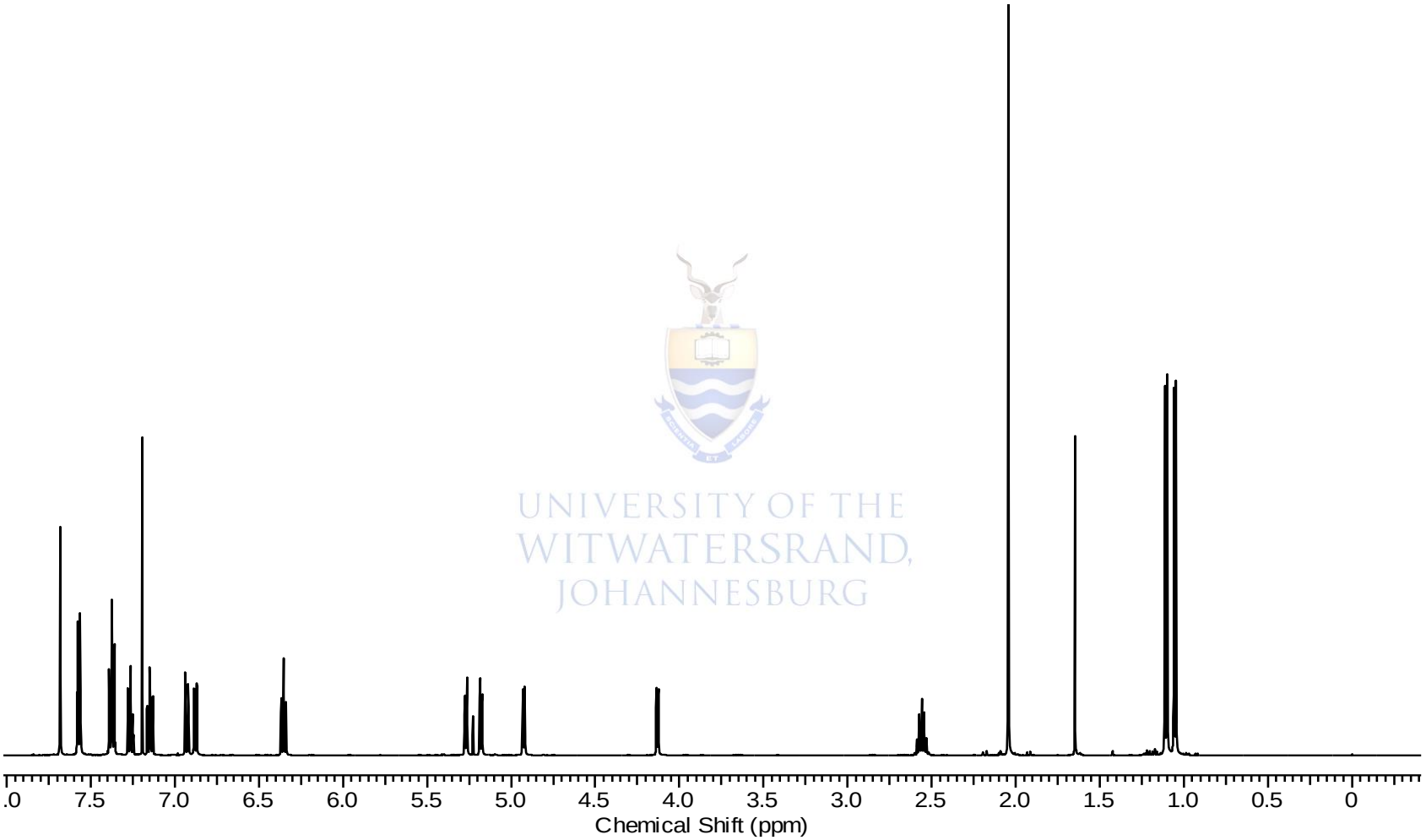

[1]H-NMR spectrum of ruthenium salicylaldimine complex ***Ru4****.*

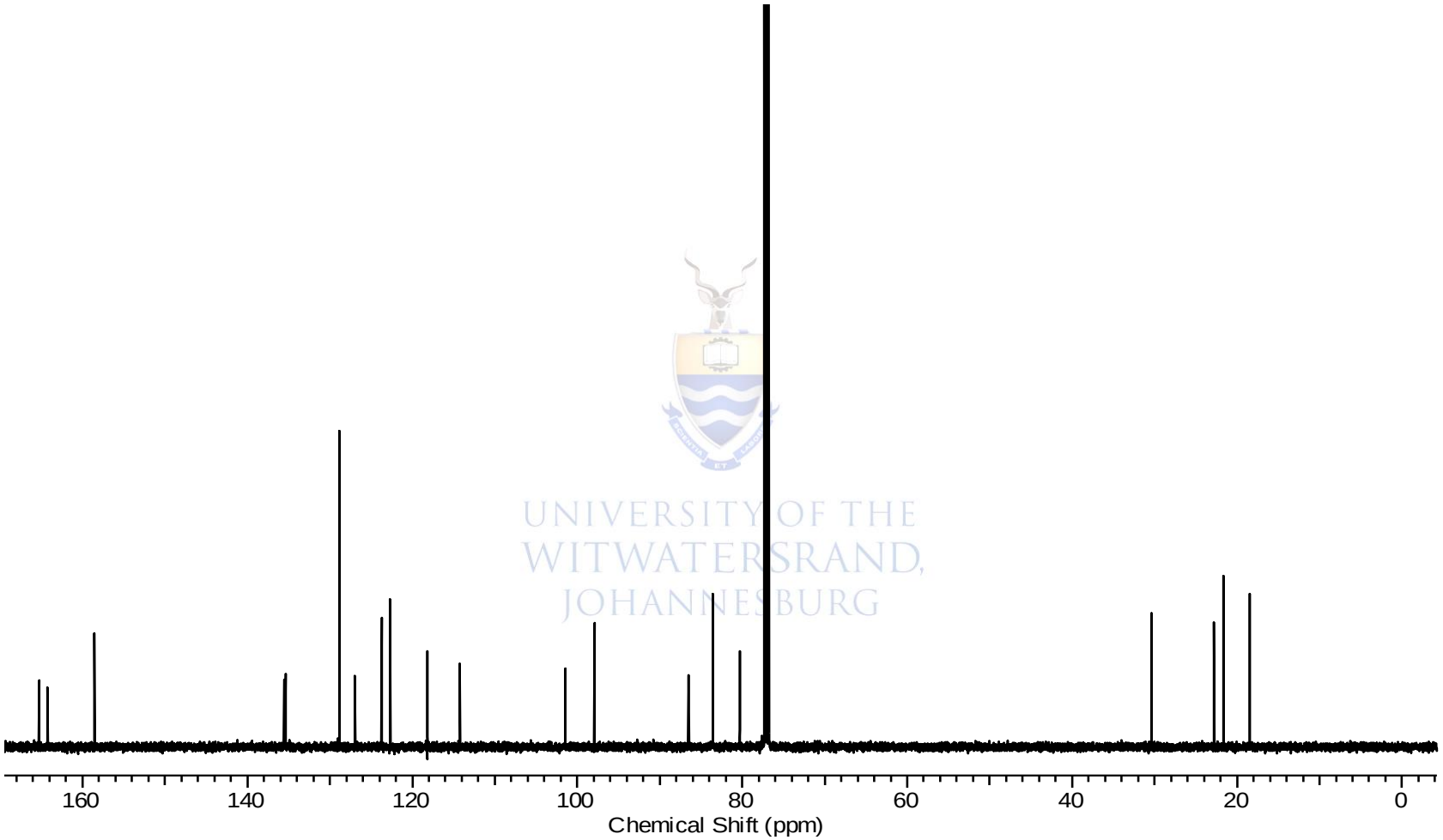

*^{13}C-NMR spectrum of ruthenium salicylaldimine complex **Ru4**.*

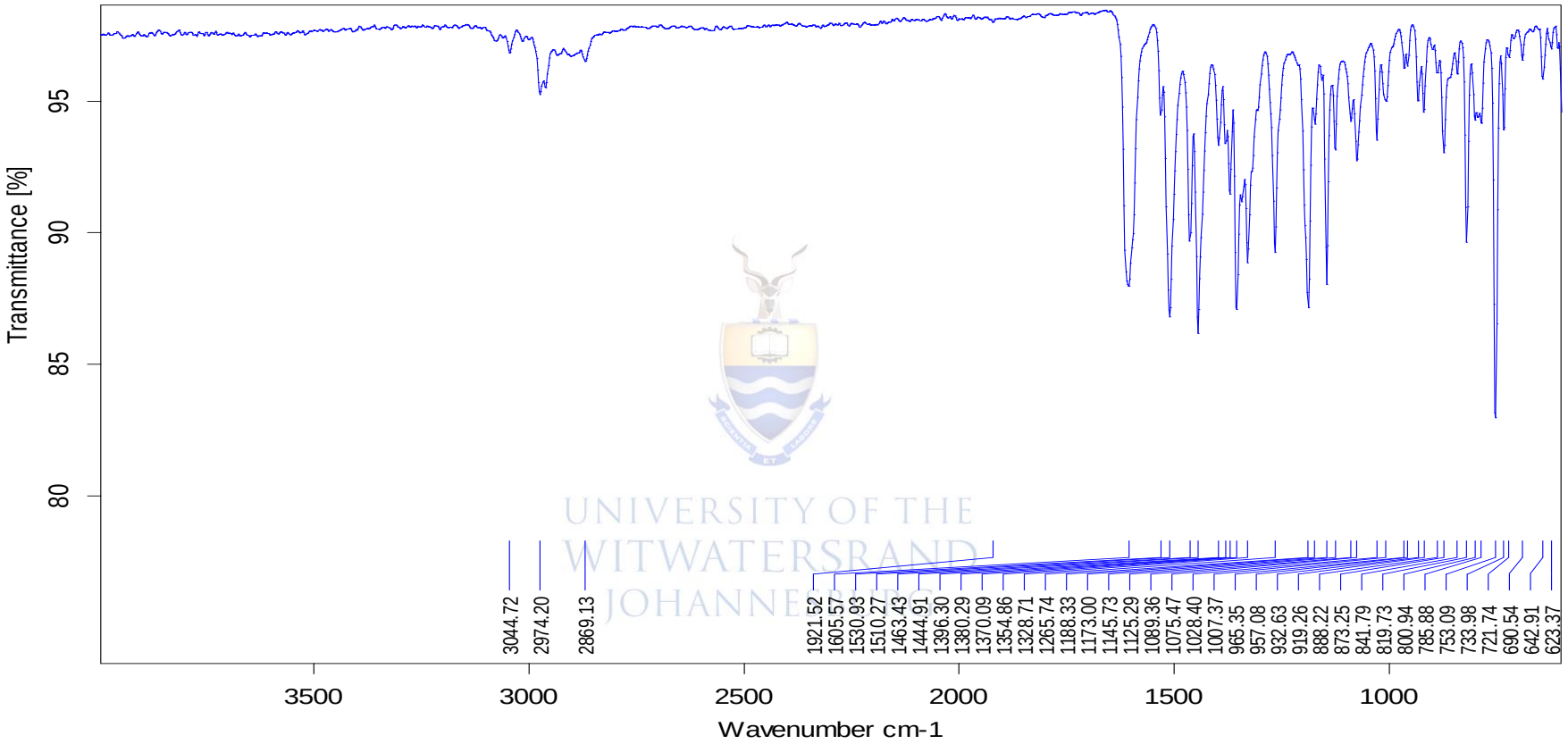

FTIR spectrum of ruthenium salicylaldimine complex ***Ru4***.

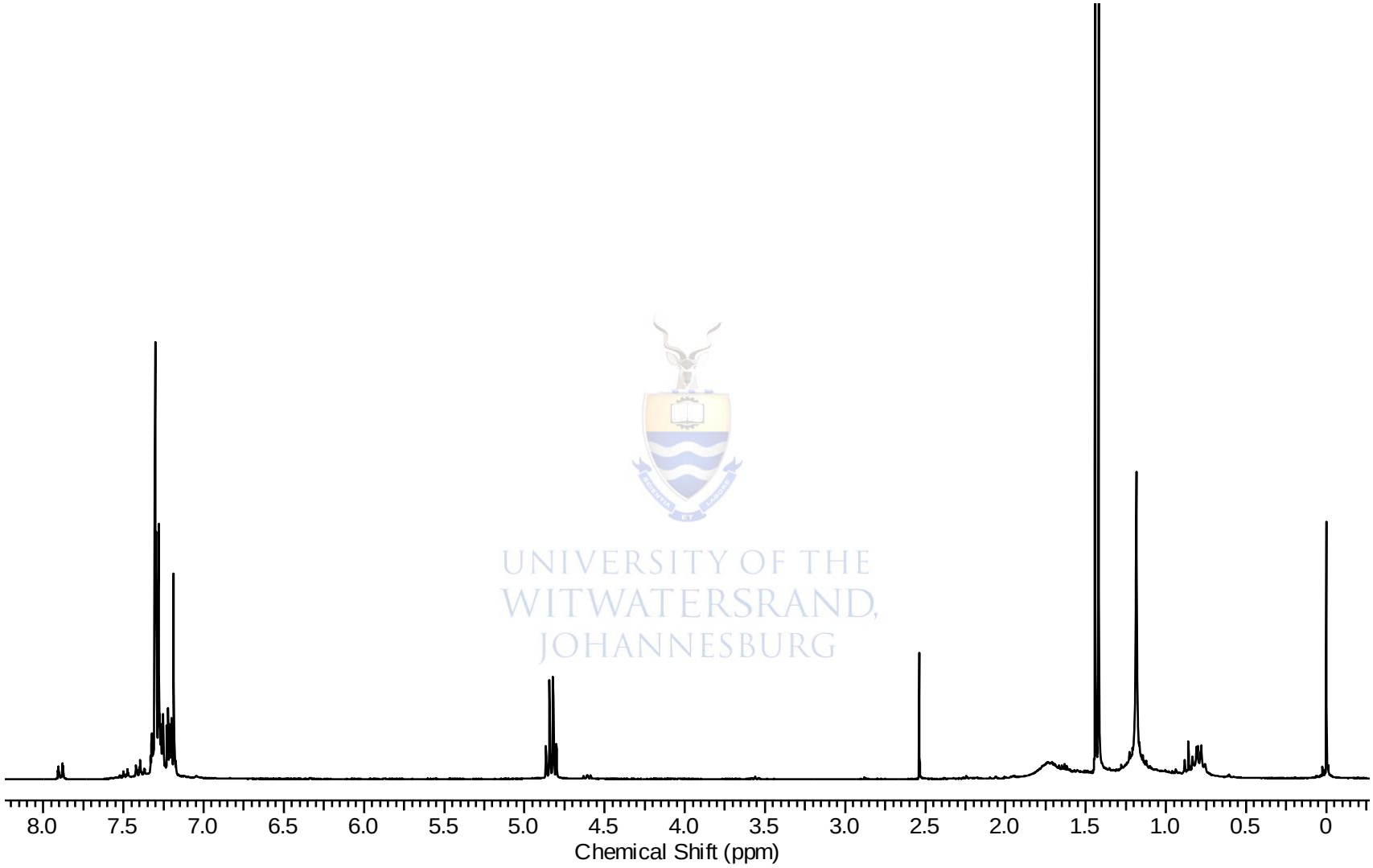

*^{1}H-NMR spectrum of reaction residue obtained after using **Ru2** as the catalyst precursor at 82 ^{o}C for 48 hours.*

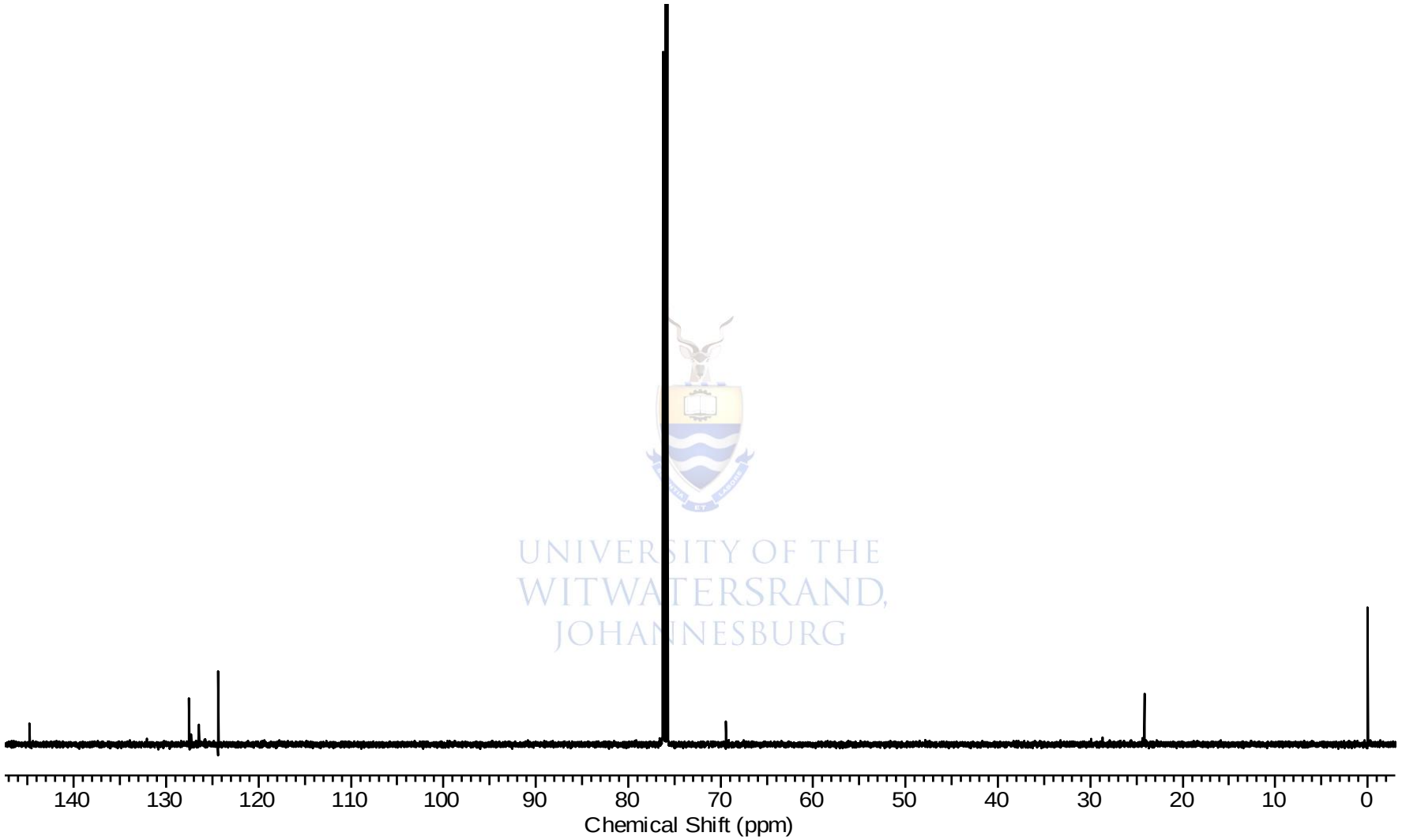

*^{13}C-NMR spectrum of reaction residue obtained after using **Ru2** as the catalyst precursor at 82 ^{o}C for 48 hours.*

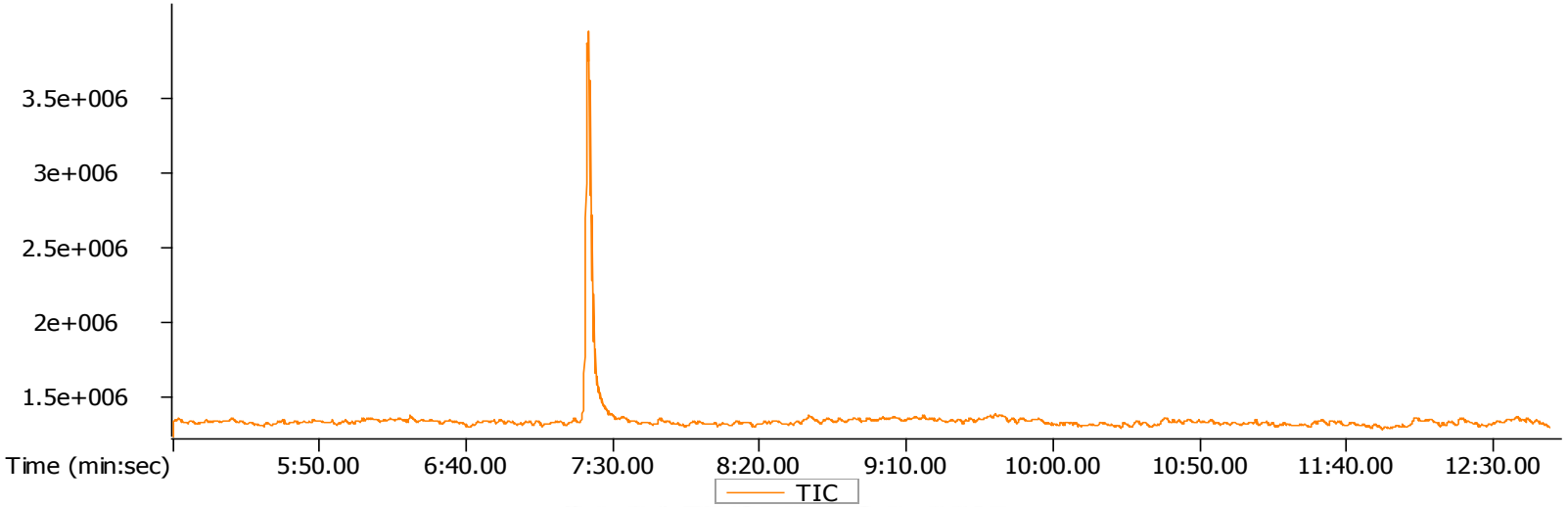

*GC chromatogram for the transfer hydrogenation of acetophenone using **Co2** as the catalyst precursor at 82 ^{o}C for 48 hours.*

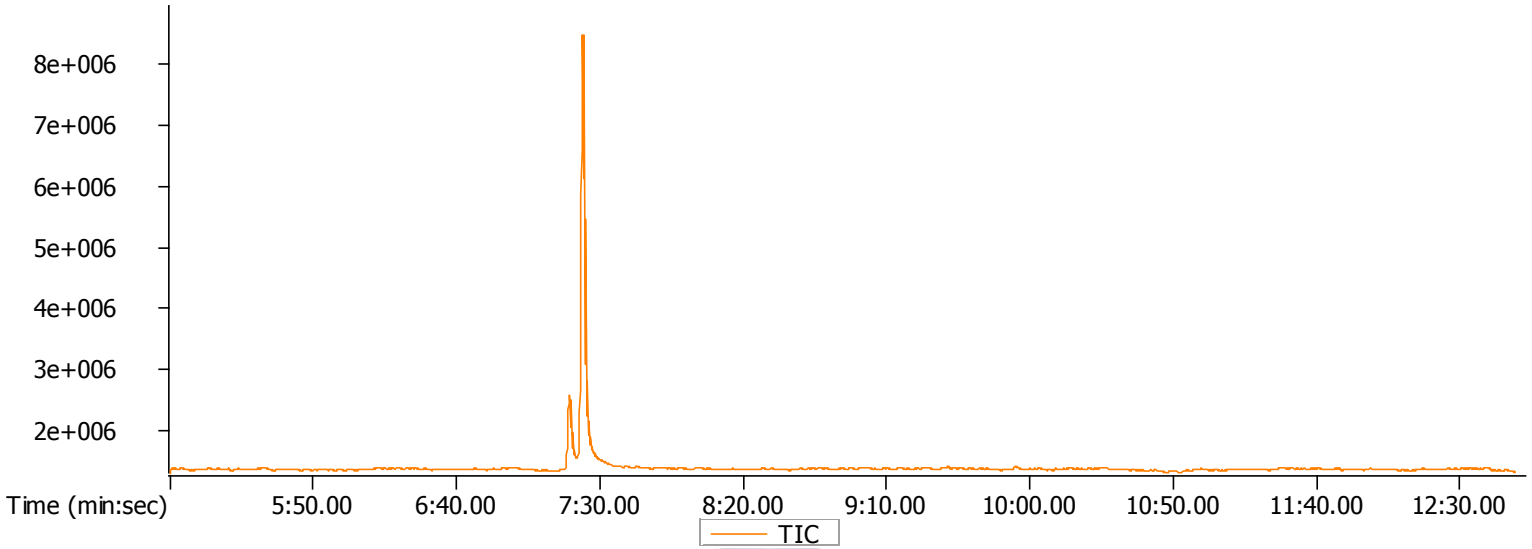

*GC chromatogram of the transfer hydrogenation of acetophenone using **Ru1** as the catalyst precursor at 82 ^{o}C for 48 hours.*